

8-2018

Hyperspectral Modeling of Relative Water Content and Nitrogen Content in Sorghum and Maize

Valerie Cross
Purdue University

Follow this and additional works at: https://docs.lib.purdue.edu/open_access_theses

Recommended Citation

Cross, Valerie, "Hyperspectral Modeling of Relative Water Content and Nitrogen Content in Sorghum and Maize" (2018). *Open Access Theses*. 1522.
https://docs.lib.purdue.edu/open_access_theses/1522

This document has been made available through Purdue e-Pubs, a service of the Purdue University Libraries.
Please contact epubs@purdue.edu for additional information.

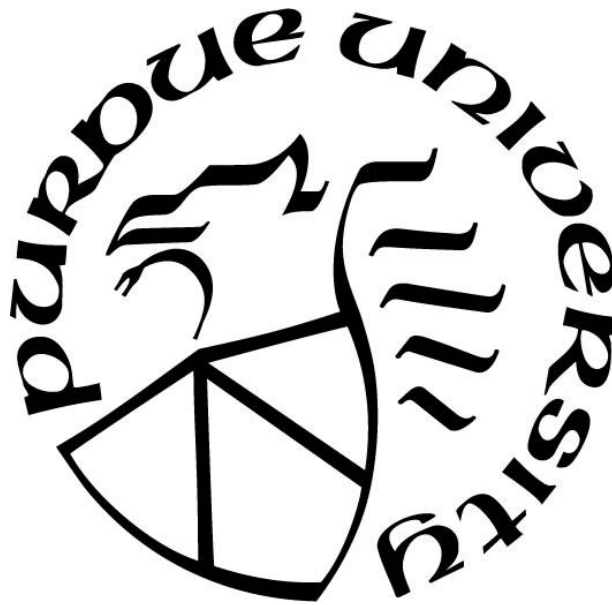
**HYPERSPECTRAL MODELING OF RELATIVE WATER CONTENT
AND NITROGEN CONTENT IN SORGHUM AND MAIZE**

by
Valerie Cross

A Thesis

*Submitted to the Faculty of Purdue University
In Partial Fulfillment of the Requirements for the degree of*

Master of Science



Department of Agronomy
West Lafayette, Indiana
August 2018

THE PURDUE UNIVERSITY GRADUATE SCHOOL
STATEMENT OF COMMITTEE APPROVAL

Dr. Mitchell Tuinstra, Chair

Department of Agronomy

Dr. Jian Jin

Department of Agricultural and Biological Engineering

Dr. Clifford Weil

Department of Agronomy

Dr. Michael Mickelbart

Department of Botany and Plant Pathology

Approved by:

Dr. Ronald Turco

Head of the Graduate Program

To Mom, Dad, and Jake.

Love Always.

ACKNOWLEDGMENTS

I would like to thank my advisor, Mitch Tuinstra, for his guidance during the past two years and throughout my undergraduate career. I would also like to thank my remaining committee members, Dr. Cliff Weil, Dr. Jian Jin, and Dr. Mike Mickelbart, for challenging me to use my brain to solve problems and answer questions.

I would also like to thank the wonderful Tuinstra lab technicians, Andy Linvill and Eugene Glover, for their wiliness to always help me out in the greenhouse. Other members of the Tuinstra lab have also become great friends and mentors during my time at Purdue.

Thank you for the support of the United Sorghum Checkoff and Sumitomo for the funding provided for the research.

Finally, I want to thank my parents for always believing in me, my grandparents for inspiring me, and my fiancé Jake for always supporting me no matter what.

TABLE OF CONTENTS

LIST OF TABLES	viii
LIST OF FIGURES	ix
ABSTRACT	xiii
CHAPTER 1: LITERATURE REVIEW	1
1.1 <i>Sorghum bicolor</i> (L.) Moench	1
1.1.2 Description	1
1.1.3 Sorghum Populations	3
1.2 <i>Zea Mays</i>	4
1.2.1 Description	4
1.2.2 Maize Populations	5
1.3 Drought	7
1.3.1 Causes and Results of Drought	7
1.3.2 Drought and Agriculture	11
1.3.3 Adaptations to Drought	12
1.3.4 Measuring Water	16
1.4 Nitrogen	18
1.4.1 Causes and Results of Nitrogen Deficiencies	18
1.4.2 Water Stress and Nitrogen	21
1.4.3 Adaptations to Nitrogen Stress	22
1.4.4 Measuring Nitrogen	25
1.5 Hyperspectral Imaging	29
1.5.1 Introduction	29
1.5.2 Vegetation Indices	31
1.5.3 Using Hyperspectral Data	35
1.6 Conclusion	38
CHAPTER 2: SORGHUM CALIBRATION STUDY	39
2.1 Introduction	39
2.2 Materials and Methods	42
2.2.1 Sorghum Seed Sources	42

2.2.2 Soil Medium.....	42
2.2.3 Design of Experiment	43
2.2.4 Application of Stress.....	43
2.2.5 Automated Imaging System.....	45
2.2.6 Relative Water Content Measurements.....	47
2.2.7 Nitrogen Content Measurements	48
2.2.8 Data Processing.....	48
2.2.9 PLS_ToolBox in MatLab.....	49
2.3 Results.....	50
2.3.1 Relative Water Content.....	50
2.3.2 Nitrogen Content.....	52
2.3.3 Relative Water Content Models using Spectral and Morphological Features	54
2.3.4 Relative Water Content Models using only Spectral Features	57
2.3.5 Summary of all Relative Water Content Models	60
2.3.6 Nitrogen Content Models using Spectral and Morphological Features	61
2.3.7 Nitrogen Content Models using only Spectral Features	64
2.3.8 Summary of all Nitrogen Content Models.....	66
2.3.9 Relative Water Content Models built using data from same nitrogen treatments	67
2.3.10 Nitrogen Content Models built using data from same water treatments	68
2.3.11 Principal Component Analysis	69
2.4 Discussion.....	71
2.4.1 Reference Measurements	71
2.4.2 Models.....	71
2.4.3 Importance of verifying the applicability of spectral only models	73
2.4.4 Importance of water and nitrogen treatments in concert.....	74
2.5 Conclusion	75
CHAPTER 3: MAIZE MULTIPLE GENOTYPE STUDY	77
3.1 Introduction.....	77
3.2 Materials and Methods.....	78
3.2.1 Maize Seed Sources	78
3.2.2 Soil Medium.....	79

3.2.3 Design of Experiment	79
3.2.4 Application of Stress	80
3.2.5 Automated Imaging System	80
3.2.6 Relative Water Content Measurements	80
3.2.7 Nitrogen Content Measurements	81
3.2.8 Data Processing	81
3.2.9 PLS_ToolBox in MatLab	81
3.3 Results	81
3.3.1 Relative Water Content Results	81
3.3.2 Nitrogen Content Results	83
3.3.3 Relative Water Content Models	85
3.3.4 Summary of all Relative Water Content Models	89
3.3.5 Nitrogen Content Models	90
3.3.6 Summary of all Nitrogen Content Models	94
3.3.7 Models built using PHP02 Half-Siblings	95
3.3.8 Models built using Sorghum Data	95
3.3.9 Combining Sorghum Calibration Data and Maize Multiple Genotype Data	97
3.3.10 Principal Component Analysis	101
3.4 Discussion	102
3.4.1 Reference Measurements	102
3.4.2 Models	102
3.4.3 Predicting Across Species	104
3.5 Conclusion	106
REFERENCES	108

LIST OF TABLES

Table 1. Genotype and treatment combinations evaluated in this experiment	43
Table 2. Analysis of Variance (ANOVA) table for reference relative water content.....	51
Table 3. Analysis of Variance (ANOVA) table for reference nitrogen content	53
Table 4. Genotype and treatment combinations evaluated in this experiment	80
Table 5. Analysis of Variance (ANOVA) table of relative water content.....	82
Table 6. Analysis of Variance (ANOVA) table of reference nitrogen content	84

LIST OF FIGURES

Figure 1. Electromagnetic spectrum	40
Figure 2. Predicted SPAD measurements in sorghum plants under six different nitrogen treatments: 0, 5, 10, 15, 20, and 40 mM ammonium nitrate	44
Figure 3. Camera and lighting system inside the imaging tower.....	46
Figure 4. Entrance to imaging tower.....	46
Figure 5. Schematic of the automated greenhouse conveyor belt system	47
Figure 6. Working conveyor belt system.....	47
Figure 7. Reference RWC by Treatment	51
Figure 8. Reference nitrogen content by treatment.....	53
Figure 9. Interaction plot of reference nitrogen content by genotype for the four N treatments	54
Figure 10. Plot of reference RWC compared to cross-validated predicted RWC using the model based on the response of all three genotypes	55
Figure 11. Plot of reference RWC compared to cross-validated predicted RWC of all three genotypes using the model based on the response of B35	56
Figure 12. Plot of reference RWC compared to cross-validated predicted RWC of all three genotypes using the model based on the response of Tx7000	56
Figure 13. Plot of reference RWC compared to cross-validated predicted RWC of all three genotypes using the model based on the response of Tx623	57
Figure 14. Plot of reference RWC compared to cross-validated predicted RWC of all three genotypes using the model based on the response of all three genotypes	58
Figure 15. Plot of reference RWC compared to cross-validated predicted RWC of all three genotypes using the model based on the response of B35	59
Figure 16. Plot of reference RWC compared to cross-validated predicted RWC of all three genotypes using the model based on the response of Tx623	59
Figure 17. Plot of reference RWC compared to cross-validated predicted RWC of all three genotypes using the model based on the response of Tx7000	60

Figure 18. Heatmap of coefficients of determination of RWC models for sorghum; <code>_s_</code> represents spectral only models and <code>_sm_</code> represents spectral and morphological models.....	61
Figure 19. Plot of reference N content compared to cross-validated predicted N content using the model developed based on the response of all three genotypes	62
Figure 20. Plot of reference N content compared to cross-validated predicted N content using the model developed based on the response of B35.....	62
Figure 21. Plot of reference N content compared to cross-validated predicted N content using the model developed based on the response of Tx623.....	63
Figure 22. Plot of reference N content compared to cross-validated predicted N content using the model developed based on the response of Tx7000.....	63
Figure 23. Plot of reference N content compared to cross-validated predicted N content using the model developed based on the response of all three genotypes	64
Figure 24. Plot of reference N content compared to cross-validated predicted N content using the model developed based on the response of B35.....	65
Figure 25. Plot of reference N content compared to cross-validated predicted N content using the model developed based on the response of Tx623.....	65
Figure 26. Plot of reference N content compared to cross-validated predicted N content using the model developed based on the response of Tx7000.....	66
Figure 27. Heatmap of coefficients of determination of nitrogen content models for sorghum; <code>_s_</code> represents spectral only models and <code>_sm_</code> represents spectral and morphological models.....	67
Figure 28. Plot of reference RWC compared to cross-validated predicted RWC of all three genotypes using the model developed on the data of different water treatments but uniform nitrogen treatments.....	68
Figure 29. Plot of reference N content compared to cross-validated predicted N content of all three genotypes using the model developed on the data of different nitrogen treatments but uniform water treatments	69
Figure 30. Principal Component Analysis of all spectral and morphological features	70
Figure 31. RWC values for maize plants by treatment	82
Figure 32. Interaction plot of RWC by genotype for the four treatments.....	83

Figure 33. Graph of reference N content by treatment	84
Figure 34. Plot of cross-validated relative water content against reference relative water content for the model built with all six genotypes.....	85
Figure 35. Plot of cross-validated relative water content against reference relative water content for the model built with B73xMo17.....	86
Figure 36. Plot of cross-validated relative water content against reference relative water content for the model built with BCC03xPHP02.	86
Figure 37. Plot of cross-validated relative water content against reference relative water content for the model built with CML550xPHP02.....	87
Figure 38. Plot of cross-validated relative water content against reference relative water content for the model built with G80xPHP02.....	87
Figure 40. Plot of cross-validated relative water content against reference relative water content for the model built with P1105AM	88
Figure 39. Plot of cross-validated relative water content against reference relative water content for the model built with PHJ33xPHP02.....	88
Figure 41. Heatmap of all coefficients of determination for relative water content models; _s_ represents spectral only models and _sm_ represents spectral and morphological models.....	89
Figure 42. Plot of cross-validated nitrogen content against reference nitrogen content for the model built with all six genotypes	90
Figure 43. Plot of cross-validated nitrogen content against reference nitrogen content for the model built with B73xMo17	91
Figure 44. Plot of cross-validated nitrogen content against reference nitrogen content for the model built with BCC03xPHP02.....	91
Figure 45. Plot of cross-validated nitrogen content against reference nitrogen content for the model built with CML550xPHP02	92
Figure 46. Plot of cross-validated nitrogen content against reference nitrogen content for the model built with G80xPHP02.....	92
Figure 47. Plot of cross-validated nitrogen content against reference nitrogen content for the model built with P1105AM.....	93

Figure 48. Plot of cross-validated nitrogen content against reference nitrogen content for the model built with PHJ33xPHP02	93
Figure 49. Heatmap of all coefficients of determination of all nitrogen content models; <u>_s_</u> represents spectral only models and <u>_sm_</u> represents spectral and morphological models.....	94
Figure 50. Plot of reference RWC against cross-validated predicted RWC for a model built using the spectral and morphological features of the four PHP02 half-siblings.....	95
Figure 51. Plot of RWC against cross-validated predicted RWC of the maize multiple genotype study using the sorghum calibration RWC model	96
Figure 52. Plot of N content against cross-validated predicted N content of the maize multiple genotype study using the sorghum calibration spectral nitrogen content model.....	97
Figure 53. Plot of cross-validated relative water content against reference relative water content generated using the spectral and morphological features of the sorghum and maize data.....	98
Figure 54. Plot of cross-validated predicted relative water content against reference relative water content generated using the spectral features of the sorghum and maize data.....	99
Figure 55. Plot of cross-validated nitrogen content against reference nitrogen content generated using the spectral and morphological features of sorghum and maize.....	100
Figure 56. Plot of cross-validated nitrogen content against reference nitrogen content generated using the spectral features of sorghum and maize.....	100
Figure 57. Principal Component Analysis of all spectral and morphological features	101

ABSTRACT

Author: Cross, Valerie, A. MS

Institution: Purdue University

Degree Received: August 2018

Title: Hyperspectral Modeling of Relative Water Content and Nitrogen Content in Sorghum and Maize.

Major Professor: Mitch Tuinstra

Sorghum and maize are two of the most important cereal grains worldwide. They are important industrially, and also serve as staple crops for millions of people across the world. With climate change, increasing frequencies of droughts, and crops being planted on more marginal land, it is important to breed sorghum and maize cultivars that are tolerant to drought and low fertility soils. However, one of the largest constraints to the breeding process is the cycle time between cultivar development and release. Early evaluation of cultivars with increased the ability to maintain water status under drought and increases nitrogen contents under nitrogen stress could be the key to decreasing breeding cycle time. New tools for non-destructive, high throughput phenotyping are needed to evaluate new cultivars. These new tools can also be used for monitoring and management of crops to improve productivity.

Hyperspectral imaging holds promise as one tool to improve the speed and accuracy of predicting numerous plant traits including abiotic stress tolerance characteristics. In this thesis, hyperspectral imaging projects were designed to develop and test prediction models for relative water content (RWC) and nitrogen (N) content of sorghum and maize. The first study utilized three different genotypes of sorghum in an automated hyperspectral imaging system in greenhouses at Purdue University. From this study, models were developed for relative water content and nitrogen content using the data from all three genotypes collectively as well as the data from each genotype individually. Models developed using the spectral and morphological features

obtained from the hyperspectral images are predictive of both relative water content and nitrogen content. The coefficients of determination (R^2) for all graphs comparing the predicted relative water content to the reference relative water content of sorghum averaged 0.90 while the same graphs for maize averaged 0.64. The coefficients of determination for all graphs comparing the predicted nitrogen content to the reference nitrogen content of sorghum averaged 0.85 while the same graphs for maize averaged 0.61. Models built only with the spectral features for sorghum were also predictive of both relative water content and nitrogen content. The coefficients of determination for all graphs comparing the predicted relative water content to the reference relative water content of sorghum averaged 0.91 while the same graphs for nitrogen content in sorghum averaged 0.85.

The nitrogen content models developed using the data from the Tx7000 genotype are highly predictive of both Tx7000 and B35 but not highly predictive of Tx623. However, models developed using the data from Tx623 are highly predictive of all three genotypes. Another important finding from this study was that the water and nitrogen signals overlap and the most predictive models are developed from data where water and nitrogen vary continuously. Models to predict one factor that do not account for variation in the other factor are not very accurate.

The second experiment utilized hyperspectral imaging to characterize RWC and N content of maize. Models for RWC and N content were developed using spectral and morphological features. The models developed for maize were not as predictive as the models for sorghum but they were still predictive of RWC and N content for the models developed using all six genotypes and the models developed using the data from the individual genotypes. Models built using the four half-sibling genotypes were not more predictive than the models based on all six genotypes.

The final portion of this thesis explored predictions across species using both the sorghum and maize data. We found that models developed using only sorghum were not predictive of the maize reference measurements. However, when the sorghum and maize data were combined and used to generate models, both the RWC model and the N content model were highly predictive for both reference measurements.

CHAPTER 1: LITERATURE REVIEW

1.1 *Sorghum bicolor* (L.) Moench

1.1.2 Description

Sorghum bicolor is a C₄, annual or short-term perennial grass that was domesticated in Ethiopia and Southern Sudan around 3000 years ago (Dial, 2012). Sorghum is an upright plant with flat leaf blades, rigid stems, and a panicle located at the apex of the plant. In 1972, Harlan and de Wet categorized sorghum into 5 basic races based on the conformation of the spikelets. These five races were bicolor, guinea, caudatum, kafir, and durra. Ten races that are hybrids of the five basic races were also categorized. Depending on the race, the panicle may be more loose or tight, the panicle may droop, and the glumes may vary in color.

Sorghum performs well on fertile, well-drained soils of pH 6.0-6.5 (Dial, 2012). General management practices for standard biomass production, especially in developed countries, include the addition of 75-100 pounds of nitrogen per acre (84-112 kilograms of nitrogen per hectare). Sorghum can also perform well in less than ideal conditions. It is adapted to grow on low fertility, moderately acidic, highly alkaline, and higher salinity soils. Its water requirements are less than maize at 400-750 mm annually (“Sorghum bicolor”, n.d.). When drought stress occurs, sorghum can become dormant. Early season severe drought stress will stop the growth and floral initiation of the plant which it then resumes at the onset of more favorable conditions. Late season drought stress stops the vegetative growth but the plant continues floral initiation to complete its lifecycle. Most sorghum requires 90-120 days for full grain maturation and will not tolerate frost, shade, or prolonged flooding.

Many plants, including sorghum, produce hydrogen cyanide (HCN) when damaged (Mithofer & Boland, 2012). These plants store these toxins as inactive conjugates, mainly as cyanogenic glycosides. Cyanogenic glycosides are stored in the vacuole of the cell, and the glycosidase, which activates the production of HCN, is present in the cytoplasm. When herbivorous animals, or damage of any kind, severs the barrier between these two compounds, toxic HCN is produced. This confers the plant defense against grazing animals, insects, and some pathogens. The cyanogenic glycoside present specifically in sorghum is β -D-glucopyranosyloxy-(S)-hydroxymandelonitrile, also known as dhurrin (Halkier & Moller, 1989). Dhurrin is derived from L-tyrosine in a sorghum specific process. Cyanogenic glucosides are dangerous to humans, as is the case in cassava, however, dhurrin is lacking in the seed.

Sorghum is the fifth most grown cereal crop in the world after rice, wheat, maize, and barley and has spread to become a highly important crop in Africa, India, Southeast Asia, Australia, and the United States (“Sorghum bicolor”, n.d.). It came to the United States in the 1850’s for syrup production (Dial, 2012). It is gluten free and a good substitute for people with Celiac Disease.

In the developed world, it is used mostly for livestock feed, wall boards, packing material, and other industrial uses. More notable uses of sorghum are to prevent soil compaction and manage weeds. In the developing world, sorghum is the main food source for 500 million people (“The Importance of Sorghum”, 2010). Most of these people reside in India and Africa. In Africa, it is the second most important grain after maize, and 60 million tons of sorghum are produced on the continent annually, which accounts for a third of the world production. Sorghum is adapted to the semiarid and arid regions of Africa, and the meal is cheaper and more accessible to rural and poor people. It is used to make semi-leavened bread, couscous, dumplings, porridge, and beer.

1.1.3 Sorghum Populations

Improvement in domesticated crops relies on the diversity of the crops germplasm. Unfortunately domesticated crops often undergo bottlenecks that have narrowed the genetic variation (Tanksley & McCouch, 1997). Early farmers domesticated crops based on desirable mutations, such as nonshattering seed, compact growth habits, and loss of germination inhibition. As selective breeding for these traits continued, the genetic variation would naturally narrow. Modern plant breeding has also been a detriment to genetic variation of crops even though the improvement of crops stems directly from the discovery of novel genes. Most modern cultivars are developed from crosses between highly related lines with little new germplasm introduced. In the 1960s, scientists recognized that sorghum bottlenecks due to breeding practices was severely limiting the breeders' ability to produce new, more productive cultivars in North America (Quinby, 1974). Sorghum lines from the tropics that possess genes that could be important in yield, insect and disease resistance, and food quality of US sorghum lines were difficult to manage in long-day environments (Stephens et al., 1967).

The Sorghum Conversion Project (SCP) was started as a joint venture between Texas A&M and the USDA (Quinby, 1974). This program sought to expand the genetic diversity of sorghum using elite tropical germplasm that had been converted into photo-period insensitive, short stature plants. This process begins with crossing elite photo-period sensitive plants to dwarf temperate zone varieties. The F1 population is grown in the tropics while the F2 seed is then grown out in a temperate location. From that population, short-statured, early maturing plants are selected. This seed is transported back to the tropics to be back-crossed to the tropical variety. The back-crossing is repeated for three or four generations until the plants appear very similar to the tropical varieties;

however, they are photoperiod insensitive and are shorter in stature. At the completion of the SCP, the diverse, tropical germplasm can be easily used in breeding programs in the temperate regions of the world.

Sorghum exhibits distinctive patterns of tolerance to drought stress conditions: drought susceptible, pre-flowering drought tolerance, and post-flowering drought tolerance. Tx623 was used as the reference genome for sorghum and is generally considered to be drought susceptible (Paterson et al. 2009). Tx7000, also known as Caprock, is an example of a variety with pre-flowering drought tolerance (Karper, 1949). Caprock was first developed in 1949 and through the years categorized as a non-stay-green sorghum line (Walulu et al., 1994) with pre-flowering drought stress tolerance (Kebede et al., 2001). B35, later released as Tx642, exhibits very good post-flowering drought tolerance commonly noted as stay-green (Walulu et al., 1994; Tuinstra et al., 1996).

1.2 *Zea Mays*

1.2.1 Description

Zea mays is an annual, C4 grass that was domesticated around 10,000 years ago in central Mexico from the progenitor teosinte (Galinat, 1971). Maize is a tall stout grass with an erect and solid stem and alternate leaves (Corn: plant, 2018). The species is also monoecious which means it develops separate male and female flowers on the same plant. The staminate flowers are born on the terminus of the stem on the tassel and produce the pollen. The pistillate flowers, the shoots, are born on the stem about halfway up the stem and consist of spikes with paired spikelets in rows that are attached to silks. The silks are pollinated by the pollen from the tassel and develop into the mature ears. Maize is generally commercially classified as dent corn, flint corn, sweet corn, or popcorn.

Maize is considered a short-day or day neutral plant (Maize, FAO, 2018). The crop is grown from temperate to tropical environments where the mean daily temperatures are above 15°C and free of frost. In temperate regions, day neutral plants are grown while short-day plants are produced in the tropics. Depending of the varieties and the latitude grown, maize can mature in 80-300 days. Maize produces best on well-aerated and well-drained soils but does well on most soils except for very heavy dense clay soils or very sandy soils. The crop is fairly sensitive to abiotic stresses including salinity and waterlogging. The fertility demands for maize are relatively high. Most maize varieties are not well adapted to low fertility soils but can generally tolerate hotter and drier conditions.

Maize is the most important crop in the world and is used widely for livestock feed, human food, biofuels, and industrial applications (Maize, FAO 2018). While maize is a major food source in many parts of the world, it does not have as much nutritional value as many of the other grains (Corn: plant, 2018). The protein in the grain has poor quality and the grain is deficient in niacin, which can lead to niacin deficiency, also known as the disease pellagra. Maize is used to make many food products including masa dough for tortillas and tamales, roasted or creamed corn, hominy, grits, cornbreads, popcorn, confections, couscous, porridge, and alcohols.

Industrial applications for maize include ethanol, starch, and oil (Corn: plant, 2018). Ethanol is a first generation liquid biofuel that is typically mixed at 10% with gasoline. Starch extracted from maize grain is widely used to produce corn syrups, an inexpensive sweetener, paper and wallboards, and industrial solvents.

1.2.2 Maize Populations

After maize was domesticated in the Balsas River valley of western Mexico, there is evidence of its migration throughout North and South America (Bedoya et al., 2017). Maize

diversified into a number of landraces that are genetically and phenotypically unique from each other. Bedoya et al. (2017) identified three main groups of maize germplasm in the new world. The first group is called the Mexico and Southern Andes group. This group was characterized by the exchange of germplasm between North and South America, both in the Pre-Columbian era and the modern era. The Mesoamerican group includes the Caribbean landraces of maize. The Andean group includes the races introduced to the Andes with little or no germplasm mixing since introduction. These landraces were maintained and slowly improved over thousands of years up until the advent of hybrid technology in maize. A separate study, Heerwaarden et al. (2012), categorized maize differently as a large and diverse group of temperate maize accessions in four different groups, landraces from pre-1930s, early inbreds from the 1930s to 1950s, advanced public inbred lines from the 1950s to the 1980s, and elite commercial inbred lines from the 1980s to now (Heerwaarden et al., 2012).

Heterosis, or hybrid vigor, was first discovered in maize in the first half of the 20th century (Meena et al., 2017). Heterosis results from the cross of two inbred lines exhibited as high vigor, growth, and yield. Heterosis is generally the greatest between heterotic groups or groups of germplasm that have similar combining ability and heterotic response when crossed with another heterotic group. The most common heterotic groups are the Iowa Stiff Stalk Synthetic and Lancaster Sure Crop. One of the most notable combinations between these two heterotic groups is B73xMo17 (Hoegemeyer, 2014). Landmark B73 hybrids, including B73xMo17, dominated the market for 5 to 7 years after 1973 when B73 was developed at the Iowa Agricultural Experiment Station at Iowa State University (“Accession: PI 550473”, USDA GRIN, n.d.). Mo17, from the non-stiff stalk heterotic group, was developed around eight years earlier than B73 at the University of Missouri (“Accession: PI 558532”, USDA GRIN, n.d.).

In the next four decades, various public and private institutions have developed a number of lines out of these two main heterotic groups used for breeding in the United States. Several such lines were developed by Pioneer Hi-bred International out of the Iowa stiff stalk heterotic group including PHG80 and PHJ33 (“Accession: PI 601037”, USDA GRIN, n.d.; “Accession: PI 601774”, USDA GRIN, n.d.). Another line developed by Pioneer is the PHP02 line out of the non-stiff stalk heterotic group (“Accession: PI 601570”, USDA GRIN, n.d.). Pioneer has also developed a series of hybrids that are considered more drought tolerant, the AquaMax lines, one of which is P1105AM (“2018 Corn Hybrid-Herbicide Management Guide”, 2018). Many other, smaller companies have also contributed to the maize germplasm in the past including Northrup, King and Company which produced an inbred called BCC03 (“Accession: PI 544065”, USDA GRIN, n.d.).

Public institutions are also generating new inbred lines. CML550 is a CIMMYT maize line released in 2013 (“CIMMYT releases 22 new maize inbred lines for the tropics and subtropics”, 2013). This line is an intermediate maturity line and is characterized as a CIMMYT heterotic group B and has good yield per se and is often used as a female parent in much the same way as the Iowa stiff stalk inbreds are used. It is considered to have very good adaptation to low nitrogen and low water conditions. Previous studies in the Tuinstra lab have determined that G80xPHP02 is drought susceptible under field conditions in Arizona, USA.

1.3 Drought

1.3.1 Causes and Results of Drought

Wladimir Koppen developed a system to classify climates in the early 1900s that is still the most widely used climate classification system (Peel et al., 2007). Climates are divided into five general categories: A, B, C, D, and E. These five categories are further broken down based

on temperature or precipitation. While four of the categories are defined by temperature, category B is defined by precipitation. Namely, by very low precipitation as it represents the semi-arid and arid regions of the world. Arid and semi-arid regions of the world are the dominant climate class and account for 30.2% of land area. These regions of the world have expanded 7% since the 1940s (Huang et al., 2016). In the Americas and west/central Australia, arid regions have generally become wetter. In the eastern hemisphere, the semi-arid regions have increased due to humid and sub-humid areas becoming dryer. This expansion of semi-arid regions has the potential to bring more semi-arid land under cultivation.

There are three classifications of drought (Dai, 2011). Meteorological drought is a period of months to years with below normal precipitation. It usually includes above normal temperatures, is caused by persistent atmospheric anomalies, and causes other types of drought. Agricultural drought is a period of dry soils that results from below average precipitation (meteorological drought), intense but less frequent rainfalls, and/or above average evaporation that results in lower crop production. Hydrological drought occurs when river streamflow and water storages in aquifers, lakes, or reservoirs fall below long term mean levels. Meteorological drought often is the cause of agricultural and hydrological drought but other factors, such as erosion and poor land management, can increase the severity and duration of drought. The major measure of drought is the Palmer Drought Severity Index (PDSI) developed in 1965 (Palmer, 1965). It models the overall difference between the moisture supply and the moisture demand at the earth's surface. It is a rather simple index that requires only the precipitation and the potential evapotranspiration as inputs.

While lack of precipitation is generally associated with drought, changes in precipitation are not the only causes of drought (Zhao & Dai, 2015). Increases in potential evapotranspiration,

decreases in precipitation frequency, and increases on the number of dry days could also cause or worsen drought. A study by Dao and Zhai (2015) evaluated a model based on the traditional PDSI and other key indices such as runoff and soil moisture. This model indicated that while precipitation may go up in the next decades, precipitation frequency will decrease and number of dry days will increase, and it also predicts that the more intense rainfall events that occur during this time will lead to more runoff and thus lower soil moisture. The predicted outcome of this model is that the frequency of future moderate to severe drought will increase over the Americas, Europe, southern Africa, and Australia.

The atmospheric influences on drought depend greatly on the region of the world (Schubert et al., 2016). El Nino-Southern Oscillation (ENSO) is a Pacific Ocean tropical Sea Surface Temperature (SST) anomaly that affects the precipitation of many regions of the world including the Americas, eastern and southwest Asia, Australia, and the maritime region. Other oceans' SST anomalies affected various parts of the world as well. The Indian Ocean affects precipitation in Australia and East Asia. The Atlantic Ocean affects northern South America, parts of the southern and eastern US, and the Sahel in Africa. The Mediterranean Sea can affect southern Europe and northern Africa. ENSO also affects the Asian-Australian monsoon system. This oscillation and a warming trend over the central eastern Pacific and the western Indian Oceans has weakened the monsoon system since the 1950s. Several regions of the world, including central Canada, northern Eurasia, and central Europe are little affected by SSTs. In northern Eurasia, drought is linked to the development of anticyclones while in the central Europe a number of factors seem to cause drought. In eastern Africa, drought is very hard to understand because of the heterogeneous local rainfalls.

A lack of water from drought can lead to plant related results of drought stress including effects in crop growth and yield, photosynthesis, and oxidative damage. Before crops even emerge, drought can cause poor germination and decreased stand counts (Fathi and Tari, 2016). Cell growth is also inhibited by drought stress. Cell elongation can be limited under water stress because of the interruption of water flow through the xylem due to the loss in turgor pressure (Nonami 1998). The development of seed on the plant is affected differently by drought stress depending on the stage of development of the crop. Drought stress before flowering in triticale reduced the time to anthesis (Estrada-Campuzano et al., 2008) while pre-flowering water stress in maize reduced the yield by delaying silking which increased the anthesis-to-silking interval which is highly negatively coordinated with grain yield (Cattivelli et al., 2008). Drought stress during flowering can result in barrenness (Yadav et al., 2004), kernel abortion in maize (Otegui et al., 1995), and reduce seed yield in crops such as in pigeon pea (Nam et al., 2001). And finally, drought stress after flowering can lead to shortened grain filling period in triticale (Estrada-Campuzano et al., 2008) and diminished grain set and kernel growth in wheat (Morgan, 1990). Farooq et al. (2009) recently reviewed the impacts of drought in agriculture and summarized drought stress effects on growth and development in that it hampers flower development and grain production that ultimately leads to smaller and fewer grains (Farooq et al., 2009).

Drought stress also reduces photosynthesis in a variety of ways. This effect is caused by the decrease of leaf expansion, impaired photosynthetic machinery, and early leaf senescence (Wahid and Rasul, 2004). Drought stress in plants causes the stomata to close due to water losses but this also limits CO₂ uptake which decreases carbon fixation and could lead to photo-damage (Cornic and Massacci, 1996). The photosynthetic machinery is also damaged by drought stress. This includes changes in photosynthetic pigments and components such as a decrease in maximum

velocity of ribulose-1,5-biphosphate carboxylation by Rubisco, speed of ribulose-1,5-biphosphate regeneration, Rubisco and stromal fructose activities, and the quantum efficiency of photosystem II (Reddy et al., 2004). Drought stress can also lead to oxidative damage to plants. The production of reactive oxygen species (ROS) has a linear correlation to the severity of drought stress (Farooq et al., 2008). ROS can induce peroxidation of membrane lipids, degradation of nucleic acids, and degradation of both structural and functional proteins targeting chloroplasts, mitochondria, and peroxisomes.

1.3.2 Drought and Agriculture

Water is the greatest constraint in many agricultural system (Harrison et al., 2014; Shao et al., 2009; Jamieson et al., 1995). Agriculture in semi-arid regions is often defined by low and uncertain rainfall and poor quality soils (Rao, 2008). Both of these factors affect the quantity and value of agricultural output which must feed 400 million people living on and surviving off these marginal lands (Borlaug & Dowsell, n.d.). The rapid expansions of populations and the subsequent demand for increased food production has pushed many farmers onto more marginal lands. This demand for immediate food has also led to less fallow time and more continuous cropping systems, which decrease soil fertility and, thus, decrease future yields. To add to these problems, the ecosystems of semi-arid regions are very fragile (Charney, 1975; Huang et al., 2010; Rotenberg & Yakir, 2010; Xue et al., 1997; Zeng et al., 1999). These regions are highly sensitive to human activities which can lead directly to climate change, and most of these activities stem from the agricultural exploitation of the land without proper land management.

Early season drought decreases germination and stand establishment of crops (Farooq et al., 2012). This is due to a lack of water during the imbibition phase of germination, a reduced energy supply, and impaired enzyme activity. Impaired enzyme activity and reduced energy

supply, along with loss of turgor, also inhibits growth through cell division and cell elongation which leads to reduced dry matter accumulation in virtually every plant organ. Drought also affects the growth cycle duration and can lead to early or delayed flowering depending on the crop species. If the drought occurs in the vegetative stage of growth, the yield decreases; however, if drought occurs during flowering or grain fill, the results are very often disastrous. Drought also decreases relative water content, leaf water potential, and osmotic potential in roots, shoots, and leaves. In the attempt to conserve water, leaves often transpire less. This can lead to damaging temperature increases in the leaves due to a lack of evaporative cooling.

1.3.3 Adaptations to Drought

There are a number of mechanisms that plants utilize to deal with drought. Among the most common are developmental techniques that plants utilize in water-limited environments. One of these techniques is drought escape (Araus et al., 2002). This refers to a plant having a shortened or modified life cycle in order to escape any effects of the water stress. This allows the plant to reproduce before the onset of the drought through modifications to flowering time and length of the life cycle. Another technique is through drought avoidance (Turner et al., 2001). Avoidance refers to the plant avoiding drought stress through morphological mechanisms such as stomatal control of transpiration or through an extensive root system for water uptake. Stomatal regulation in maize is a well-researched phenomenon. Maize *viviparous14* encodes a step in the synthesis of abscisic acid which regulates stomatal opening and closing (Ribaut et al., 2009). Maize is considered an “isohydric” species which means the plants are very sensitive to lower water potentials so it limits water loss at the earlier stages of water deficit so water content can be maintained in later stages of drought. A final mechanism for drought tolerance is phenotypic

flexibility. Some plants reduce leaf area for water loss by producing smaller leaves or by shedding leaves (Farooq et al., 2009).

Plants also utilize several physiological mechanisms, such as osmotic adjustment, and molecular mechanisms, such as stress proteins. Osmotic adjustment is characterized by the accumulation of solutes in the cell (Inada et al., 1992). This accumulation of solutes retains water in the cell through the principle of osmosis during times of low water potential. In times of low water potential, osmotic adjustment can stabilize various macromolecular structures. Plants also produce stress proteins under times of drought (Wahid et al., 2007). These stress proteins are soluble in water which means the proteins contribute to stress tolerance by hydration of cellular structures.

In maize, Monneveux et al. (2005) evaluated the drought tolerance progress in several tropical maize populations under recurrent rounds of selection under drought. The study found that yield increases, the measure of progress in maize drought tolerance, was more associated with improved partitioning of assimilates rather than an improvement of other physiological or molecular improvements. This study found that there were increases in the number of ears per plant and grains per ear and decreases in the abortion rates and the anthesis-to-silking interval. This improvement also resulted in an increase of ear dry weight and harvest index at the cost of tassel and stem dry weights.

Sorghum genotypes have some unique tolerances to drought. Sorghum germplasms exhibit variation in two different forms of drought tolerance. The first type is pre-flowering drought resistance which, as the name suggests, is expressed when plants are exposed to drought conditions prior to flowering. Susceptibility to pre-flowering stress is manifested as leaf rolling, uncharacteristic leaf erectness, leaf bleaching, leaf tip and margin burn, delayed flowering, saddle

effect, reduced panicle exertion, floret abortion, and small panicle size. The other type is post-flowering drought tolerance that is expressed during grain development. Susceptibility to post-flowering drought is manifested as premature plant death, stalk lodging, stalk rot, and reduction in seed size. Very few genotypes exhibit high levels of pre-flowering and post-flowering drought tolerance.

Stay-green is a post-flowering drought adaptation in sorghum (Borrell et al., 2014). There are four major quantitative trait loci (QTL) for stay-green: Stg 1, Stg 2, Stg 3, and Stg 4 (Xu et al., 2000). The stay-green trait is expressed as delayed leaf and stalk senescence during grain fill in sorghum, hence the name, stay-green. This delayed leaf senescence is largely due to the more efficient balance between the supply and demand for water in these plants. These traits can reduce the transpiration per unit leaf area through changes in stomatal density, stomatal aperture, and timing of stomatal opening which in turn reduces the water demand (Borrell et al., 2014). The supply of water available can be modified by altering tillering patterns (van Oosterom et al., 2011), leaf number per culm, and individual leaf size (Borrell et al., 2000).

Borrell et al. (2014) revealed some very specific physiological effects of the stg QTL on stay-green sorghum lines. They found that the stg loci increased grain yield under drought stressed conditions and only minimally cost yield under well-watered conditions. The increased grain yield was connected to reduced canopy size at flowering which was a direct result of reduced tillering and smaller upper leaves under drought stress which allowed for greater grain fill even under stress. This decrease in canopy size shifted a significant amount of water use from pre-flowering (water goes to the canopy) to post-flowering (water used for grain fill). The stg loci may also reduce the transpiration per unit leaf area in the remaining canopy according to this study. While not

conclusive, there was evidence that the *stg* genes also modify the root architecture and water extraction patterns of drought stressed sorghum to better utilize soil water.

There have been several studies of the differences in drought tolerance between maize and sorghum. Analyses of sweet sorghum and maize performance under well-watered and drought conditions showed that sweet sorghum performed better under drought stress (Zegada-Lizarazu et al., 2012). The ratio of plant height under drought and well-watered conditions shows that sorghum plants maintained height more than maize throughout the growing season. This indicates that the stem elongation and growth rates were less affected by drought in sweet sorghum. Sweet sorghum also significantly reduced its LAI compared to maize under drought stress to moderate water use. While this could equate to a reduction in the available photosynthate, it also means a reduction in transpiration. Sweet sorghum also maintained physiological activity, including rates of photosynthesis, transpiration, stomatal conductance, and leaf water potential, under drought stress while the physiological activity of maize was hampered. Sweet sorghum had higher water use efficiency (WUE) at the end of the season as opposed to maize because of an end of season rise in the WUE in the drought stressed plants. This indicates that sorghum has the ability to increase its WUE in response to drought while maize under drought stress has a much more limited ability to improve its WUE. Maize also had decreased performance from photosystem II because of the inability to absorb light and dissipate energy.

Aboveground biomass and root mass were reported to be important components differentiating drought tolerance of maize and sweet sorghum. Drought stressed sweet sorghum produced 90% of the biomass produced under well-watered conditions while maize under drought stress only produced around 40% of the biomass of its well-watered counterpart at the beginning of the growing season (Zegada-Lizarazu et al., 2012). By the end of the growing season, the

drought stressed sorghum had a 38% reduction in biomass while the maize had a 47% reduction in biomass as compared to their respective well-watered counterparts. The sweet sorghum also developed a larger and more evenly distributed root system that penetrated deeper into the soil profile as compared to maize. In another study, the above ground dry weight of the sweet sorghum and the maize showed almost no difference under well-watered conditions; however, the aboveground dry weight of sweet sorghum was significantly more than that of maize under drought conditions (Schittenhelm & Schroetter, 2014). Sweet sorghum also exhibited greater rooting in the subsoil than maize and penetrated more extensively into the deeper soil horizons. Sweet sorghum also had higher root length densities than maize under low water conditions. These studies helped solidify sorghum's higher drought tolerance in comparison to maize.

1.3.4 Measuring Water

Relative water content (RWC) can be easily measured by harvesting plant leaf samples and immediately weighing them to obtain the fresh weight (FW) (Turner, 1981). The leaf material can then be floated on water until it becomes completely turgid to obtain the turgid weight (TW). These samples can be dried to obtain the dry weight (DW). These values can be plugged into the equation $RWC = [(FW - DW) / (TW - DW)] * 100$ to obtain the relative water content of a plant. While this measure is very accurate and straightforward, it is destructive and very time and labor intensive over a large number of plants. Non-destructive, machine-based methods are being developed to overcome these challenges.

Terahertz time-domain spectroscopy has been used to develop an algorithm that could accurately predict the relative volumetric fraction of water in plant tissues (Gente et al., 2013). Terahertz time-domain spectroscopy measures the transmission of light through the plant that

changes based on the water content of the leaves. This algorithm requires the species specific dielectric functions (that are impacted by air space, water space, and solid tissue space of the leaf).

Remote thermal sensing has also been used to study plant water relations of soybean leaves (Swain et al., 2012). Thermal imaging registers the temperature of leaves and varies based on changes in rates of transpiration. Transpiration rate can be roughly correlated with the water content present in leaves. This type of remote sensing could be advantageous in some situation because it is not limited by leaf area index like many of the reflectance indices.

Radar has also been used to estimate water content (Ulaby & Bush, 1976). While most of the remote sensing techniques are limited by weather conditions, radar is not. Synthetic aperture radar is an all-weather solution that has been explored in the past but never widely adopted. Ulaby and Bush (1976) studied the backscattering coefficient of the radar and how it related to water content. They found a linear correlation between higher backscatter on the radar and lower water content of a plant. This could possibly be the result of a slight decrease in canopy size because of water loss allowing the radar to “see” more of the underlying soil which causes more backscatter.

Remote sensing of shortwave infrared (over 1500 to 1700 nm) and near infrared (around 820 nm) light reflectance was able to accurately predict Equivalent Water Thickness (EWT) (Ceccato et al., 2001). EWT is the ratio between the quantity of water and the area of the leaf. It corresponds to a hypothetical thickness of a single layer of water spread evenly over the whole leaf area and is another measure of the water content in plants. Remote sensing can detect the changes in the reflectance of a plant surface based on how dehydrated the plant is.

1.4 Nitrogen

1.4.1 Causes and Results of Nitrogen Deficiencies

Nitrogen content of plants can be impacted by several factors. The first is a lack of nitrogen in the soil. There are many inputs into the soil and losses from the soil system during to nitrogen cycle (Lamb et al., 2014). The inputs of nitrogen into the system includes atmospheric fixation, industrial fixation, soil organic matter, crop residues, and animal manures. Leguminous crops can contribute to soil nitrogen inputs because they contain nitrogen in high levels. Nitrogen from soil organic matter is composed mainly of a stable material called humus that has accumulated over long periods of time. Many parts of the world do not have the advantage of historic plant organic matter, such as in semi-arid and arid regions, and this could lead to nitrogen deficiency in the soil.

Industrial fixation refers to the production of industrial fertilizers (Lamb et al., 2014). Many parts of the developed world use fertilizers to overcome nutrient depletion. Industrial fertilizers are made by combining atmospheric nitrogen (N_2) with hydrogen (H_2) to form ammonia (NH_3). Anhydrous ammonia can be used to manufacture other commercial fertilizers. While commercial fertilizers are the most common way to deal with nitrogen deficiency, commercial fertilizers are not equally available to all farmers across the world (Sanchez, 2002). In Africa, commercial fertilizers are usually two to six times more expensive than in Europe, North America, or Asia.

The final nitrogen input into the soil is through the atmosphere (Lamb et al., 2014). There are two ways in which this happens: biological fixation and precipitation deposition. The nitrogen in the atmosphere is generally unavailable to plants even though there is an abundance in the atmosphere. However, legumes form a symbiotic relationship with different strains of *Rhizobium* bacteria that inhabit nodules on the roots of the legumes. These *Rhizobium* bacteria are able to fix

nitrogen from the atmosphere. The legumes use this nitrogen and the bacteria have shelter and carbohydrates. The addition of nitrogen to the soil through symbiotic nitrogen fixation is substantial. Non-symbiotic nitrogen fixers also exist in the soil, however, the nitrogen added to the soil via these organisms is negligible. Additionally, very small amounts of nitrogen are also deposited into the soil through precipitation.

Nitrogen is lost from the soil in a variety of ways. One of those ways is through leaching (Lamb et al., 2014). Leaching refers to the loss of nitrate from the soil via the nitrogen traveling with excess water down through the soil profile below the root zone. Excess water can be added through excess rainfall or excess irrigation. Soils that have a low water holding capacity, such as coarser, sandier soils, also leach nitrogen more than finer, siltier soils. Nitrogen can also be lost through soil erosion and runoff. This is another process that can result from poor management of soils and can lead to ground surface contamination problems.

The processes of denitrification and volatilization also result in the loss of nitrogen from soils (Lamb et al., 2014). Denitrification can occur when soils are warm and highly saturated for several days. In this process, bacteria convert nitrate back in to nitrogen gas which is released in to the atmosphere. The other process, volatilization can occur when nitrogen sources are applied at the surface level. In this process, these nitrogen sources volatilize and turn to ammonia gas which is lost to the atmosphere.

Finally, the majority of nitrogen is lost from the soil system through crop removal (Lamb et al., 2014). This is the process by which crops remove the nitrogen from the soil and store it in the seeds. When that crop is harvested, the nitrogen leaves the system. In developing parts of the world, such as much of Africa, soil fertility is becoming a large problem because small scale farmers have removed large quantities of nitrogen from the soil but have not replaced the nutrient

with any additional nitrogen sources (Sanchez, 2002). Africa has, on average, a very high depletion rate with an estimated 22 kilograms of nitrogen per hectare being removed from the early 1970s to the early 2000s and not replaced.

Whether from a lack of nitrogen input or an excess of nitrogen output, nitrogen deficiencies happen around the globe to a variety of crop species and affect plants in a variety of ways. Nitrogen deficiency leads to several visible symptoms (Tucker, 1984). When plants are nitrogen deficient from planting, the plants appear small with thin leaves, small stems, fewer lateral tillers, fewer branches, and fewer shoots. In early growth stages, the leaves are pale yellowish-green because of the lack of chlorophyll which is produced using nitrogen. As the plants get older, the nitrogen deficiency is visible in different ways. Nitrogen is a mobile nutrient in plant tissue which means that the plant will reuse nitrogen from old tissue and move it to newer tissue. This often leads to older leaves that become yellow and then brown. This older tissue might also develop red or purple coloration because of the predominance of other pigments over chlorophyll. Eventually, if there is not enough nitrogen to support the new growth, newer tissues will also turn yellow and pale. In grass species, such as in maize and sorghum, nitrogen deficiency leads to very specific symptoms. These symptoms include the tips of older leaves turning yellow and then “firing” or dying. In maize, a V-shaped pattern of dead tissue proceeds up the leaf from the tip. In sorghum, nitrogen deficiency may appear similar to potassium deficiency where the margins of the leaves begin to deteriorate.

While the visible symptoms might be the most telling sign of nitrogen deficiency, the internal results of nitrogen deficiency are what kill the plant. Much of the plant response to nitrogen deficiency is centered on photosynthetic elements. One study concluded that nitrogen deficiency leads to a breakdown of proteins in wheat chloroplasts, peroxisomes, and cytosol

(Crafts-Brandner et al., 1998). Another study concluded that the degradation of photosynthetic pigments and proteins is a typical characteristic of leaf senescence due to nitrogen deficiency (Deng et al., 2001). Ribulose-1,5-bisphosphate carboxylase/oxygenase (Rubisco) is the first enzyme that degrades in the Calvin Cycle during senescence in wheat plants and this decrease occurred within the first day of nitrogen stress. Zhao et al. (2005) determined that nitrogen deficiency decreased the leaf area, chlorophyll content, and photosynthetic rates of sorghum plants. The decreased photosynthetic rate was mainly due to the decrease in stomatal conductance and intercellular CO₂ concentration. Nitrogen deficiency ultimately resulted in lower dry matter accumulation (Zhao et al., 2005).

1.4.2 Water Stress and Nitrogen

Nitrogen deficiency as a result of drought is the largest contributor to the decrease of growth under drought stress (Heckathorn et al., 1997). Nitrogen is one of the most important macronutrients for a plant (Marschner, 1995). Organically bound nitrogen in the form of glutamine and glutamate are used to build all amino acids, amines, ureides, peptides, and proteins. Structural proteins are necessary to maintain the structure and function of the plant. Chlorophyll, another protein rich in nitrogen, is an extremely plant important protein critical for photosynthesis and plant growth. Applications of nitrogen can help increase antioxidative defense mechanisms. These are important when light is not limiting to protect the photosynthetic pigments from photooxidation and the leaves from senescence. One study found that in sorghum, severe nitrogen deficit affected the height of the sorghum plants (Zhao et al., 2005). Even moderate nitrogen deficit decreased the leaf area and dry matter accumulation in sorghum.

Plant nitrogen content decreased by almost 4% in one drought stress study (He & Dijkstra, 2014). In other studies, drought reduced plant growth by reducing nitrogen uptake, transport, and

distribution (Rouphael et al., 2012) because of a decline in soil moisture (Fierer & Schimel, 2002; Chapin, 1991; Schimel et al., 2007). Water stress can reduce plant nutrient uptake by reducing nutrient supply through mineralization (Sardens & Penuelas, 2012; Cramer et al., 2009). It can also reduce plant nutrient uptake by reducing nutrient diffusion and mass flow in the soil, and decreased leaf litter N composition by more than 50% compared to regular weather conditions (Sanaullah et al., 2012). Within the plant, nitrate reductase has decreased activity under water stress (Azedo-Silva et al., 2004), and nitrogen content in the leaves partially regulates transpiration (Cramer et al., 2009).

1.4.3 Adaptations to Nitrogen Stress

Plants adapt to low nitrogen in a variety of ways including nitrogen transport, photosynthetic elements, cell biochemistry, and morphology. In one study, low nitrogen stress revealed differentially expressed genes between nitrogen stress tolerant and sensitive sorghum genotypes (Gelli et al., 2014). Low nitrogen treatments increased the high-affinity transport system for nitrate and ammonium in all sorghum genotypes; however, the tolerant genotypes expressed the high affinity transporters much more than the sensitive genotypes. This indicates that the tolerant genotypes increased these transporters in order to uptake more nitrogen from the soil. The same study also found that tolerant genotypes increase the high affinity amino acid transporters for more efficient uptake of amino acids from the soil.

Plants also modify a number of photosynthetic elements in response to nitrogen deficiency. One of the most notable changes in the photosynthetic elements is the decrease in chlorophyll content and the drastic increase in zeaxanthin (Khamis et al., 1990). The dramatic increase in zeaxanthin is related to protection of photosystem II (PSII). This photosystem is one of the first,

and major, steps in photosynthesis. Since the light saturation point of nitrogen limited plants is reduced, PSII is more easily damaged. Nitrogen limited plants do not appear to suffer large amounts of photoinhibitory damage when exposed to high irradiance because of the protective zeaxanthin which dissipates the excitation energy. The decrease in the amount of chlorophyll is significant but the photosynthetic efficiency doesn't drop as much. The nitrogen stressed plants were much more efficient in terms of carbon assimilation per photosynthetic unit. Mu et al. (2016), showed that maize plants displayed a 54% increase in photosynthetic N-use efficiency and that the plants invested more nitrogen to sustain electron transport while the amount of chlorophyll was actively reduced to control excess electron production.

Analyses of gene expression under N sufficient and limited conditions also suggested numerous cell biochemistry adaptations that plants undergo due to nitrogen limitations (Gelli et al., 2014). First, this study shows the transcripts most abundantly expressed in sensitive genotypes include an increase in secondary metabolites such as flavonoids and anthocyanins, as well as an increase in the production of Cytochrome P450s which are related to anthocyanin production. The researchers also noticed an increase in a transcript involved in the synthesis of glycine betaine. Glycine betaine is an osmoprotectant that accumulates in the cell and has been associated with abiotic stress protection. Another important change found in sensitive genotypes were changes in the cell wall biochemistry including proteins responsible for wall assembly, remodeling during growth, development, and stress responses. One of these proteins was β -expansin which plays a key role in the cell wall expansion and in root growth and development. Gelli et al. (2014) also found that auxins and cytokinins were altered in sensitive genotypes. Under stress, several auxin response factors were more highly expressed in the sensitive genotypes as opposed to the tolerant genotypes which may have resulted in the reduced root mass noticed under nitrogen stress. Five

different kinases were similarly altered under nitrogen limitations in the sensitive genotypes which may be important in adaptation to low nitrogen stress.

The nitrogen stress tolerant genotypes accumulated a transcript for cell wall invertase-2 that was “massively increased” in the tolerant genotypes under nitrogen limitation (Gelli et al., 2014). This enzyme is related to the sucrose degradation in the cell which could promote the carbon partitioning in favor of sucrose accumulation in order to counteract some of the stress symptoms. Another transcript, SEC14 cytosolic factor, was also highly expressed in the tolerant genotypes and acts as a signal precursor that activates stress response genes that increase the stability of the membrane. Finally, the study mentions a structural constituent of ribosomes and translation elongation factors that were abundant in the low-N tolerant genotypes.

Much of the plant adaptation to low-N environments has to do with root morphological features. On a grand scale, plants tend to modify root morphology by increasing root length, root hair density, and lateral root number in low-N environments (Miller and Cramer, 2005). Gelli et al. (2014) found that tolerant sorghum genotypes produce higher root mass compared to the sensitive genotypes under nitrogen limitation (Gelli et al., 2004). In maize, Chun et al. (2005) demonstrated that shoot growth is reduced in low-N environments, but root biomass is not altered resulting in an increase in the root to shoot ratio. Maize increases the total root length per plant, elongates individual axial roots, and enhances lateral root growth all while decreasing the number of axial roots per plant. This provides an opportunity for the plant to explore the soil for nitrogen sources while not producing too much root biomass. Saengwilai et al. (2014) determined that a certain type of cell, root cortical aerenchyma (RCA), also plays key role in low-N stress tolerance. RCA expression is increased in plants under low-N stress in both the field and the greenhouse which led to reduced root respiration and reduced tissue nitrogen content. These RCA cells

resulted in a substantial increase in yield for the high-RCA producing genotypes versus the low-RCA producing genotypes under low nitrogen conditions. This study concluded that the RCA reduced root metabolic costs, permitted greater rooting depth, and enhanced nitrogen acquisition.

Leaf morphology is also modified in low-N environments. Photosynthesis is maintained by a reduction in leaf expansion which ultimately leads to lower leaf areas (Me et al., 2016). This reduction in leaf area sustains the leaf nitrogen concentrations better because there is less leaf area for the same, or lower amounts, of nitrogen under conditions in which the plant is not taking up enough nitrogen. Interestingly, the stay-green morphology in sorghum also plays a role in nitrogen stress tolerance. Studies of stay-green sorghums at ICRISAT suggested that the stay-green characteristics of some sorghum genotypes translated into higher leaf nitrogen status resulted in the ability to maintain photosynthetic capacity, produce higher yield, and resist lodging under lower nitrogen situations (Borrell et al., 1999).

1.4.4 Measuring Nitrogen

One of the earliest methods of determining the nitrogen content of organic compounds was developed in 1883 by Johan Kjeldahl (Munoz-Huerta et al., 2013). The Kjeldahl digestion method has been widely used to determine nitrogen content of food, beverages, grain, manure, waste water, soils, and plants. This method consists of three general steps. The first step is wet digestion where a concentrated acid is mixed with the sample in a Kjeldahl flask and heated until it clarifies as the CO₂ evolves. This results in an ammonium sulfate solution. The second step is to add NaOH to the ammonium sulfate and distill the solution. The addition of the NaOH turns ammonium ions into ammonia which is then passed through the condenser with heat and is trapped in a receiving solution. The ammonia concentration in the solution is proportional to the nitrogen content of the

sample. An estimate of the ammonia concentration in the solution is reached through a titration in the third general step.

Other methods for measuring the ammonia concentration in step three have also been evaluated. Clifton & Clifton (1991) used an indophenol calorimetric procedure to estimate the ammonia content using a spectrophotometer. Lee et al. (2008) used diffusion conductimetry which passed the solution through a gas-permeable membrane and carries the ammonia to a conductivity cell where the ammonia concentration is measured. This test produced more accurate results compared to titration and calorimetry methods. Pontes et al. (2009) used an ion chromatography to determine the ammonia concentration. This test was more sensitive than other methods and used no carcinogenic materials; however, the test was significantly more expensive than indophenol calorimetry. The most pressing problem with the Kjeldahl digestion is the fact that it can only measure organically bound nitrogen and not other forms of nitrogen such as nitrate and nitrite (Munoz-Huerta et al., 2013).

In the early 1900s, Jean-Baptiste Dumas developed another nitrogen content determination process based on combustion (Munoz-Huerta et al., 2013). The method he starts by heating the sample in a tin capsule to temperatures between 800 and 1000°C. The water vapor created during the combustion is removed. Then, the nitrogen oxides in the sample are reduced, turning them into N₂ gas. The other gases present with the N₂ gas are removed and the gaseous nitrogen content is measured. The Dumas procedure uses no toxic reagents and is more accurate when the sample has a substantial amount of nitrate (Watson & Galliher, 2001). The Dumas combustion method has several drawbacks. This procedure requires a very small sample size, and incomplete combustion of the sample can produce inaccurate measurements of nitrogen level (Unkovich et

al., 2008). In addition, both the Kjeldahl digestion and the Dumas combustion methods involve destructive sampling of part of the plant or the whole plant (Munoz-Huerta et al., 2013).

Optical measurements can provide non-destructive estimates of plant N content (Munoz-Huerta et al., 2013). These sensors can be categorized in a variety of ways. They can be either leaf level or canopy level. Leaf level sensors take measurements of individual leaves one at a time. Canopy level sensors take measurements of the whole canopy at once. Sensors can be passive or active sensors. Passive crop canopy sensors take their measurements using only the sunlight available while active sensors have an integrated light source. Sensors can also be categorized by the type of light they measure. Transmittance measurements are the measure of light not absorbed by the chlorophyll that instead passes through the plant (“Fluorescence vs Transmittance”, n.d.). This is obtained by putting a light source in line with the sensor with the plant in between. Fluorescence measurements are obtained by placing a light source perpendicular to the line of sight of a sensor. Fluorescence meters measure the small amounts of longer wavelengths emitted by the chlorophyll in a short amount of time after being absorbed (Tremblay et al., 2012). This light is emitted due to the plant absorbing excess light energy and having to dissipate it. And finally, reflectance is the measurement of the light that is reflected off the surface of a plant (“Reflectance and Transmittance”, 2016).

Soil plant analysis development (SPAD) meters determine the relative amount of chlorophyll in a leaf by measuring the transmittance of light through the leaf in two wavebands (600 to 700 nm and 400 to 500 nm) (Loh et al., 2002). It essentially measures the greenness of the leaf in a nondestructive way. Because chlorophyll is the greatest sink of nitrogen in the leaves, SPAD meters can be used to estimate the relative nitrogen content in leaves. SPAD meter readings and actual chlorophyll concentration are highly correlated (Xiong et al., 2015). SPAD readings

and nitrogen content are also highly correlated, but the correlation was lower than the correlation between SPAD and chlorophyll content. The relationship between SPAD readings and nitrogen content is significantly affected by environmental factors and leaf features of the specific crop.

Plant stress, such as lower or higher concentrations of nitrogen, can alter the chlorophyll fluorescence which can be read by a fluorescence sensor, such as a Multiplex sensor (Tremblay et al., 2012). The Dualex sensor is another example of a fluorescence sensor (Samborski et al., 2009). As opposed to reading the fluorescence from the chlorophyll, this sensor measures the fluorescence from the polyphenolics in the plant. Polyphenolics are secondary metabolites produced and stored in a plant during periods of stress, namely low nitrogen availability. The sensor uses chlorophyll as a photosensor that emits fluorescent light in response to the light reaching the mesophyll. The phenolics contribute to UV absorption in the leaf so the content of polyphenolics can be assessed and used as a proxy for nitrogen content. As nitrogen content increases, the concentration of polyphenolics in the cells decrease.

There are a multitude of sensors that measure the reflectance of plants (Samborski et al., 2009). The Yara N-Sensor is a passive sensor with two spectrophotometers. One spectrophotometer measures the crop light reflectance and the other permanently corrects the reflectance signal under changing levels of light. The GreenSeeker is an active sensor that emits light energy from diodes and uses a spectrophotometer to read the crop light reflectance.

More obscure and less widely used methods are also employed to determine nitrogen content of plants. The nitrogen status of a plant can be determined by evaluating the nitrate concentration of the leaf or petiole sap (“Petiole sap nitrate guidelines”, 2011). The sap is squeezed from the leaf or the petiole and evaluated with nitrate test strips. Nitrate-selective electrodes can also be used to determine nitrate concentration (Parks et al., 2012).

1.5 Hyperspectral Imaging

1.5.1 Introduction

Phenomics is the “acquisition of high-dimensional phenotypic data on an organism-wide scale” (Houle et al., 2010). Put very simply, phenomics is large scale phenotyping. The field of phenomics is used to determine ideal ecotypes for an area, evaluate a trait or series of traits of interest, and establish how a phenotype relates to a genotype. The current difficulty in agriculture’s ability to implement wide scale phenomic applications is a bottleneck in the detection and utilization of genetic variation present in crop species (Araus & Cairns, 2014). Robotic, environment controlled, fully automated phenotyping pipelines have been developed in greenhouses and growth chambers. High-throughput field phenotyping techniques are now being established.

Remote sensing has been utilized to generate agricultural data for a number of years. Remote sensing is defined as deriving data from earth’s land and water surfaces using overhead images that are produced using reflected or emitted light from some region of the electromagnetic spectrum (Campbell & Wynne, 2011). The origins of using images to gather information aerially began in World War I to gather military information. There have been a number of applications of remote sensing to agriculture over time. Remote sensing has been used to estimate both nitrogen and water contents of plants. Remote sensing has also been used to develop calendars for specific crops and specific regions, crop identification, determination of crop growth stages and harvest readiness, and determination of water content to aid irrigation schedules. Much of the remote sensing has been done using multispectral sensors that examine a few, very broad bands of the electromagnetic spectrum. Hyperspectral remote sensing is based on the evaluation of many (around 200), narrow (around 10 nm wide) bands as they reflect off the area of interest. The

objective lens collects this radiation and the collimating lens projects the radiation as a beam of parallel rays through a diffraction grating. The diffraction grating separates the radiation into distinct spectral bands. The energy contained in the specific bands is detected by linear arrays of silicon and indium antimonide. The output of the hyperspectral sensor is a relative value based on the qualities of the radiation.

Remotely sensed images are defined by spectral resolution and spatial resolution (Govender et al., 2007). Spectral resolution has to do with the number and width of the bands measured in the electromagnetic spectrum. Multispectral sensors have lower spectral resolution as compared to hyperspectral sensors because they only measure a small number of wide bands while hyperspectral sensors measure a large number of narrow bands. Spatial resolution refers to the level of detail in an image as a function of the design of the sensor. Level of detail is described as a measure of the smallest object that the sensor can measure with the smallest object being larger than a pixel.

Recent implementation of satellites with hyperspectral sensors and the decreased cost of hyperspectral sensors has allowed more access to hyperspectral data. Hyperspectral remote sensing was used to identify nonnative, invasive species (Underwood et al., 2003). This study showed a 97% accuracy in identifying whether the invasive plant, iceplant, was present in California ecosystems. In another application, the analysis of hyperspectral data collected in soybeans was used to predict the sucrose, glucose, fructose, and nitrogen content of different cultivars of soybeans (Monteiro et al., 2007).

Hyperspectral images collected on stands of wheat infected with leaf rust were used to detect leaf rust as soon as five days after inoculation when there were only very slight visible symptoms of the disease (Franke et al., 2005). In this study, the hyperspectral data was more

informative than the multispectral data due to the multispectral sensor's lower spectral sensitivity, thus it was much more susceptible to external factors such as illumination conditions. A different study mapping California marshland also compared multispectral data to hyperspectral data (Rosso et al., 2005). This study determined that multispectral data was insufficient to distinguish vegetation species in wetland environments because the divisions between species are very fine and the low spectral and spatial resolution of the multispectral sensors could not be used map the vegetation accurately.

1.5.2 Vegetation Indices

Vegetation indices are mathematical equations that use reflectance values of specific wavelengths or ranges of wavelengths and transform these reflectance values to mitigate the effects of atmosphere, solar illumination, soil background, and sensor viewing geometry to make the reflectance values more accurate (Jain et al., 2007). These transformed reflectance values are then correlated to a trait of interest such as stress detection, pigment estimation, and biophysical properties. The multiple ways to categorize vegetation indices reveals the diversity, applicability, and structure of vegetation indices.

Perhaps the broadest definition of vegetation indices divides them into two categories: broadband and narrowband (Agapiou et al., 2012). Vegetation indices are sorted into these two categories based on the wavelength characteristics used in their formula. Broadband indices use reflectance measurements from a region of the electromagnetic spectrum, such as red, near infrared, or green region. Broadband indices can be calculated using multispectral data. Narrowband indices use reflectance measurements from specific wavelengths in their equations, such as 670 nm or 800 nm. Narrowband indices can be calculated using multispectral data. Many handheld devices have been developed to calculate either broadband or narrowband indices.

Thenkabail et al. (2011) divided vegetation indices into structural, biochemical, and physiological indices. Structural indices include fractional cover, green leaf biomass, leaf area index, senesced biomass, and photosynthetically absorbed radiation. Biochemical indices measure compositional variation such as water, pigments (chlorophyll, carotenoids, and anthocyanins), protein and amino acids, and plant structural materials (lignin and cellulose). Physiological/stress indices measure the minute difference in reflectance induced by stress from changes in xanthophylls, chlorophyll content, or leaf moisture.

Jain et al. (2007) characterized vegetation indices into three categories: structural, chlorophyll and red-edge indices. Structural indices vary based on internal structures of the cell. Chlorophyll indices measure the chlorophyll content in plants as indicated by greenness and can be used to roughly determine nitrogen content in the plant. The red edge indices utilize the red-near infrared transition zone based on the strong absorption of chlorophyll in the red wavelengths and strong reflectance in the near infrared wavelengths.

Stagakis et al., (2010) divided the vegetative indices into 5 categories based on their mathematical design and intended areas of use. The first category is broadband greenness indices. They measure the chlorophyll content of the plant (aka the greenness) using broadband reflectance. Narrowband greenness predicts the same properties but use narrowband reflectance measures. Both of these can be used to measure chlorophyll content, nitrogen content, and sometimes even water content. Leaf pigment indices include both broadband and narrowband indices and measure the carotenoid or anthocyanin content of a plant. Stress indices were developed to monitor stress conditions in the plant including the water status in the canopy.

The structure and the equations used to compute these vegetation indices reveal much about intended use and applications. One of the simplest indices is the difference vegetation index. It is

simply the reflectance in the near infrared region minus the reflectance in the red region. There are simple ratios which take one number divided by another. The simple ratio is reflectance in the near infrared region divided by reflectance in the red region of the electromagnetic spectrum. Because it is a ratio, it reduces the effects of atmosphere and topography by eliminating irradiance and transmittance (Sutton, 2012). The normalized difference vegetation index (NDVI) is one of the most widely used indices (Jain et al., 2007). It was developed for use with broadband multispectral data (Jurgens, 1997). Its original equation, $(\rho_{\text{NIR}} - \rho_{\text{Red}}) / (\rho_{\text{NIR}} + \rho_{\text{Red}})$, is a classic example of a normalized equation (Sutton, 2012). Normalized equations seek to mitigate errors and variation. Many of the most important indices, such as NDVI, have been modified for application using hyperspectral data (Jurgens, 1997). NDVI was modified via experimentation to find the ideal wavelengths to give the most accurate measurements with the resulting equation $(\rho_{800} - \rho_{680}) / (\rho_{800} + \rho_{680} - 2(\rho_{445}))$. While normalized indices are efficient at reducing errors, they do not eliminate them (Sutton, 2012).

There are hundreds of vegetation indices. A few examples are explored in the following pages to demonstrate the range and breadth of the applicability of the most common vegetation indices. One study used the NDVI to generate a plot of the vegetation profiles across Africa over time to be analyzed for variations in rainfall and vegetative cover types (Townshend & Justice, 1986). Hansen and Schjoerring (2003) used NDVI generated from hyperspectral data to evaluate green biomass, leaf area index, leaf chlorophyll concentration, leaf chlorophyll density, leaf nitrogen concentration, and leaf nitrogen density of wheat in order to determine the most predictive statistical model. NDVI at the V8 stage was used to model yield and nitrogen demand for maize (Teal et al., 2006).

Another vegetation index measured is the photochemical reflectance index (PRI). This index is derived from the reflectance at 531 nanometers and 570 nanometers. This index is a good indicator of the photosynthetic radiation use efficiency which is defined as the net CO₂ assimilation rate per incident photon flux density. The PRI was used to correlate with the zeaxanthin content of barley under two different nitrogen treatments (Fillela et al., 1996). The zeaxanthin content of the plants was shown to be different under the two different nitrogen treatments and could be detected by the PRI. Only one year later, another study analyzed the zeaxanthin contents and a fluorescence-based index of photosystem II photochemical efficiency and related it back to the PRI in 20 different species of annuals, deciduous perennials, and evergreen perennials (Gamon et al., 1997).

Photochemical reflectance index can be highly correlated to water content and nitrogen content because photosynthesis is dependent on both water and nitrogen. The nitrogen reflectance index (NRI) was used in a different study for nitrogen management of maize in the field (Bausch et al., 1996). This study determined that NRI represents the plant N status of the maize plants in the field.

Several other indices including the anthocyanin reflectance index (ARI) have been used to predict to estimate plant pigments in leaves (Gitelson and Solovchenko, 2017). ARI was used to estimate the anthocyanin content of leaves which have been used to monitor plant stresses and has been correlated with the physiological status of the plant. The physiological reflectance index (PhRI) has been used to sense the de-epoxidation state of the xanthophyll cycle (Peguero-Pina et al., 2007). This measures the breakdown of a photochemical process, the xanthophyll cycle, in response to drought stress which can indicate the water status of a plant as photosynthesis is highly affected by lack of water.

The structure-insensitive pigment index (SIPI) is related to the carotenoid/chlorophyll *a* ratio (Penuelas et al., 1995). SIPI is related to the ecophysiological status of the leaf and the plant. In sunflower, physiological changes related to nitrogen and water limitations were associated with the normalized pigment chlorophyll ratio index (NCPI). NCPI was used to analyze the carotenoid/chlorophyll ratio and was inversely related to the chlorophyll content and nitrogen content of the leaves. The plant senescence reflectance index (PSRI) was developed to monitor the response of grassland species to climate change (Ren et al., 2017). The PSRI could predict precipitation based on the water content of the foliage.

1.5.3 Using Hyperspectral Data

Several recent studies have used hyperspectral imaging to predict nitrogen and water status of plants. Optimized spectral indices and partial least squares regression models were developed to predict nitrogen content of winter wheat (Li et al., 2014). This team found that the optimized spectral indices were weak predictors of canopy nitrogen content before flowering, and only NDVI and Normalized Area Over reflectance Curve (NAOC) showed consistent performance across different calibration datasets. The optimum bands determined through partial least squares regression increased the predictive power of the hyperspectral data.

Nigon et al. (2015) utilized partial least squares regression to predict nitrogen content of potatoes. Two different cultivars of potatoes were grown under five different nitrogen treatments to produce a hyperspectral imaging dataset that encompasses several genotypes and a wide range of nitrogen contents. While this study analyzed several narrowband indices, it ultimately determined that partial least squares regression produced better predictions than the indices. This is due to the sensitivity in the changes within the spectral bands that are predictive of nitrogen content, namely the red edge region. Narrowband indices cannot capture these sensitive changes

while partial least squares models do capture these changes. Nigon et al. (2015) pointed out that one of the key downsides to PLS is that one must understand the number of latent variables and how they change in response to environment.

Cotrozzi et al. (2017) related hyperspectral imagery with leaf water potentials to estimate plant water relations in the foliage in Encina oak trees. Leaf water potential was measured at predawn and midday, on different leaves under different levels of water availability. Ge et al. (2016) conducted a similar study modeling plant water relations of maize in an automated imaging system in a greenhouse at the University of Nebraska-Lincoln. The University of Nebraska-Lincoln study utilized PLS regression to predict shoot fresh and dry weights, plant area, and leaf water content. Leaf areas and shoot weights were highly correlated to hyperspectral imaging in the younger growth stages; however, as the two genotypes in this study became less phenotypically similar, these correlations weakened. Plant water content was well predicted using PLS models from the hyperspectral data for both genotypes, but the prediction was better for one genotype, B73, because it had simpler morphological structure in later growth stages.

While PLS regression shows up in literature more frequently than other modeling techniques, another common technique is machine learning. Kersting et al. (2012) developed a type of regression called Dirichlet-Aggregation Regression of phenotypes. This employs a matrix factorization approach that can impose a natural distribution of only a handful of extreme data samples across all clouds and time steps. This led to the first AI technique to detect early drought stress in barley.

Another machine learning technique is support vector machine (SVM). Moshou et al. (2012) used least square support vector machine (LSSVM) for modelling plant phenotypes. SVM builds models by assigning samples to preassigned categories based on a training set. LSSVM is

a version of SVM for regression that is developed by solving a series of linear equations as opposed to a quadratic equation as in traditional SVM. These models were used for modeling water stress and disease infection in wheat. LSSVM was used to analyze optical hyperspectral data to predict the pathogen infection and the water status of wheat plants. The LSSVM technique reportedly increased the classification performance of the model to 99%. Behmann et al. (2014) used ordinal SVM to model drought stress phenotypes in barley. This is another regression technique in SVM that works by labeling the training samples by rank which orders the different categories. Using this technique, the researchers detected drought stress in the barley plants using hyperspectral imaging before drought stress was apparent to the human eye.

Bhugra et al. (2017) used simplex volume maximization (SiVM) to model drought tolerance phenotypes in three different genotypes of wheat in India. This technique works by fitting a simplex with the maximum volume to the data. This essentially clusters different treatments together in a similar result as support vector machine. This technique resulted in the clustering of the different genotypes under different treatments indicating these models may be good for classifying cultivars.

Several studies have analyzed both nitrogen and water together using hyperspectral imaging. Pandey et al. (2017) phenotyped maize and soybean plants under different levels of nutrient stress or water stress. Macronutrients, micronutrients, and water content were all predicted using PLS regression. Water content was predicted with the highest accuracy followed by nitrogen, phosphorus, potassium, and sulfur. A similar study of nitrogen and water stresses in spinach demonstrated that hyperspectral data could be used to predict the biomass, water content, and nitrogen content (Corti et al., 2017). This study also performed partial least squares regression in order to build the prediction models but came to an interesting conclusion. Reflectance and

morphological based models for the entire plant worked best to estimate water content and biomass, but for the nitrogen content, models developed from single leaves actually predicted the nitrogen content better. This is one of the very few experiments that has evaluated nitrogen and water treatments in concert.

1.6 Conclusion

Sorghum and maize are important cereal crops around the world with diverse industrial and food-related applications and diverse responses to drought and nitrogen stresses. In the past, these crops have been studied by hyperspectral imaging, and abiotic stress phenotypes have been predicted using statistical models. However, past experiments have suffered from lack of wavelengths from the imager and from lack of genetic diversity in the crop of interest.

In the following chapters of this thesis, I will describe studies that utilize information obtained through hyperspectral imaging to predict the relative water content and the nitrogen content of sorghum and maize. The first chapter will focus on sorghum hyperspectral imaging using three genotypes of sorghum selected for variation in drought tolerance and stay-green capacity. The second chapter will focus on maize hyperspectral imaging using six genotypes of maize selected for variable drought tolerance and low-N tolerance.

CHAPTER 2: SORGHUM CALIBRATION STUDY

2.1 Introduction

Sorghum is a C4 grass that was domesticated in Ethiopia and southern Sudan about 3000 years ago (Dial, 2012). This annual or short-term perennial grass grows ideally on fertile, well-drained soil with the addition of 75-100 pounds of nitrogen per acre. However, sorghum is also well adapted to less than ideal conditions such as low water and low nitrogen. Sorghum can even go dormant in the event of early season drought stress, where the plant will halt the vegetative growth and floral initiation until better growing conditions (“Sorghum bicolor”, n.d.). Late season drought stress will halt vegetative growth but the plant will still continue floral initiation and complete its lifecycle. While this is advantageous in regions of low fertility and low water, these conditions still limit the productivity of the crop, thus it is important to breed varieties with drought stress and nitrogen stress tolerance.

There are a variety of ways to analyze the water and the nitrogen status of plants in a breeding program. However, most of these analyses are slow, labor intensive, and destructive to the plant. Remote sensing of plant water and nitrogen status could speed up the process and preserve the plants used in a breeding program. Phenomics is the intense study of the physical aspects of an organism to evaluate traits of interest and establish how phenotype relates to genotype in a species (Araus and Cairns, 2014). However, the wide range of genetic variation within crop species is considered a bottleneck to phenomics applications in agriculture. This study seeks to utilize hyperspectral imaging to predict the nitrogen and water status of sorghum by establishing a calibration model that predicts these traits in several genotypes.

Hyperspectral imaging is a type of remote sensing defined by the evaluation of many, narrow bands across the electromagnetic spectrum (Campbell & Wynne, 2011). The many bands refer to anywhere from 20 to over 500 bands across the electromagnetic spectrum from 400 nanometers up to 2500 nanometers (Fig. 1). The information is collected every 10 to 20 nanometers, which refers to the narrowness of the bands as well.

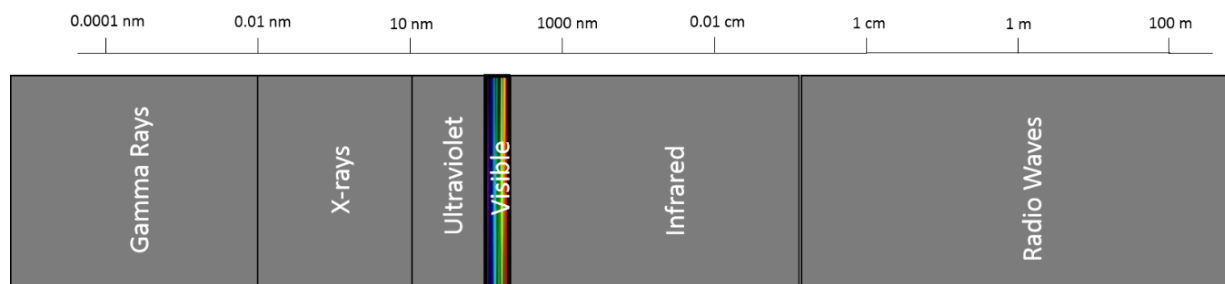


Figure 1. Electromagnetic spectrum

With this information collected from a hyperspectral sensor, models can be built that can predict the nitrogen and water status of the plant. The hyperspectral data has been used to build these models in a variety of ways in the past. These ways have included partial least squares regression to predict both nitrogen and water contents of the plants (Li et al., 2014; Nigon et al., 2015; Cotrozzi et al., 2017; Ge et al., 2016). Another popular technique is through machine learning, such as variations on support vector machine (SVM), to predict water contents (Kersting et al., 2012; Moshou et al., 2012; Behmann et al., 2014). Other techniques such as simplex volume maximization to predict drought tolerance in wheat in India have also been applied in the past (Bhugra et al., 2017).

However, all of these past studies have evaluated either water stress or nitrogen stress separately save a few studies. One study out of the University of Lincoln-Nebraska combined

water and nutrient stress in one genotype of maize and one genotype of soybean (Ge et al., 2016). This study did not evaluate nitrogen stress by itself or evaluate more than one genotype of either species. The lack of genetic variation in the species is one of the challenges of phenomics mentioned above and could result in prediction models that are not able to be used for more than one genotype. In a 2017 study in spinach, water and nitrogen stress were applied in concert and hyperspectral models were built for water content, nitrogen content, and biomass (Corti et al., 2017).

Previous studies have determined that nitrogen and water stress interact in expression of plant phenotypes. One of the largest contributors to a decrease in growth under drought stress is nitrogen deficiency (Hechathorn et al., 1997). In a 2014 study, over short term drought stress, the plant nitrogen content decreased by almost 4% (He & Dijkstra, 2014) most likely due to a decrease in nitrogen uptake, transport, and distribution (Rouphael et al., 2012) and reduced nitrate reductase activity (Azedo-Silva et al., 2004) under drought stress. In the soil, nutrient diffusion and mass flow as well as a decreased leaf litter nitrogen composition have also been observed under drought stress conditions (Sanaullah et al., 2012).

Taking into consideration the goal of phenomics and the challenge of genetic variation in crop plants, the methods for developing prediction models, and the importance of observing nitrogen and water stress together, this study was implemented with the goal of developing nitrogen and water content prediction models with wide applicability and high accuracy.

2.2 Materials and Methods

2.2.1 Sorghum Seed Sources

For this project, three lines out of a Sorghum Association Panel were selected. A 1949 line known as Tx7000, or Caprock was selected for several of its unique properties. This line is categorized as a non-stay-green genotype (Walulu et al., 1994) that displays pre-flowering stress tolerance (Kebede et al., 2001). Pre-flowering drought tolerance is particularly important in sorghum from the panicle differentiation stage to just before flowering (Kebede et al., 2001).

The second line that was chosen was B35, which, in contrast to Tx7000, displays strong stay-green characteristics (Walulu et al., 1994) and post-flowering drought tolerance from right after flowering through maturation of the seeds (Tuinstra et al., 1996).

The final line selected for this project was the genotype BTx623. In 2009, Tx623 was used as the reference for the complete sequencing of the sorghum genome (Paterson et al., 2009).

2.2.2 Soil Medium

A soil media was developed by our team to grow sorghum with much the same characteristics as field conditions in 1.5 gallon pots that would still allow the application of long term nitrogen stress and short term water stress. This was achieved by combining one third topsoil, one third sand, and one third Turface Athletics MVP. Topsoil and sand were combined to provide a substrate with low water holding capacities and low nutrient content. Turface is a calcined, non-swelling illite clay with 60% minimum amorphous silica with 5% or less iron oxide, aluminum oxide, calcium oxide, magnesium oxide, potassium oxide, sodium oxide, and titanium oxide with strong cation exchange capacity. The mixture was mixed thoroughly to maintain uniformity across the entire experiment.

2.2.3 Design of Experiment

The experiment was designed as a randomized complete block with nine blocks. Each combination of genotype and treatment was represented in each block of the design. The treatments are shown in Table 1.

Table 1. Genotype and treatment combinations evaluated in this experiment

<u>Genotype</u>	<u>Nitrogen (mM)</u>	<u>Water</u>
Tx623	40	Fully watered
	40	Severe drought stress
	5	Fully watered
	5	Severe drought stress
B35	40	Fully watered
	40	Severe drought stress
	5	Fully watered
	5	Severe drought stress
Tx7000	40	Fully watered
	40	Severe drought stress
	5	Fully watered
	5	Severe drought stress

2.2.4 Application of Stress

Nitrogen treatments were applied over the entirety of plant growth for the sorghum treatments. These treatments were established through the use of two different Hoagland's solutions with different levels of nitrogen. Preliminary studies had shown that the minimum nitrogen rate for normal sorghum growth was 300 ml of Hoagland's solution with 40mM

ammonium nitrate applied weekly. Hyperspectral imaging revealed that 20 mM ammonium nitrate solution produced plants that were not as green as plants grown using the 40 mM solution (Fig. 2). Plant's watered weekly with a Hoagland's solution containing 5 mM ammonium nitrate solution produced plants that were visually deprived of nitrogen but not significantly stunted in grown.

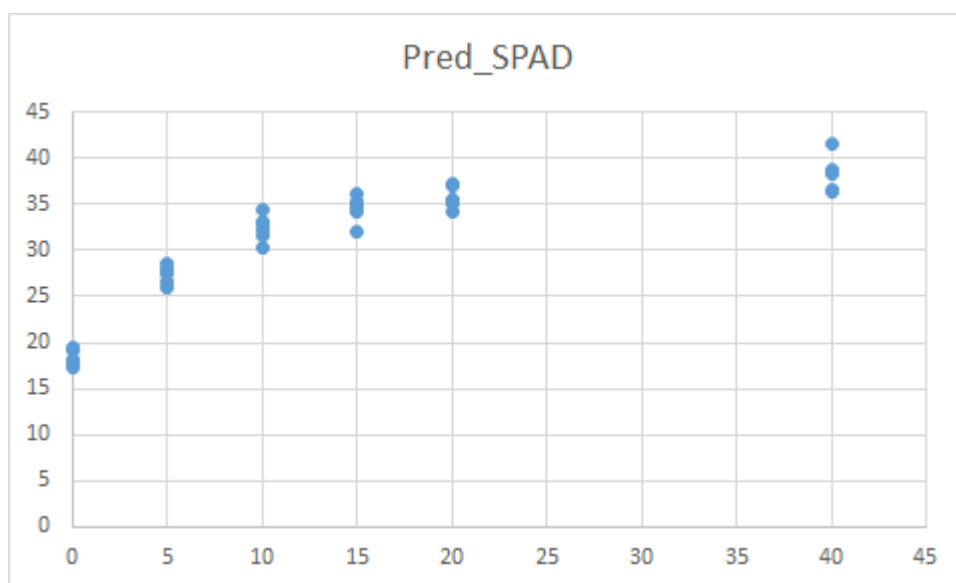


Figure 2. Predicted SPAD measurements in sorghum plants under six different nitrogen treatments: 0, 5, 10, 15, 20, and 40 mM ammonium nitrate

The original Hoagland's solution was developed in 1938 by D.R. Hoagland and D.I. Arnon and revised in 1950 by D.I. Arnon (Hoagland and Arnon, 1950). The solutions used in this experiment were modified from the original recipe in order to provide all macronutrients and micronutrients with two different levels of nitrogen. Five stock solutions were used to produce the desired Hoagland's solution including 1 M potassium phosphate monobasic solution, 0.33 M magnesium sulfate anhydrous solution, 0.017 M ferrous sulfate heptahydrate solution, 1 M calcium nitrate solution, and a micronutrient stock solution. The micronutrient stock solution contained 50

mM potassium chloride, 25 mM boric acid, 2 mM manganese sulfate tetrahydrate, 2 mM zinc sulfate, 0.5 mM cupric sulfate, and 0.5 mM molybdic acid.

The 5 mM ammonium nitrate solution, equivalent to a 0.6 mM nitrogen, combined 12 mL KH_2PO_4 , 6 mL MgSO_4 , 8 mL $\text{FeSO}_4/\text{EDTA}$, 2 mL micronutrient stock, and 5 mL $\text{Ca}(\text{NO}_3)_2$ stock were used. To each plant, every week, 300 milliliters of solution was given. The 40 mM ammonium nitrate solution, equivalent to a 4.15 mM of nitrogen, combined 12 mL KH_2PO_4 , 6 mL MgSO_4 , 8 mL $\text{FeSO}_4/\text{EDTA}$, 2 mL micronutrient stock, and 5 mL $\text{Ca}(\text{NO}_3)_2$ stock were used. To each plant, every week, 300 milliliters of solution was given with an additional 0.9489 g of ammonium nitrate in a total volume of 1 L. Each week, 300 mL of these solutions were applied to each plant according to the treatment designations.

While the nitrogen treatments were applied over the life of the plant, drought treatments were applied a short periods of time. From vegetative growth stage four until vegetative growth stage six, all the plants received 600 mL of water from the automated conveyor belt system. After vegetative growth stage six, the plants assigned to receive drought stress were watered with 150 mL of water each day for a week. The other plants assigned to the well-watered treatment received 600 mL of water each day. These two treatments produced drought symptoms in plants with moderate to severe stress or well-watered plants with no drought stress symptoms.

2.2.5 Automated Imaging System

An automated, high-throughput imaging system installed in a greenhouse at Purdue University was used in these studies. The system included a hyperspectral imaging tower that accommodates top-view and side-view hyperspectral (HS) cameras. The tower can image plants up to 1.5 meters tall. The HS cameras are Middleton Spectral Vision MSV 500 cameras with push broom style scanning. The cameras scan from 400 to 1100 nanometers with a spectral resolution

of 2.8 nanometers. Inside the imaging tower (Fig. 3), there are 8 studio halogen lamps to provide lighting. The openings where the plant enters the towers (Fig. 4) have doors that automatically close when imaging the plants, and the imaging time is approximately 1 minute per plant. The plants were automatically rotated on the imaging platform so the widest plane of the plant is facing the camera.



Figure 3. Camera and lighting system inside the imaging tower

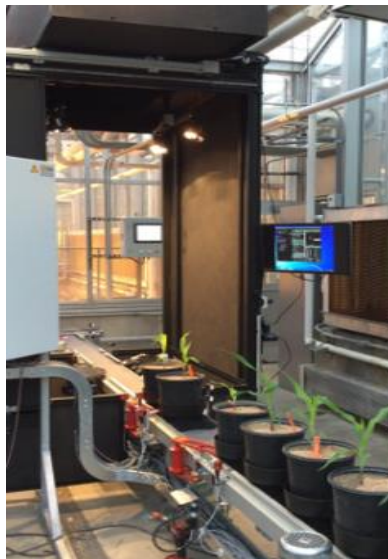


Figure 4. Entrance to imaging tower

The automated system contains a conveyor belt system that can accommodate up to 108 pots that sit in carriers on the conveyor belt (Figs. 5 and 6). Each carrier and plant, is identified by an RFID tag for imaging purposes.

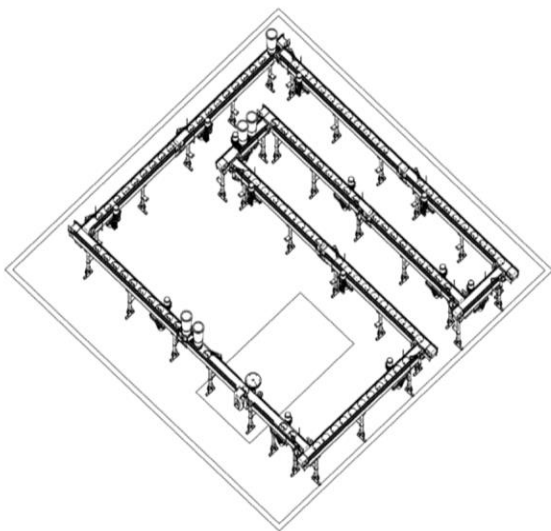


Figure 5. Schematic of the automated greenhouse conveyor belt system



Figure 6. Working conveyor belt system

2.2.6 Relative Water Content Measurements

The process to measure relative water content (RWC) begins by harvesting and obtaining the fresh weight (FW) of a portion of plant tissue (Turner, 1981). Then the plant material is floated or submerged in water until the material is completely turgid and the plant tissue is weighed to obtain the turgid weight (TW). Finally, the plant tissue is fully dried to obtain the dried weight (DW). These values are used to determine the RWC using the equation $RWC = [(FW - DW) / (TW - DW)] * 100$. In this experiment, the plant tissue sampled from the sorghum plant was approximately 2.5 cm x 5.0 cm. The samples were submerged in deionized water overnight to ensure the tissue was fully turgid without risking degradation. Finally, all samples were dried in

a 90° F dryer until samples weighed the same on consecutive days. All weights were obtained using the Mettler AJ100L balance with a readability of 0.1 mg, a tolerance of 0.1 mg, and a linearity of 0.2 mg (D. Yaconis - Weighing Solutions Technical Specialist METTLER TOLEDO, personal communication, June 13, 2018).

2.2.7 Nitrogen Content Measurements

Nitrogen content of leaf samples was analyzed by the Brouder lab in the Agronomy Department at Purdue University using a Thermo Scientific FlashEA 1112 Nitrogen and Carbon Analyzer for Soils, Sediments, and Filters (CE Elantech, Lakewood, NJ). This analyzer uses “flash dynamic combustion” to convert organic and inorganic substances into combustion gases with oxygen in the auto sampler.

This analyzer has three basic steps after combustion. First, the gas mixture enters reactor one, a quartz oxidation of components, at a temperature of 950°C. The next step takes place in reactor two, made of copper, at a temperature of 840°C where nitrogen oxides are converted to elemental nitrogen. Finally, the sample is filtered through an adsorption filter into a chromatographic column and from there to a conductivity conductor that generates electrical signals that are translated into percentage of nitrogen.

2.2.8 Data Processing

The hyperspectral imaging data was processed by the Jin lab in the Agricultural and Biological Engineering Department at Purdue University. The images were processed using a segmentation procedure (Fig. 7) and then subjected to morphological analysis, reflectance calculation, and spectral indices calculation. Segmentation utilizes plant materials distinct spectral

reflectance signature, particularly at the “red-edge”, to segment the image into a black and white image to distinguish plant material from surrounding material. This allows the calculation of morphological traits such as canopy area, leaf area, number of leaves, height of the plant, and angle of the leaves. This also allows for the calculation of the reflectance of every pixel of the plant. Such reflectance across the entire range creates a profile of the entire, individual plant.

Along with the entire spectral reflectance, 9 different plant indices are calculated including Normalized Difference Vegetation Index (NDVI), Narrow Band Normalized Difference Vegetation Index (NBNVDI), Transformed Chlorophyll Absorption in Reflectance Index (TCARI), Structure-Insensitive Pigment Index (SIPI), Plant Senescence Reflectance Index (PSRI), Physiological Reflectance Index (PhRI), Normalized Pigment Chlorophyll Ratio Index (NPCI), Anthocyanin Reflectance Index (ARI), and Nitrogen Reflectance Index (NRI). These can be quickly used to evaluate the spectral response of a plant to different treatments. The hyperspectral imaging also produces a reflectance data point at every pixel of every plant at every wavelength. The average of all the pixels is calculated for every plant at every wavelength and this average was used to represent the plant at a specific wavelength. Finally, all the results including plant reflectance at every wavelength, plant morphology, and spectral indices were output into a results table.

2.2.9 PLS_ToolBox in MatLab

The PLS_Toolbox is a software developed by Eigenvector Research Incorporated for use in MATLAB (PLS_Toolbox, 2018). This software can perform Partial Least Squares (PLS) regression, as was used in this study, but it can also perform many other functions including Principal Components Regression, Support Vector Machine Regression, Artificial Neural

Networks, and more. The interface involves loading x variables and y variables, selecting the proper preprocessing steps, and the proper cross validation. The x variables can be any combination of spectral and morphological features including the values for the bands at measured wavelengths, spectral indices calculated using the hyperspectral data, and morphological features calculated using the segmentation.

A leave one out technique was used for cross-validation. The preprocessing steps vary depending on the use of only spectral data or spectral and morphological data. Transmission or reflectance was converted to absorbance in a log/1 conversion, multiplicative signal correction (MSC) where the weighted normalization and baseline were removed using the mean, and the mean offset was removed for each variable if PLS regression was applied to spectral data. Each variable was mean centered and scaled to unit standard deviation and Savitzky-Golay smoothing and derivatives were applied if PLS regression was applied to spectral and morphological data.

After a model was generated, the predicted values for the data set used to generate the model were extracted. This model can be applied to any data set with the same number of bands in the x variable.

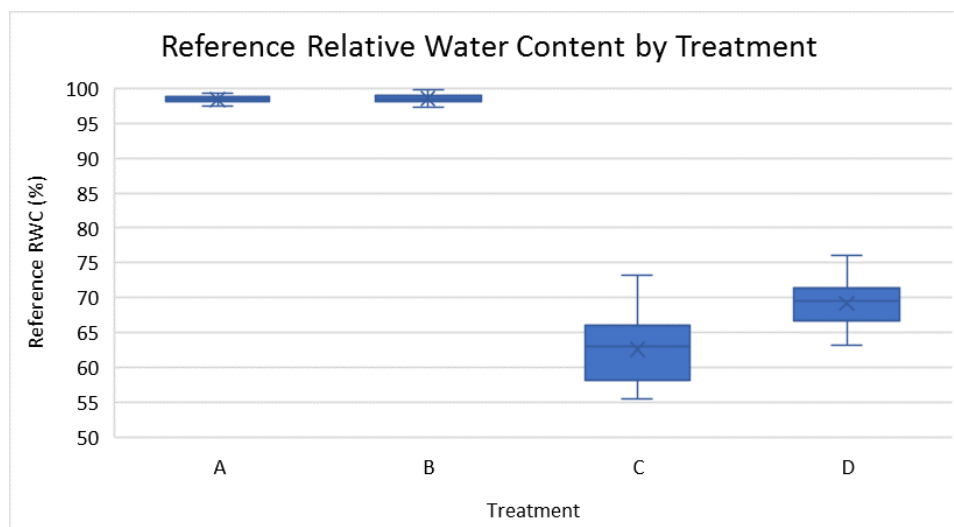
2.3 Results

2.3.1 Relative Water Content

The relative water content (RWC) of the sorghum plants ranged from 55.5% to 99.7% of the leaf section (Fig. 7). Both of the well-watered treatments had consistently high RWC close to 100% because the plants were well watered every day while the drought stressed treatments had RWCs between 55% to 80%. There is a clear treatment effect. The statistical analysis of the RWC is shown in Table 2. The formula used for the ANOVA is:

$$\text{RWC} \sim \text{Treatment} + \text{Genotype} + \text{Treatment} * \text{Genotype}$$

The type III sums of squares were used because of the imbalance in the replications of treatment C for the B35 genotype. The treatment effect was confirmed by the ANOVA, but no genotype or treatment by genotype effects were observed.



A	Well-Watered; 40 mM N
B	Well-Watered; 5 mM N
C	Severe Drought Stress; 40 mM N
D	Severe Drought Stress; 5 mM N

Figure 7. Reference RWC by Treatment

Table 2. Analysis of Variance (ANOVA) table for reference relative water content

ANOVA Table (Type III tests)					
Response: RWC					
	Sum Squares	Df	F Value	Pr(>F)	
(Intercept)	87145	1	10146.8129	<2e-16	***
Treatment	9299	3	360.9054	<2e-16	***
Genotype	0	2	0.0271	0.9732	
Treatment x Genotype	42	6	0.8243	0.5539	
Residuals	816	95			
Significance codes: 0, '***' 0.001, '**' 0.01, '*' 0.05					

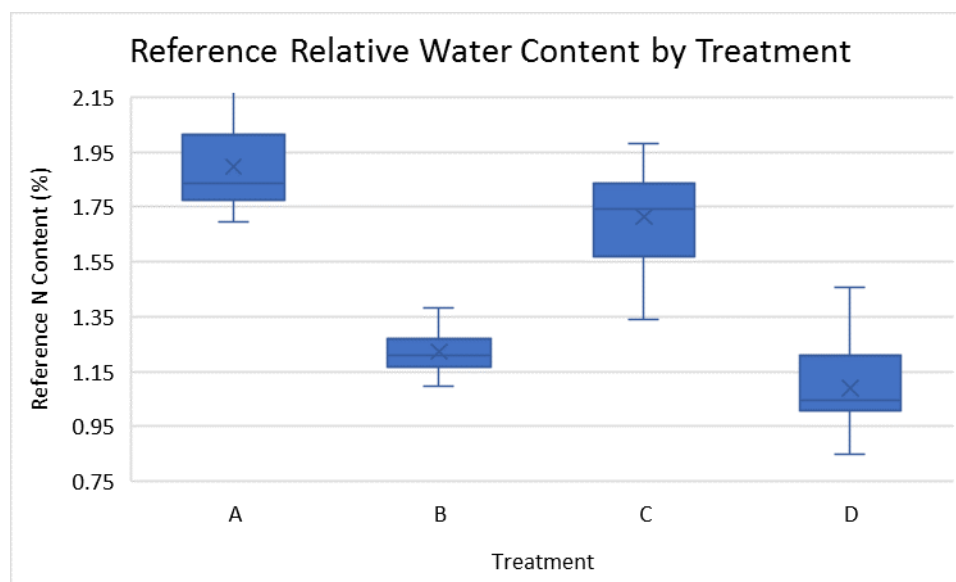
2.3.2 Nitrogen Content

The N content of the sorghum plants ranged from 0.85% to 2.27% of the leaf section (Fig. 8). This graph shows a treatment effect based on nitrogen levels and appears to show a treatment interaction between the drought stress and the nitrogen stress. The well-watered, high nitrogen treatment shows higher nitrogen content than the drought stressed, high nitrogen treatment. The same was true for the low nitrogen treatments as well. The statistical analysis of the N content is shown in Table 3. The formula used for the ANOVA is:

$$N_{\text{content}} \sim \text{Treatment} + \text{Genotype} + \text{Treatment} * \text{Genotype}$$

The type III sums of squares were used because of the imbalance in the replications of treatment C for the B35 genotype. The ANOVA confirms that there is a treatment effect based on the nitrogen but also shows a strong genotype effect and a strong treatment by genotype effect (Table 3).

An interaction plot was generated (Fig. 9) to visualize the interaction between genotype and treatment. Tx623 displays the most consistent response to nitrogen treatments. The average N content for both of the high N treatments was similar, and the average N content for both of the low N treatments was also similar. B35 had a different response to the treatments. The plants under high water, for both high and low N treatments, had higher average N contents than the low water counterparts. The same trend was present for Tx7000; however, the average N content of Tx7000 under the high water and low nitrogen treatment was not as low as the other two genotypes.



A	Well-Watered; 40 mM N
B	Well-Watered; 5 mM N
C	Severe Drought Stress; 40 mM N
D	Severe Drought Stress; 5 mM N

Figure 8. Reference nitrogen content by treatment

Table 3. Analysis of Variance (ANOVA) table for reference nitrogen content

ANOVA Table (Type III tests)					
Response: N content					
	Sum Squares	Df	F Value	Pr(>F)	
(Intercept)	38.314	1	3423.636	<2e-16	***
Treatment	5.721	3	170.4072	<2e-16	***
Genotype	0.381	2	17.0098	4.850e-07	***
Treatment x Genotype	0.6	6	8.9288	9.994e-08	***
Residuals	1.063	95			
Significance codes: 0, '***' 0.001, '**' 0.01, '*' 0.05					

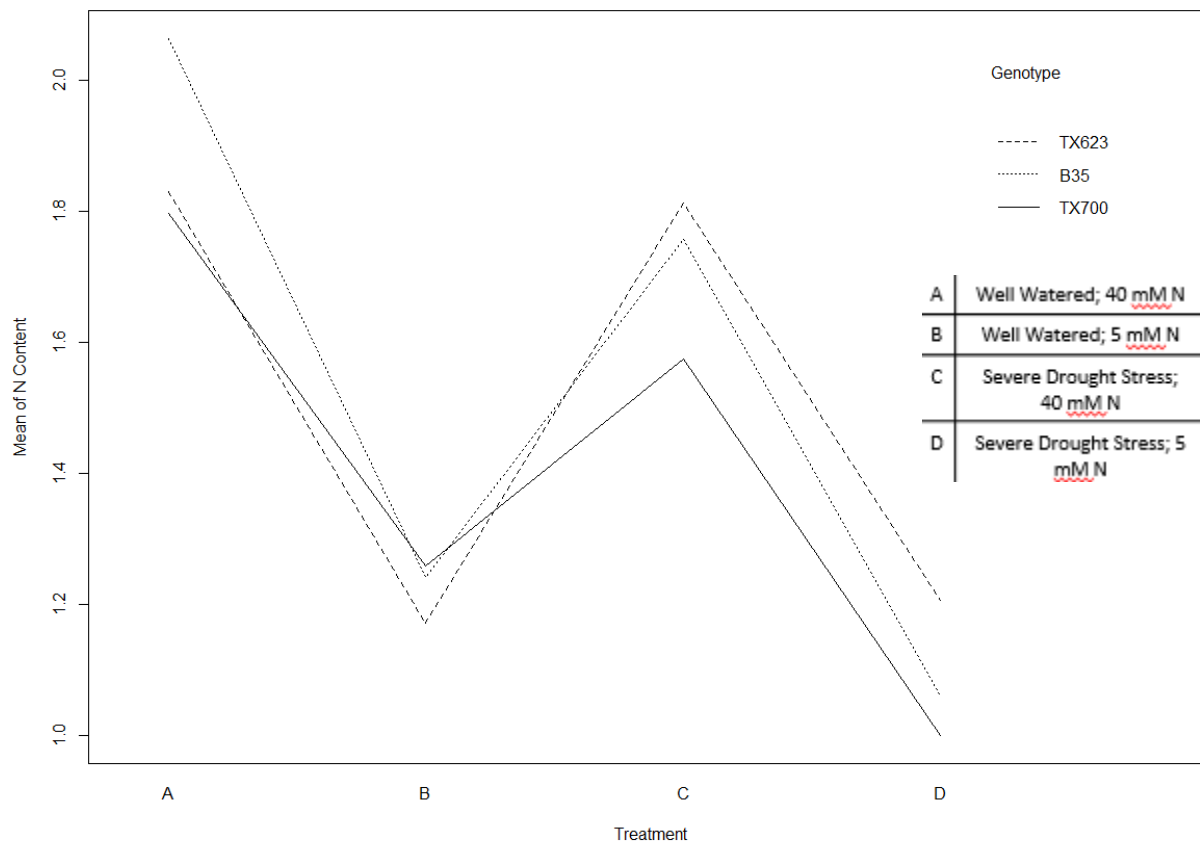


Figure 9. Interaction plot of reference nitrogen content by genotype for the four N treatments

2.3.3 Relative Water Content Models using Spectral and Morphological Features

Spectral and morphological data from B35, Tx623, and Tx7000 were used to develop models for predicting variation in RWC using PLS regression. The predictions were then compared to the reference relative water content measurements (Fig. 10). The coefficient of determination for this model is 0.906. This model was compared to models built using spectral and morphological data from B35, Tx623, and Tx7000 individually (Figs. 11, 12, and 13). The coefficients of determination for the models developed from the individual genotypes were 0.928, 0.900, and 0.896, respectively.

All four models had a coefficient of determination around 0.9. In these models developed using the data from all plants in the experiment, the model developed using the response from B35 was slightly better than the other two models developed using the data from Tx623 or Tx7000. However, other models were developed using a randomly selected 70% of the data for the models developed based on the response of all three genotypes individually. From these models, it was clear that B35 is not consistently better at predicting the responses of the other two genotypes.

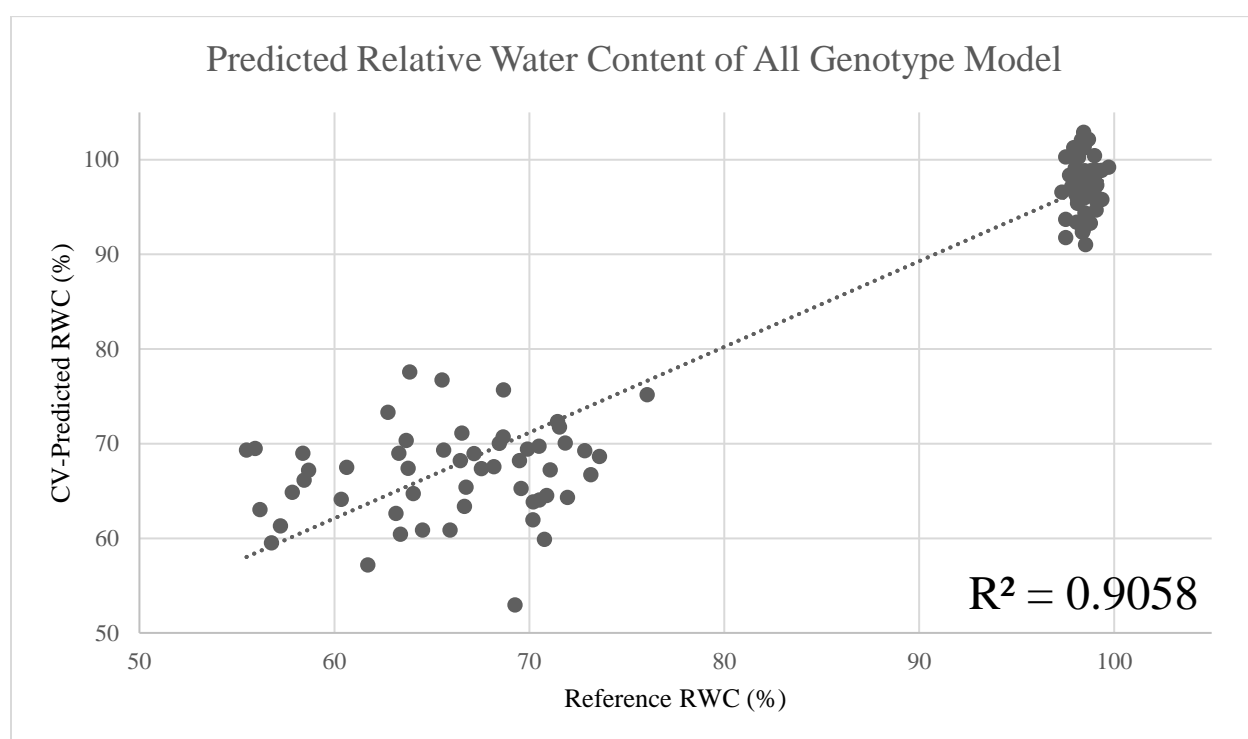


Figure 10. Plot of reference RWC compared to cross-validated predicted RWC using the model based on the response of all three genotypes

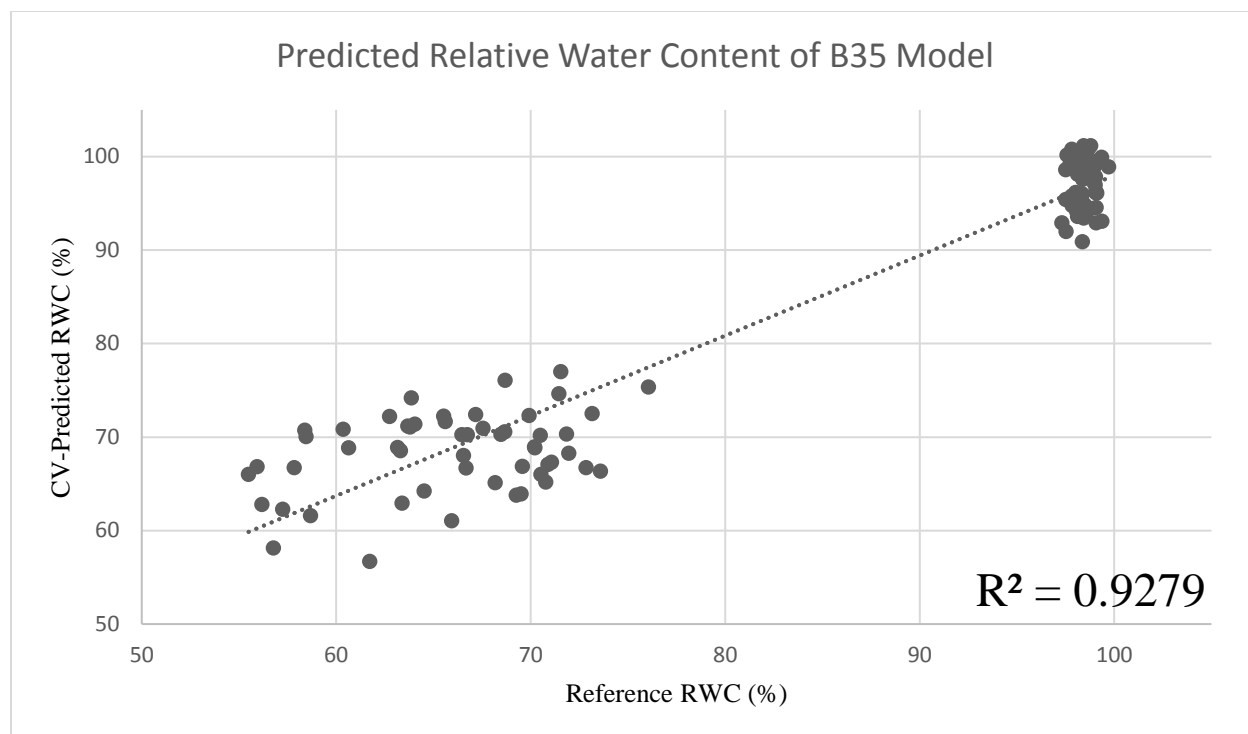


Figure 11. Plot of reference RWC compared to cross-validated predicted RWC of all three genotypes using the model based on the response of B35

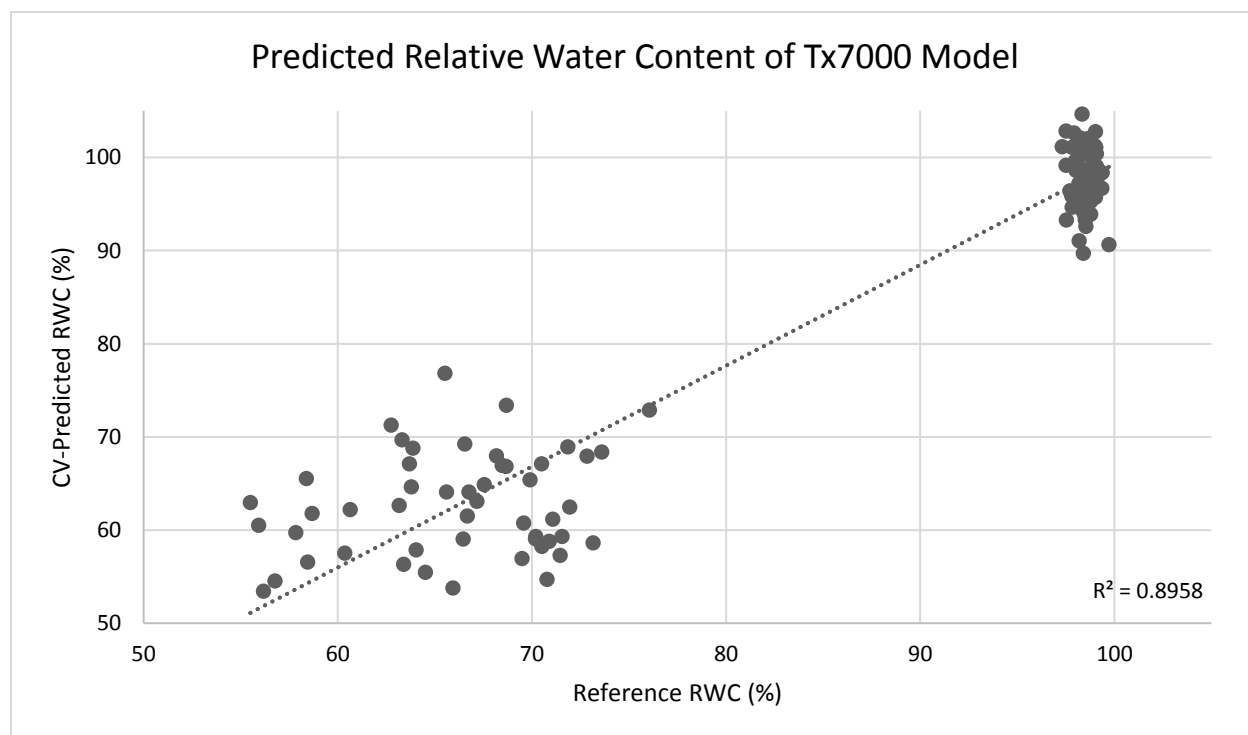


Figure 12. Plot of reference RWC compared to cross-validated predicted RWC of all three genotypes using the model based on the response of Tx7000

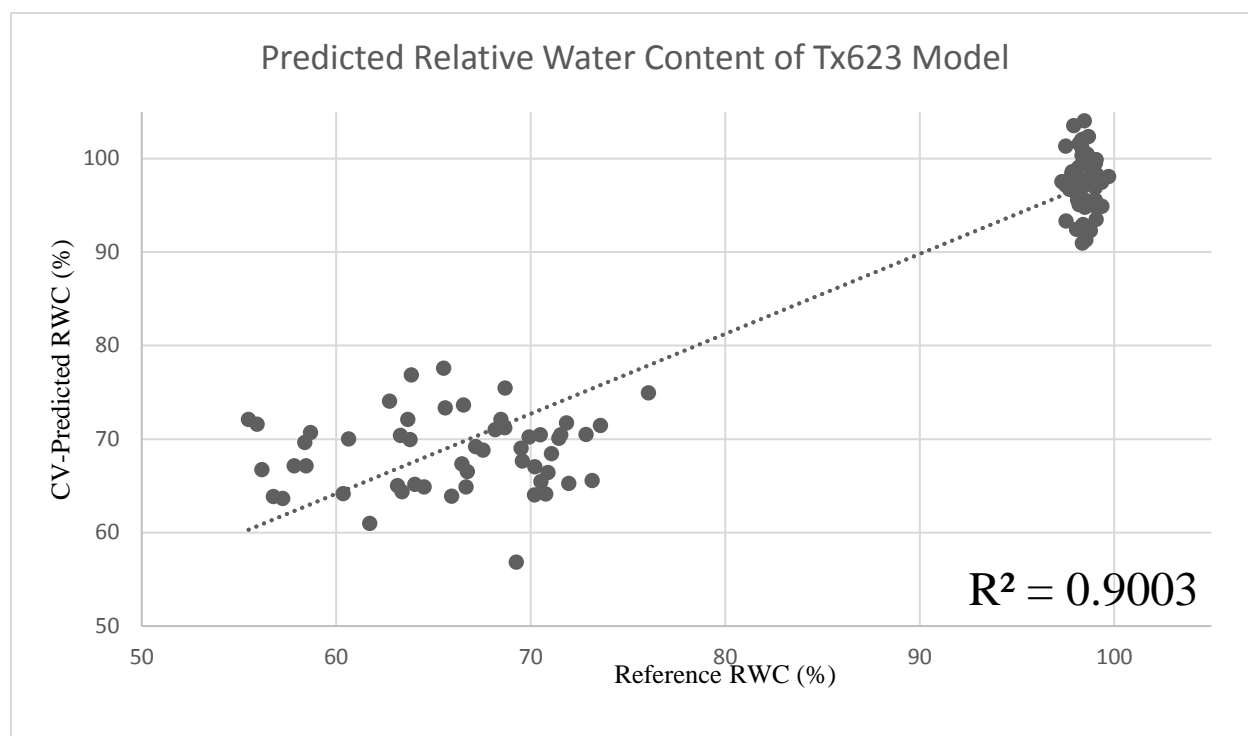


Figure 13. Plot of reference RWC compared to cross-validated predicted RWC of all three genotypes using the model based on the response of Tx623

2.3.4 Relative Water Content Models using only Spectral Features

PLS models developed using spectral and morphological data were compared with models developed using only the spectral features of the hyperspectral data from B35, Tx623, and Tx7000. The predictions of the models developed using the spectral features were then compared to the reference measurements RWC (Fig. 14). The coefficient of determination for this model is 0.948. Three more models were produced using the spectral features of the hyperspectral data for each of the individual genotypes (Figs. 15, 16, 17) with coefficients of determination of 0.843, 0.843, and 0.796 respectively.

Models built using spectral and morphological features of the plant extracted from the hyperspectral images were, in general, slightly, but not significantly more accurate than models

built using only spectral features of the plant for both relative water content and nitrogen content predictions. One notable exception was the full model using all genotypes to predict the relative water content of all genotypes, where the coefficient of determination increased when the model was built with spectral features only. The models developed using the spectral data only of B35, Tx623, and Tx7000 respectively were slightly, but not significantly, less accurate.

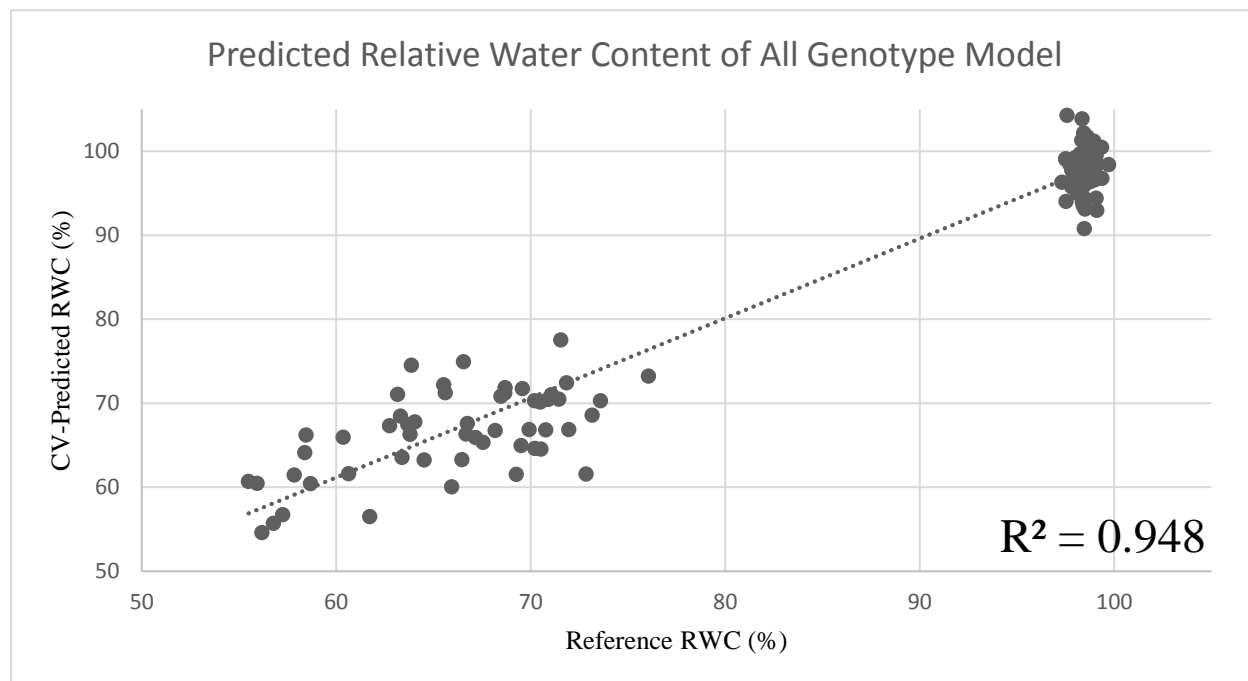


Figure 14. Plot of reference RWC compared to cross-validated predicted RWC of all three genotypes using the model based on the response of all three genotypes

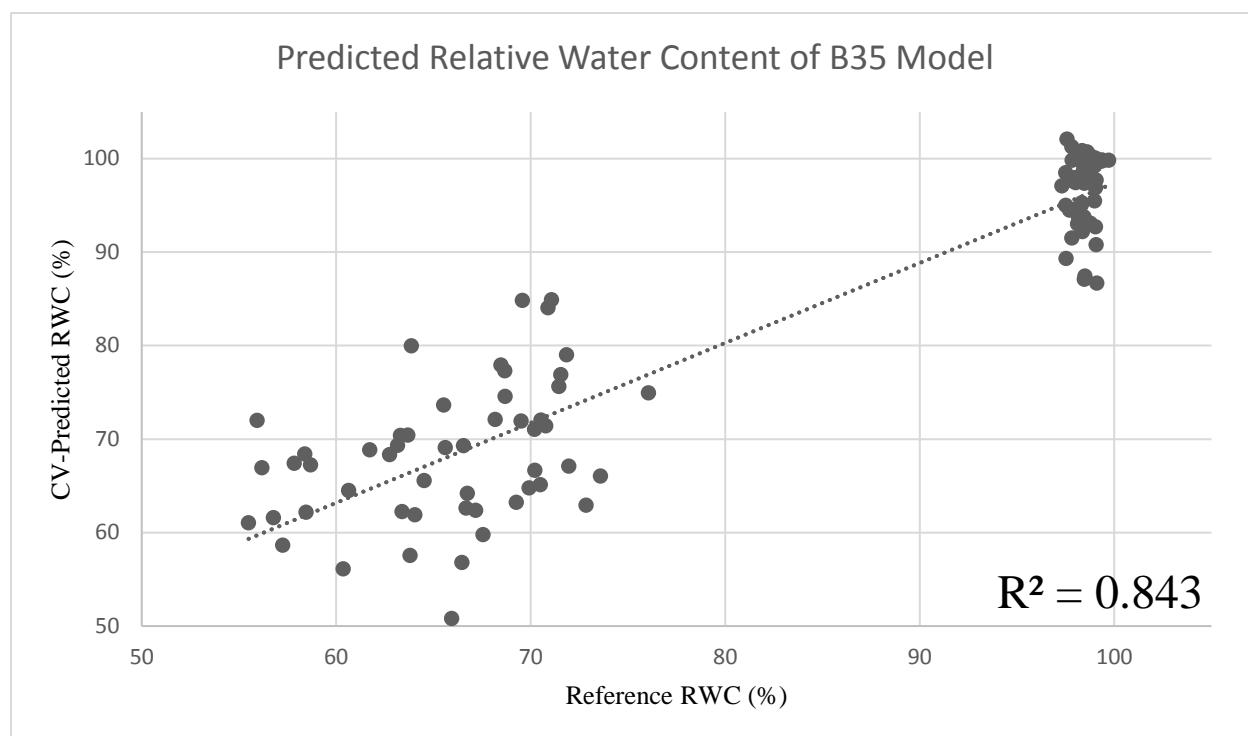


Figure 15. Plot of reference RWC compared to cross-validated predicted RWC of all three genotypes using the model based on the response of B35

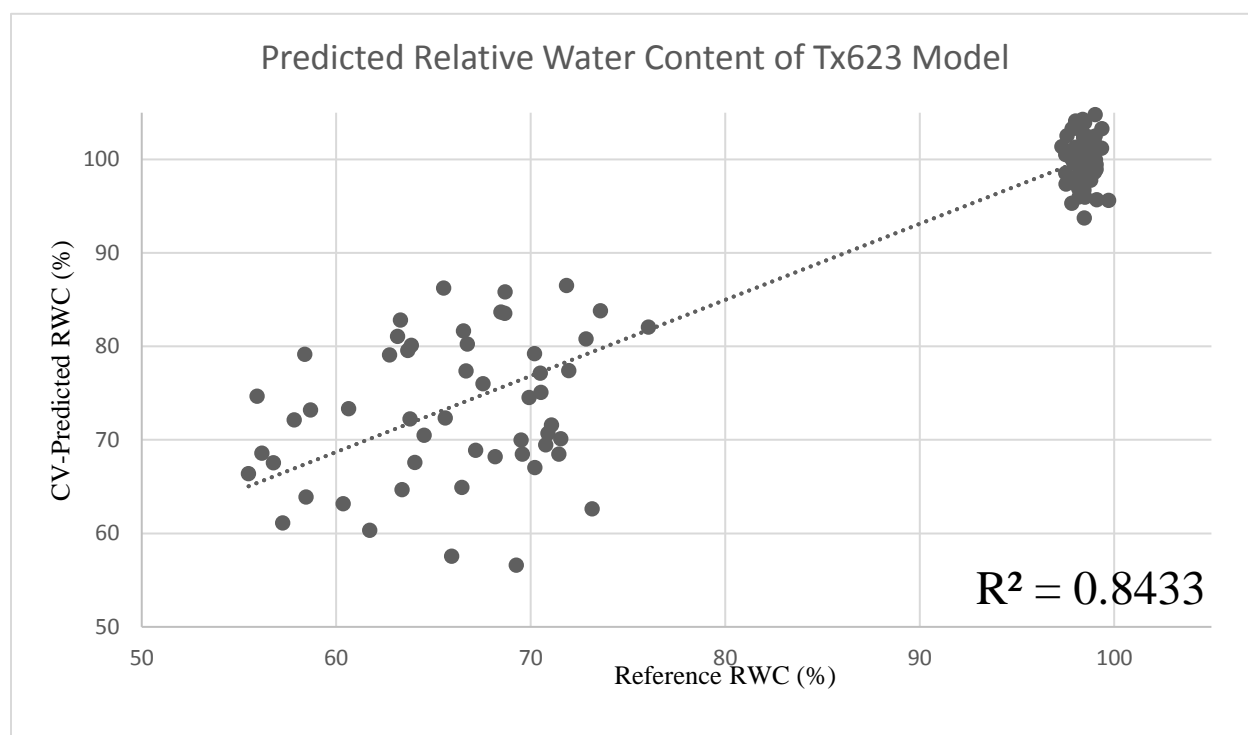


Figure 16. Plot of reference RWC compared to cross-validated predicted RWC of all three genotypes using the model based on the response of Tx623

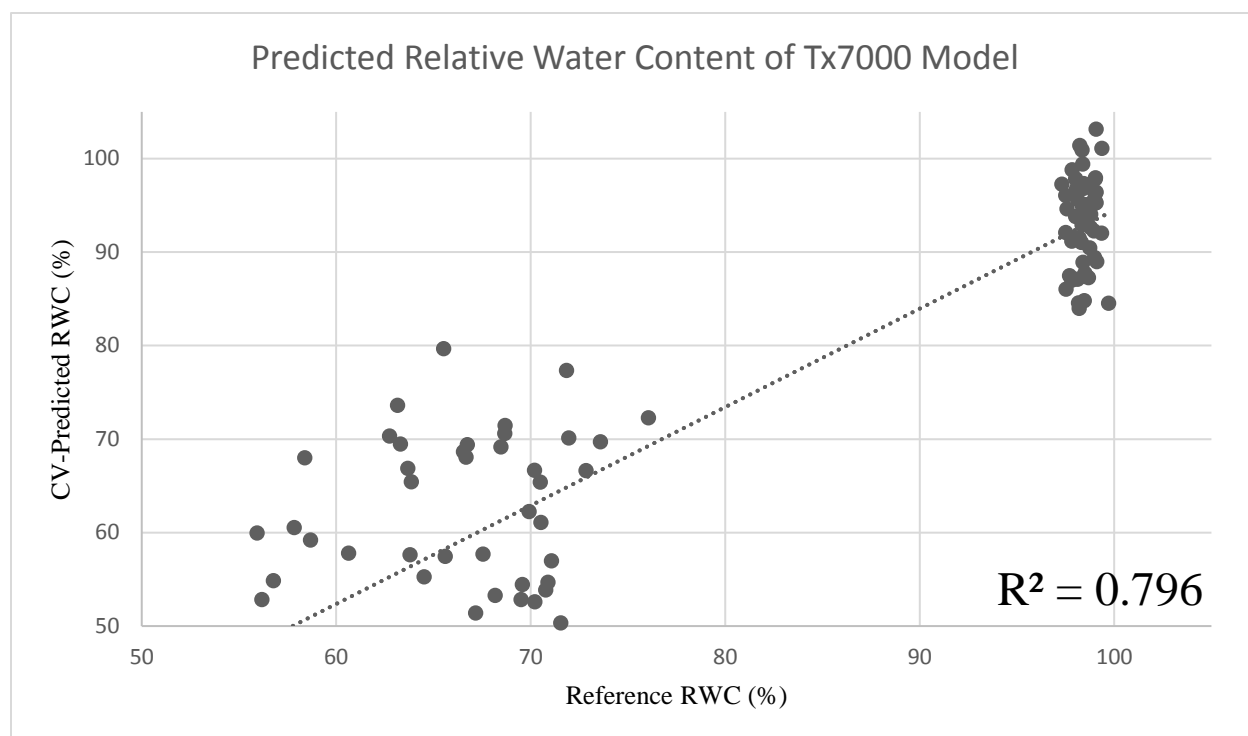


Figure 17. Plot of reference RWC compared to cross-validated predicted RWC of all three genotypes using the model based on the response of Tx7000

2.3.5 Summary of all Relative Water Content Models

Coefficients of determination for RWC models developed using spectral and morphological features and using spectral features of combined and individual genotypes of sorghum are shown in Figure 18. This heatmap shows that most of the RWC models, whether models developed with spectral and morphological features or with spectral features have coefficients of determination between 0.8 and 0.95. The only coefficient of determination lower than 0.8 is the coefficient of determination of the model developed using the spectral and morphological features of B35.

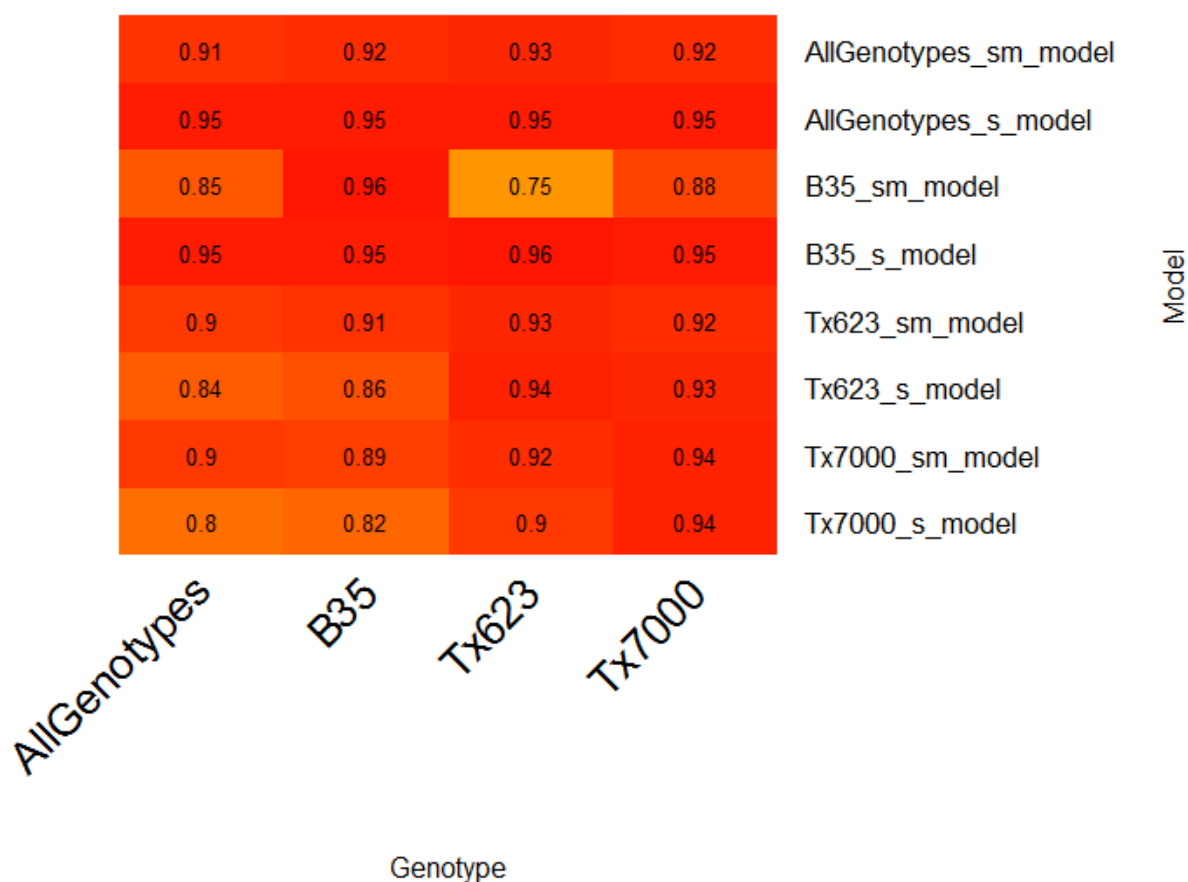


Figure 18. Heatmap of coefficients of determination of RWC models for sorghum; _s_ represents spectral only models and _sm_ represents spectral and morphological models

2.3.6 Nitrogen Content Models using Spectral and Morphological Features

PLS models for nitrogen content developed using the spectral and morphological data were compared to the reference nitrogen contents of measured sorghum plants (Fig. 19). The coefficient of determination for this model was 0.925. The three subsequent models were built using the spectral and morphological data from each genotype individually (Figs. 20, 21, and 22) and have coefficients of determination of 0.792, 0.812, and 0.81 respectively. The model developed based on all three genotypes was more accurate than the models developed based on each genotype individually.

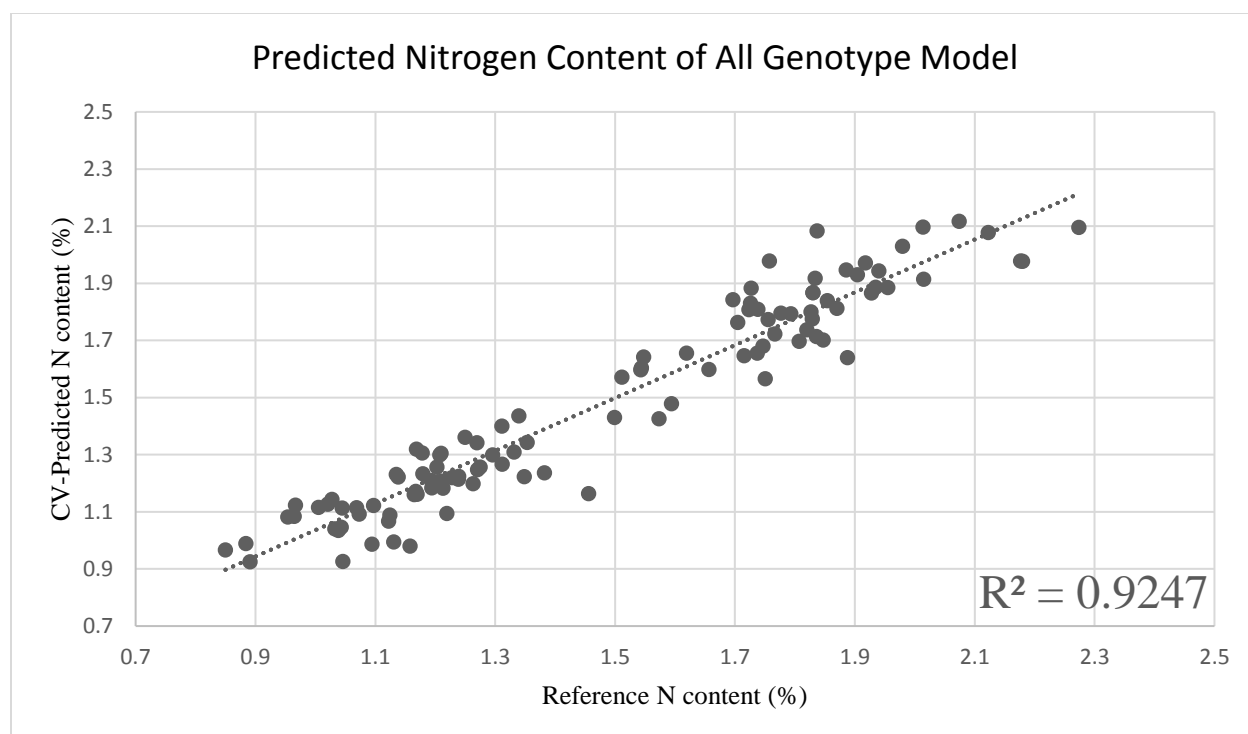


Figure 19. Plot of reference N content compared to cross-validated predicted N content using the model developed based on the response of all three genotypes

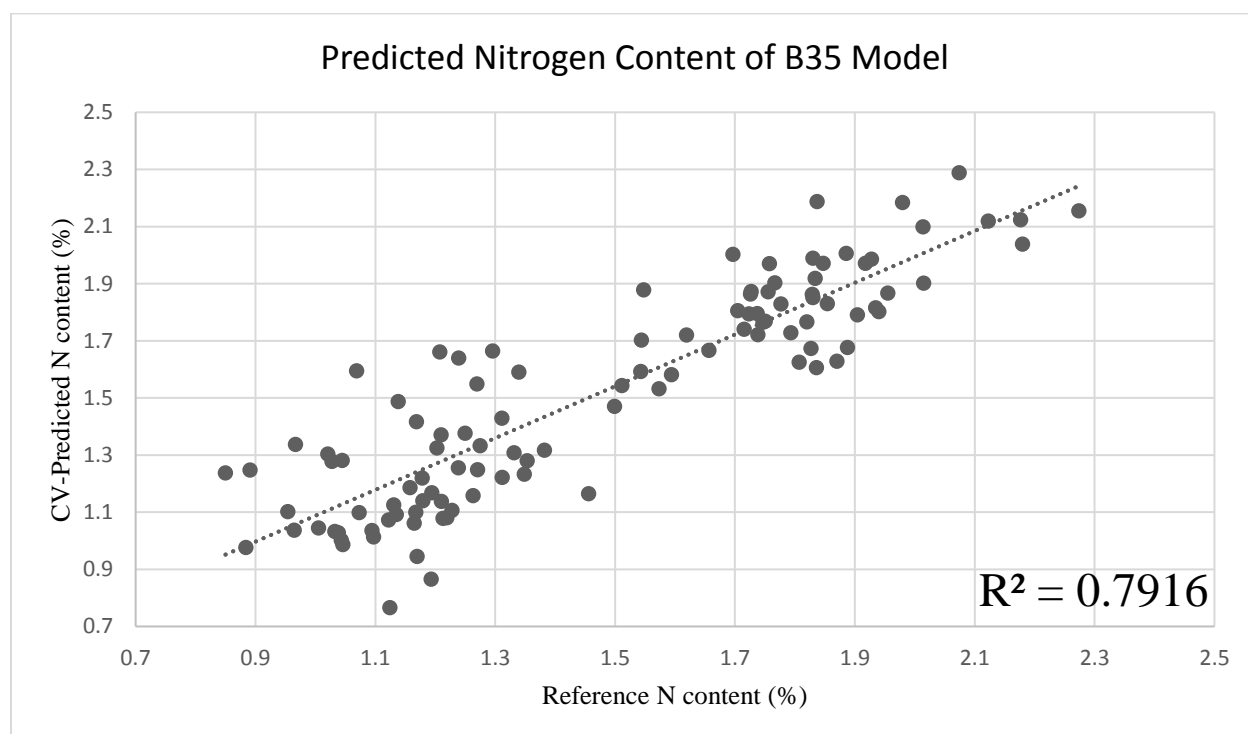


Figure 20. Plot of reference N content compared to cross-validated predicted N content using the model developed based on the response of B35

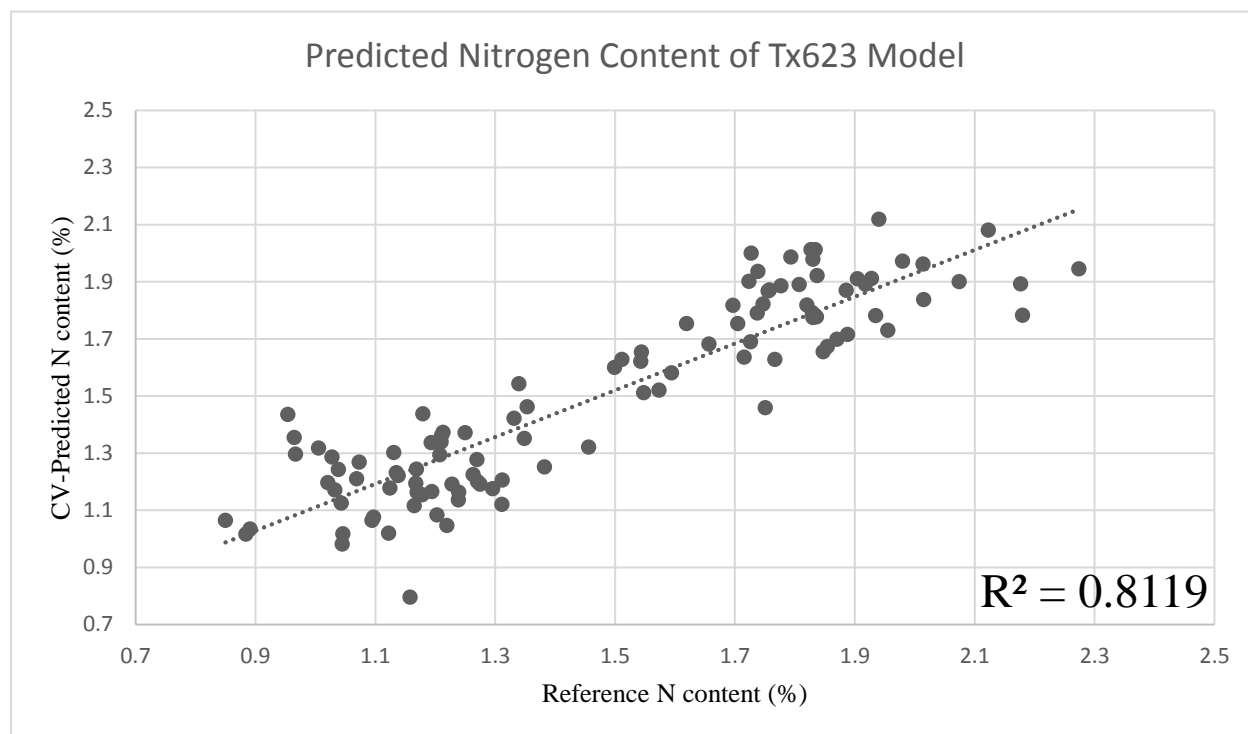


Figure 21. Plot of reference N content compared to cross-validated predicted N content using the model developed based on the response of Tx623

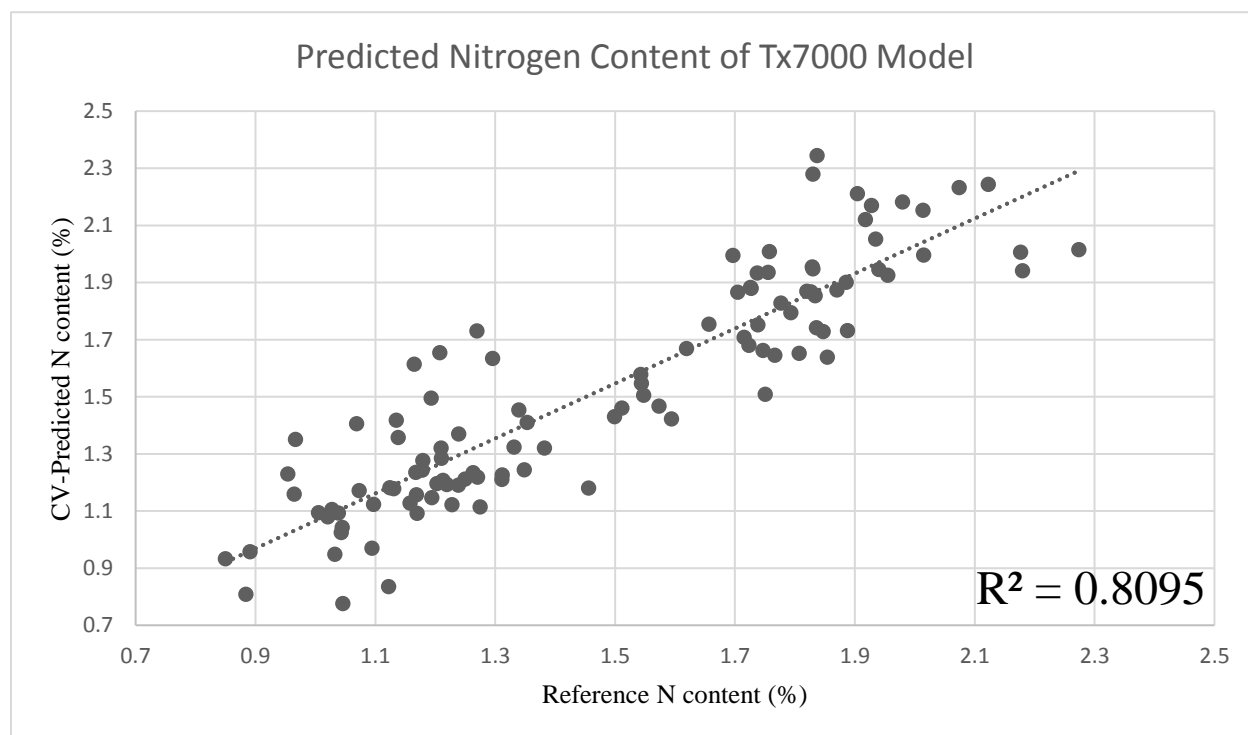


Figure 22. Plot of reference N content compared to cross-validated predicted N content using the model developed based on the response of Tx7000

2.3.7 Nitrogen Content Models using only Spectral Features

After the nitrogen models were developed using the spectral and morphological features, new models were generated using only the spectral features to predict nitrogen content. Nitrogen content models were developed using the spectral data from B35, Tx623, and Tx7000. The predictions were then compared to the reference nitrogen contents from this experiment (Fig. 23). The coefficient of determination for this model was 0.9079. Three additional models were generated using each of the individual genotypes (Figs. 24, 25, and 26) and predictions from each model were compared to the reference nitrogen contents with coefficients of determination of 0.734, 0.871, and 0.764, respectively. The N content models developed with the spectral features only were not significantly different than those developed using the spectral and morphological features. The models developed using all three genotypes were generally more predictive than the models developed with only one genotype.

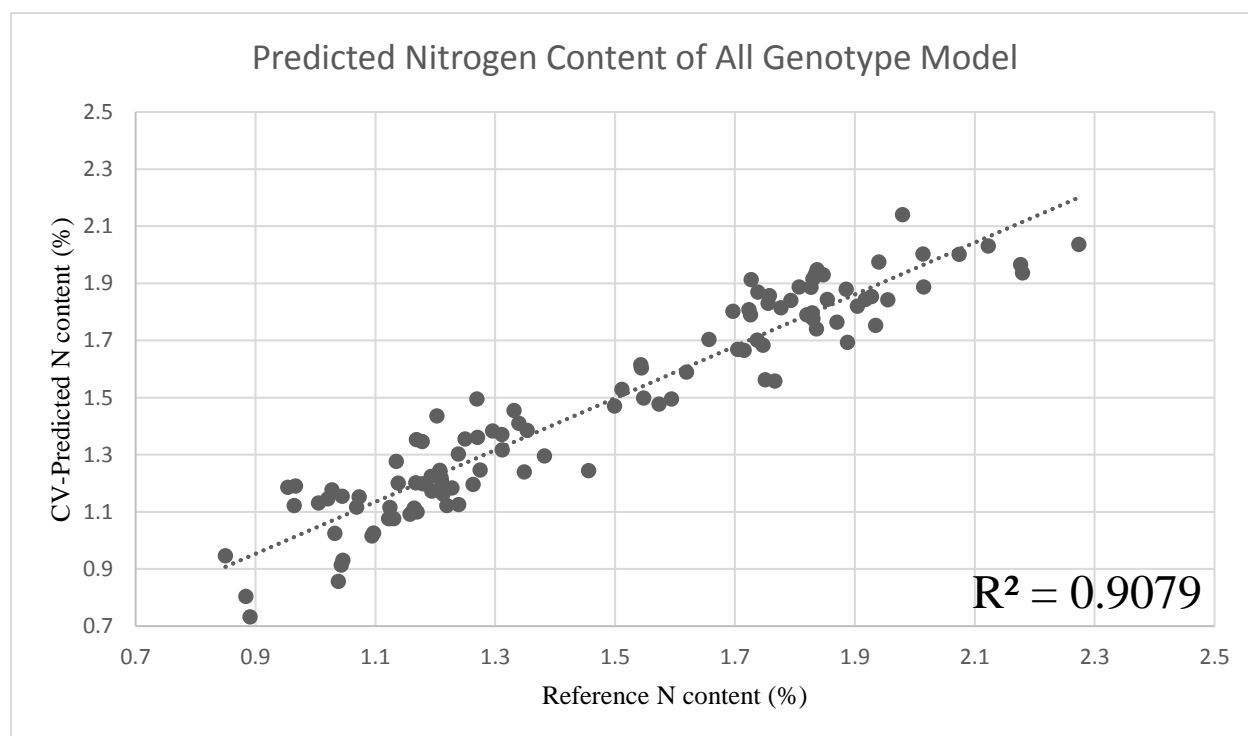


Figure 23. Plot of reference N content compared to cross-validated predicted N content using the model developed based on the response of all three genotypes

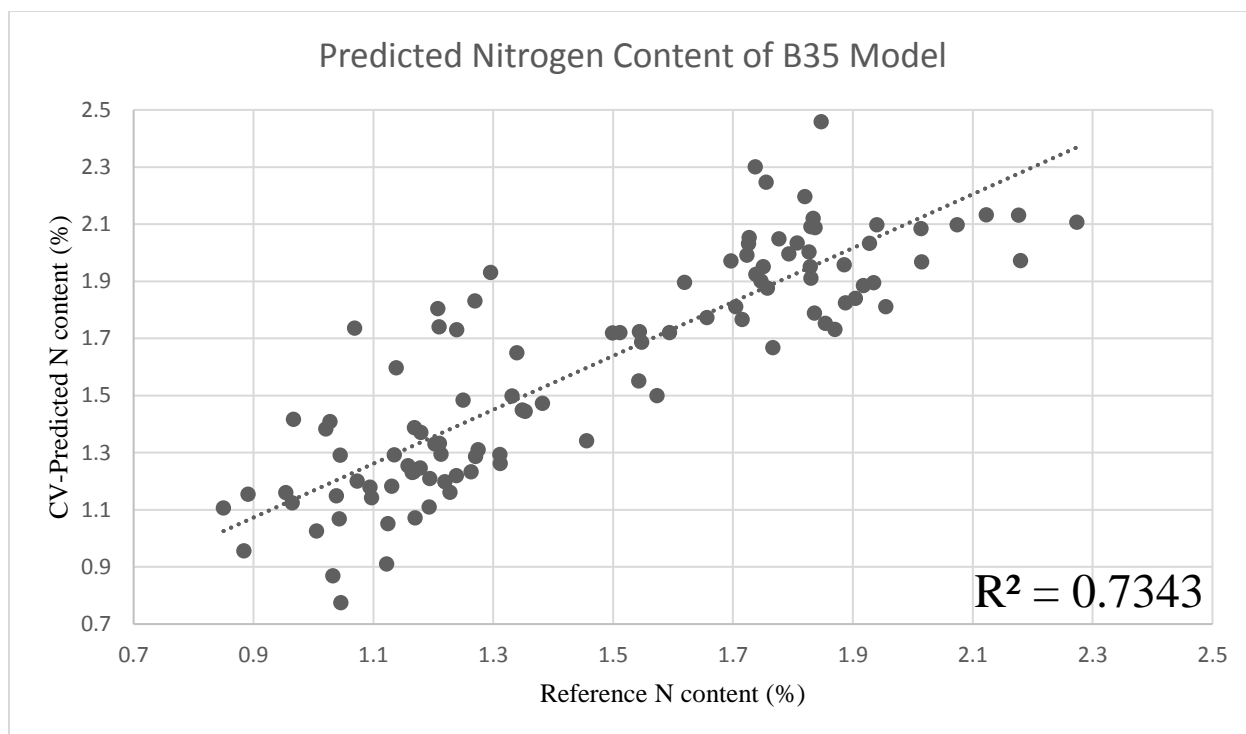


Figure 24. Plot of reference N content compared to cross-validated predicted N content using the model developed based on the response of B35

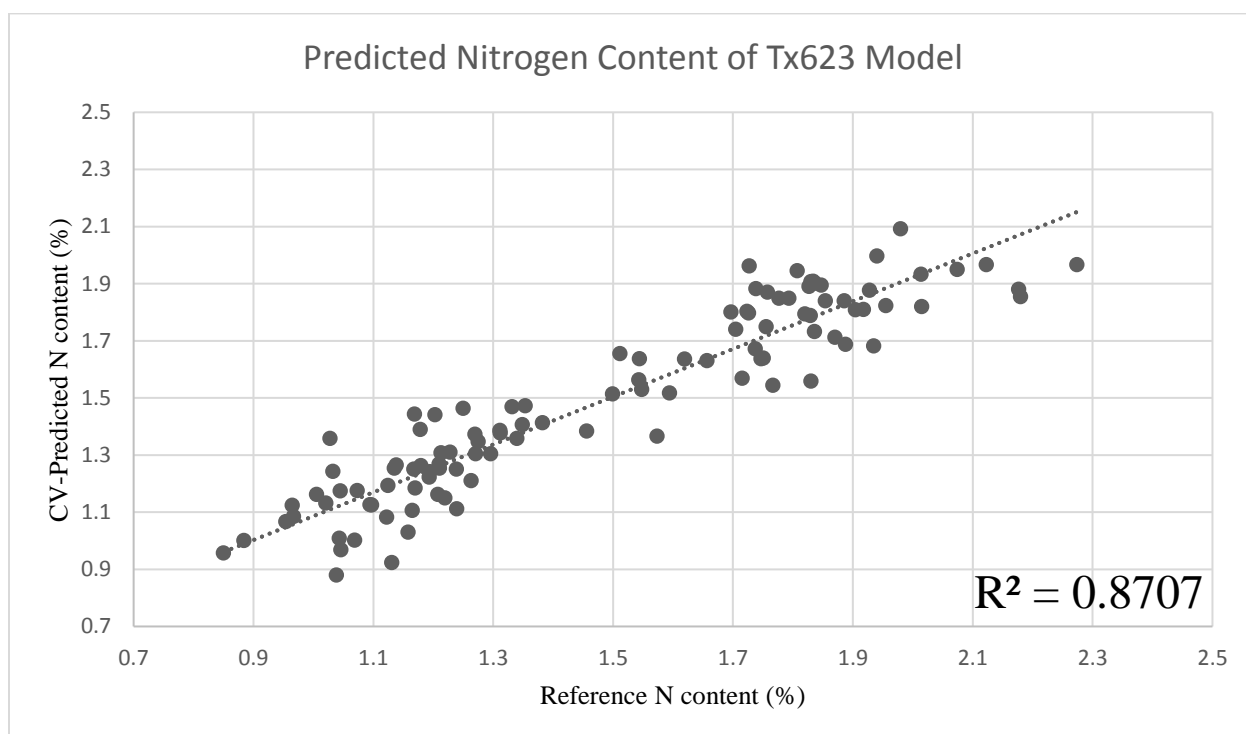


Figure 25. Plot of reference N content compared to cross-validated predicted N content using the model developed based on the response of Tx623

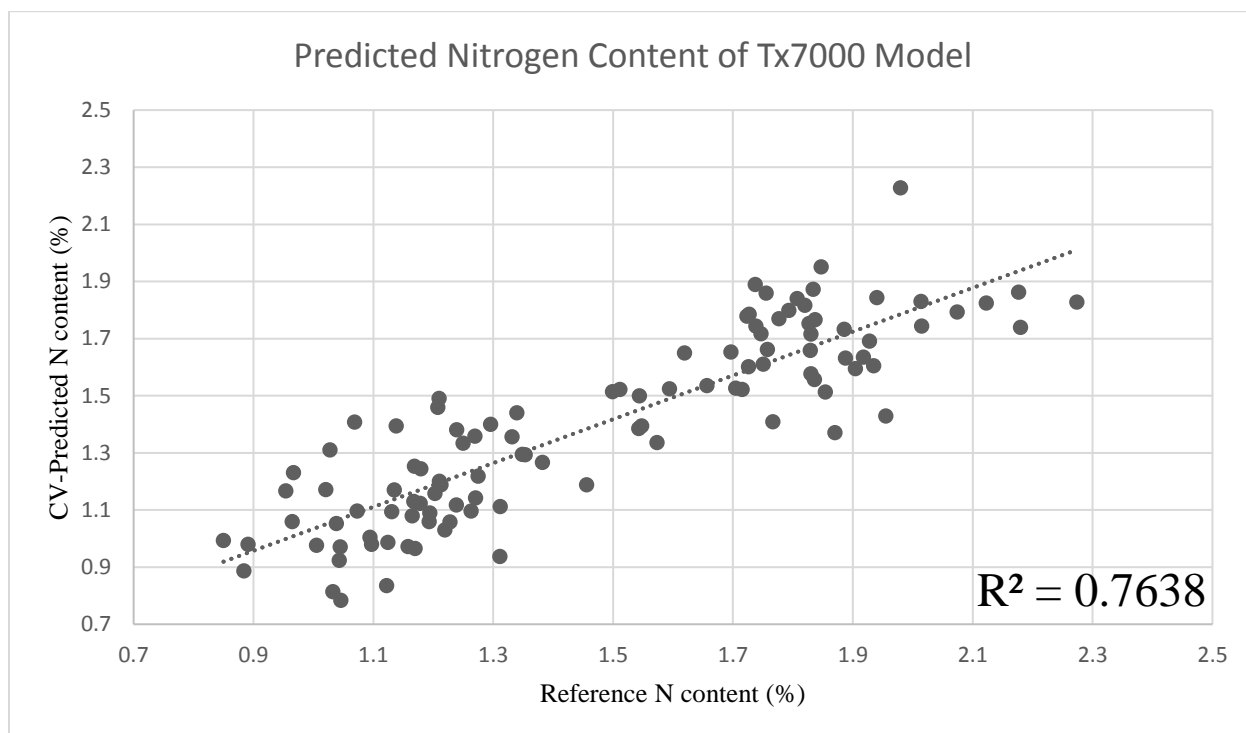


Figure 26. Plot of reference N content compared to cross-validated predicted N content using the model developed based on the response of Tx7000

2.3.8 Summary of all Nitrogen Content Models

To summarize all the nitrogen content models, a heatmap was generated to compare all of different models to each of the three genotypes and all of the genotypes in Fig. 27. The models developed for the nitrogen prediction had a coefficient of determination above 0.7 except for the B35 and Tx7000 models when predicting Tx623. The models generated using B35 and Tx7000 do not predict Tx623 as well as the Tx623 models predict both B35 and Tx7000. This could indicate that some genotypes, such as Tx623, make better models than others.

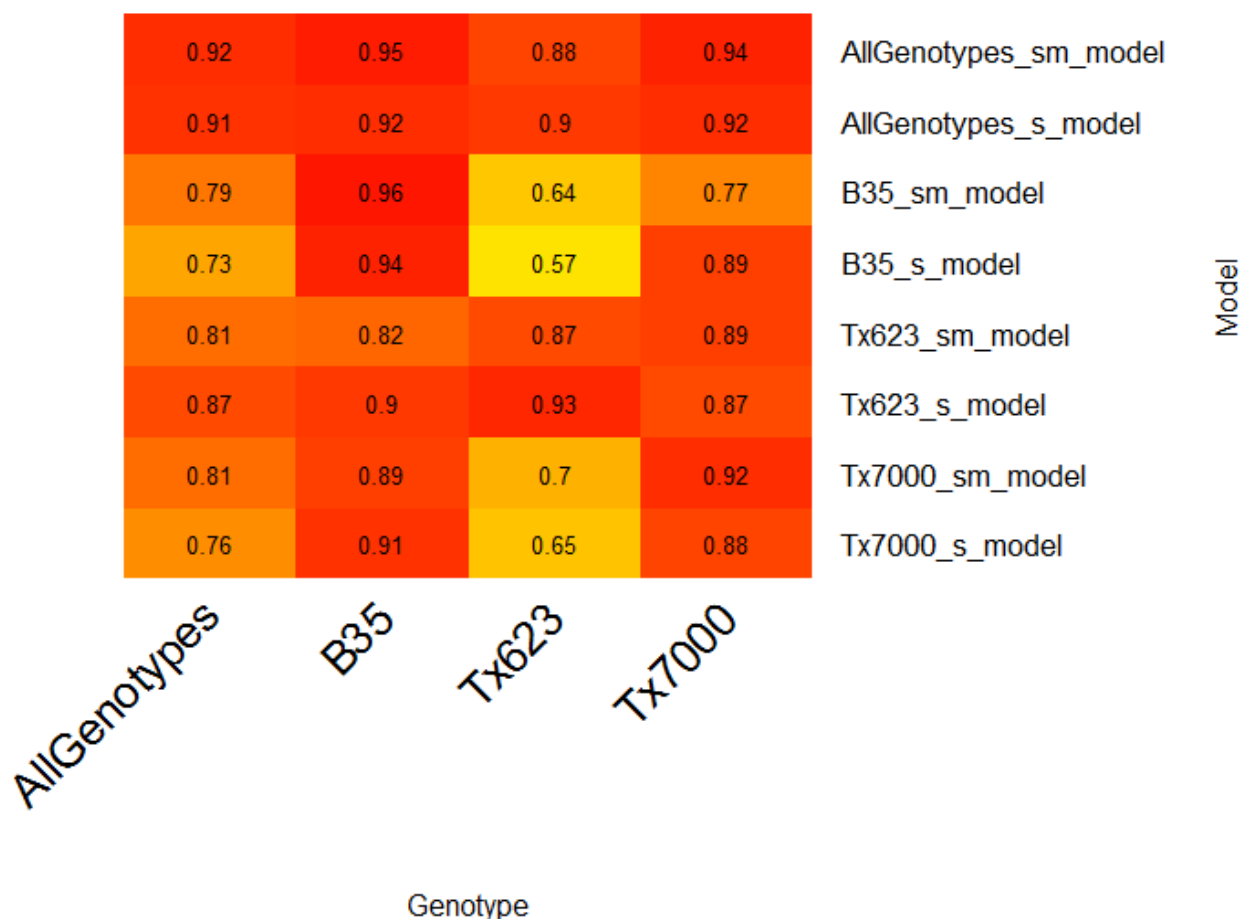


Figure 27. Heatmap of coefficients of determination of nitrogen content models for sorghum; _s_ represents spectral only models and _sm_ represents spectral and morphological models

2.3.9 Relative Water Content Models built using data from same nitrogen treatments

Drought and nitrogen stresses are often confounded and produce overlapping symptoms of plant stress. To determine how these interactions influence trait predictions, models were built using the data from the two high nitrogen treatments with varying drought stress levels. This model was then applied to the full data set, all four treatments, to predict the relative water content of all plants and the predicted RWC from that model was plotted against the reference RWC (Fig. 28).

The predictions separate based on treatments in the graph. When looking at the high water treatments, the higher nitrogen levels cause the predictions to be higher than the reference measurements and the lower nitrogen levels cause the predictions to be lower than the reference measurements. The low water treatments display a similar trend.

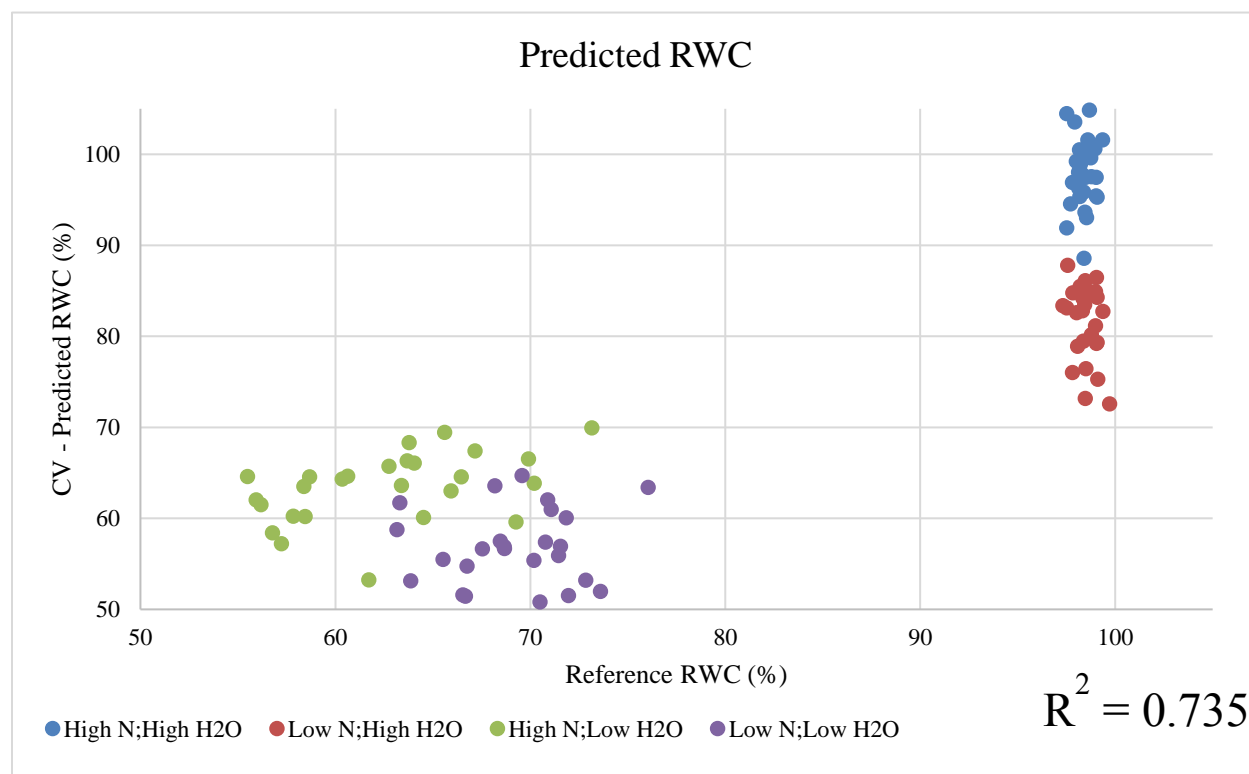


Figure 28. Plot of reference RWC compared to cross-validated predicted RWC of all three genotypes using the model developed on the data of different water treatments but uniform nitrogen treatments

2.3.10 Nitrogen Content Models built using data from same water treatments

A similar model was developed using the data from the two well-watered treatments with varying nitrogen levels. This model was then applied to the full data set, all four treatments, to predict the nitrogen content of all plants and the predicted nitrogen from that model was plotted against the reference nitrogen content (Fig. 29).

Figure 29 does not display the same distinct separation of treatments as figure 28 does. The coefficient of determination is lower and the accuracy was decreased by not taking the different water treatments in account when developing the N content predictions.

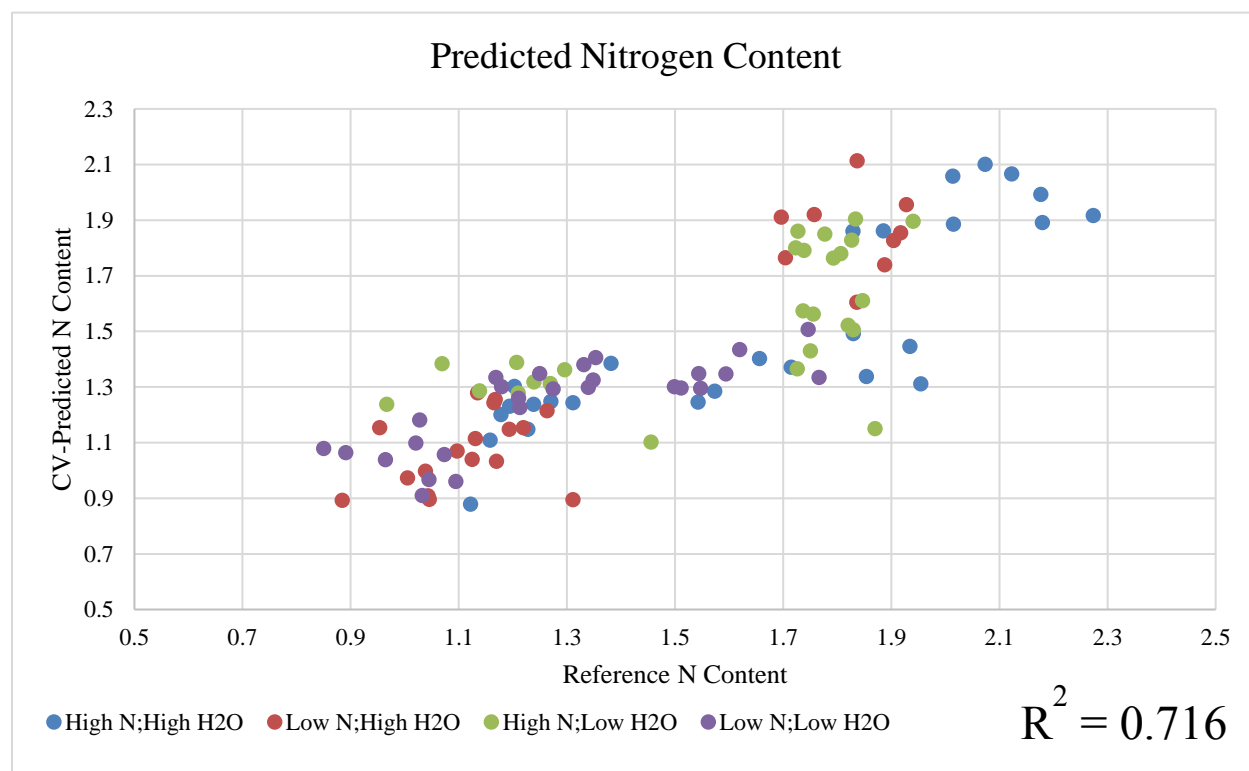


Figure 29. Plot of reference N content compared to cross-validated predicted N content of all three genotypes using the model developed on the data of different nitrogen treatments but uniform water treatments

2.3.11 Principal Component Analysis

In an attempt to explain some of the differences between the predictions of the models built using the three genotypes, a principal component analysis was generated using the spectral and morphological features of the three genotypes. The two principal components (PC1 and PC2) explain 96.5% of the explained variation. Confidence ellipses summarize the mean point of each genotype to compare the differences between the genotypes.

The PCA shows that the mean values of Tx7000 are centered on a different value than both B35 and Tx623. B35 and Tx623 are centered on the same mean. This could indicate that there are spectral or morphological differences between the B35 and Tx623 cluster and the Tx7000 cluster. Unfortunately, the PCA does not indicate why the models developed using B35 and Tx7000 are not accurate predictors of Tx623 reference N content.

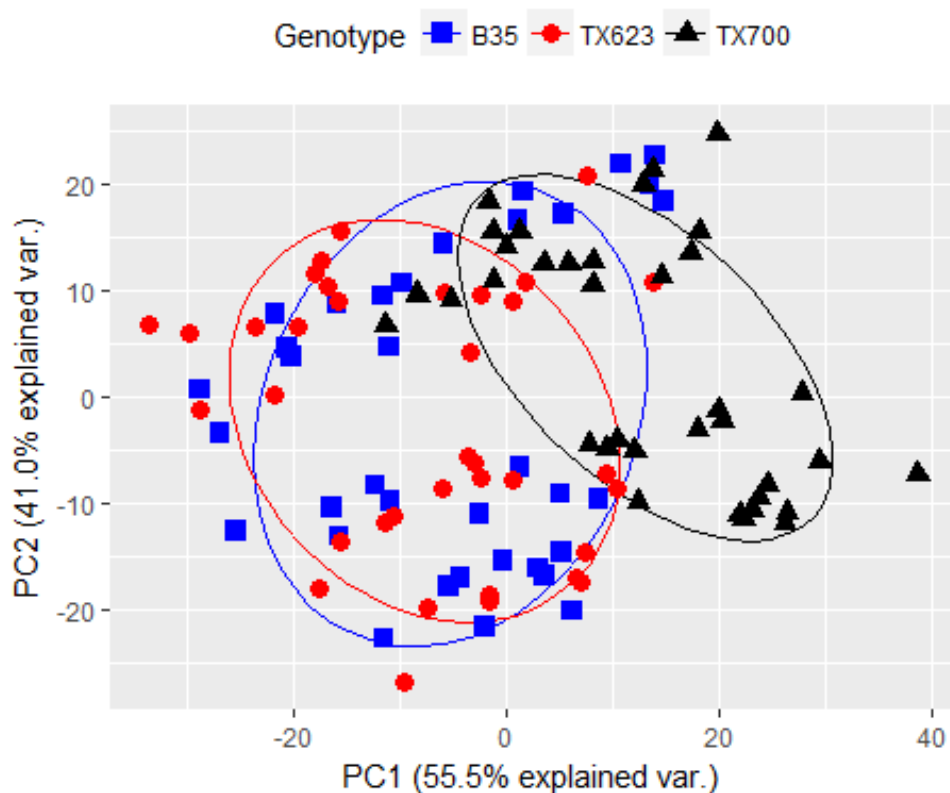


Figure 30. Principal Component Analysis of all spectral and morphological features

2.4 Discussion

2.4.1 Reference Measurements

The three varieties of sorghum, B35, Tx623, and Tx7000, were selected to represent varying mechanisms of drought tolerance. According to literature, Tx623 is generally considered to be drought susceptible (Paterson et al., 2009), Tx7000 has pre-flowering drought stress tolerance (Karper, 1949), and B35 has post-flowering drought stress tolerance (Walulu et al., 1994; Tuinstra et al., 1996). None of the genotypes displayed any difference in response to drought treatments. Tx7000, which displays pre-flowering drought stress tolerance in literature showed no differential response to pre-flowering drought stress that was present in this study. Due to height constraints, the imaging system could not image the plants are flowering, so this is probably why we saw no difference in drought response for these sorghum genotypes because the differences present themselves just before flowering in the case of Tx7000 and just after flowering in the case of B35.

There was a treatment, genotype, and a treatment by genotype effect in the nitrogen treatments. B35, which displays post-flowering drought stress, is considered a stay-green line (Walulu et al., 1994). Borrell and Hammer (2000) and Borrell et al. (1999) determined that stay-green sorghum lines stay green for longer after flowering due to higher leaf nitrogen status. This could account for the differential response of B35 under nitrogen stress.

2.4.2 Models

PLS regression is one of the more popular prediction methods used in the literature for hyperspectral imaging of both water status and nitrogen status in plants. Ge et al. (2016) used PLS regression to predict the water status of two genotypes of maize. This study found that when the predicted values were compared to the reference values, the coefficient of determination was 0.87.

Our study found a coefficient of determination of 0.91 when comparing the predicted to the reference values. The coefficients of determination are very comparable; however, our study evaluated three genotypes while Ge et al. only evaluated two genotypes. Ge et al. did evaluate the coefficients over time and determined that the two genotypes were less tightly correlated as they matured. This is something that our study did not evaluate. The Ge et al. study also evaluated plants on across a spectrum of relative water content from 68% to 93% while our study had two distinct clusters of RWC.

Li et al. (2013) and Nigon et al. (2014) both used PLS regression to predict the nitrogen status of plants. The Li et al. study used a dataset containing the data from two cultivars, two locations, and three years that was all sampled prior to the wheat flowering. This dataset had a coefficient of determination of 0.79 when the predicted values were compared to the reference values. Nigon et al. modeled the leaf N concentration in two genotypes of potato over a growing season with multiple imaging dates. The coefficient of determination across all dates when the predicted values were compared to the reference values was 0.78. Our study had a coefficient of determination of 0.90 when the predicted values were compared to the reference values of all three genotype when predicting nitrogen content. Both of these studies highlighted new approaches that could be utilized to improve our future projects including sampling over multiple dates or multiple locations.

There are only a few studies that develop PLS regression prediction models that combine both water and nitrogen treatments. One of these is Pandey et al. (2017) that collected hyperspectral images in order to predict a number of macro- and micronutrients, including N, as well as RWC. This study collected data from one cultivar of soybean and one cultivar of maize and combined the data to develop the prediction models. The coefficient of determination for the

water status was 0.97 when comparing the predicted values to the reference values while the N content prediction was 0.88 when comparing the predicted values to the reference values. However, this study didn't treat the same plants with both nitrogen and water treatments. Corti et al. (2016) combined water and nitrogen stresses when developing PLS regression models for spinach. This study found the coefficient of determination of the model developed using one variety of spinach for water content was 0.87 when the predicted values were compared to the reference values, but the coefficient of determination of the model developed for nitrogen content was only 0.41 when comparing the predicted and the reference values. The coefficients of determination in our study for RWC and N content were 0.91 and 0.90, respectively, when comparing the predicted values to the reference values.

The predictions developed in this study are comparable to previous predictions in the literature. However, the prediction models developed in this study utilized three distinct genotypes with differing drought adaptations and a combination of water and nitrogen stresses, which makes this study unique. From this study, we would recommend the RWC and N content models developed using the data from all three genotypes because these three genotypes represent three different drought tolerance responses in sorghum.

2.4.3 Importance of verifying the applicability of spectral only models

Models built using spectral and morphological features of the plant extracted from the hyperspectral images were, in general, slightly, but not significantly more accurate than models built using only spectral features of the plant for both relative water content and nitrogen content predictions. It may be important in the future to build models using strictly spectral features. Morphological features are available for this study because of the unique design of the automated greenhouse. The imaging tower can be used to collect data on the plant from the top and the side

with controlled lighting. After segmentation, the morphological features of the plant can be calculated. However, a handheld device which may be more easily managed and accessible for collecting field measurements for a wider variety of people, would only use spectral features so it is important to test and verify the robustness and applicability of spectral only models. The three spectral only models had coefficients of determination of 0.843, 0.843, and 0.796, respectively.

Models developed using spectral only features may also be highly valuable when plants exhibit physiological changes related to drought. When sorghum is water stressed, the leaves roll and thus the leaf area of the plant is reduced (O'Toole & Cruz, 1980). Zhao et al. (2005) found that moderate nitrogen deficit resulted in decreased leaf area and dry matter accumulation while severe nitrogen deficit affected the height of the plant. In models built with morphological features, the leaf area and the plant height may be components used in the prediction model. However, when predicting the water status of plants with only moderate drought stress, the leaf area may not be as reduced as in severe stress due to a lack of severe leaf rolling. This will be important in breeding programs in the identification of lines that can maintain plant water content under moderate drought stress as opposed to severe drought stress.

2.4.4 Importance of water and nitrogen treatments in concert

Figure 29 shows a clear differentiation in prediction based on the treatment. This model was built using varying water treatments with varying relative water contents but with the same nitrogen treatments. This affirms one of the objectives of this experiment. We expected nitrogen and water stress phenotypes to interact because nitrogen deficiency as a result of drought is the largest contributor to the decrease of growth under drought stress (Heckathorn et al., 1997). He & Dijkstra (2014) found N content decreased by almost 4% in a drought stress study. Other studies have also observed drought reducing nitrogen content through reduction in nitrogen uptake and

distribution (Rouphael et al., 2012), a decline in soil moisture (Fierer & Schimel, 2002), and reduction in mineralization (Sardens & Penuelas, 2012; Cramer et al., 2009). In our study, the nitrogen content became a large factor in predicting the RWC of the plant as shown in Figure 29 where the four treatments are in four distinct groups. Conversely, the model developed with the high water treatments to predict the nitrogen content produced a graph (Fig. 30) without the distinct groups seen in the graph of the model built using high nitrogen treatments to predict RWC but has a lower accuracy of prediction. This confirms the importance of growing plants under both water and nitrogen stresses.

2.5 Conclusion

The goal of the sorghum calibration experiment was to develop a robust model to predict the relative water content of sorghum and a model to predict the nitrogen content of sorghum. While this experiment utilized only three genotypes, it revealed some interesting conclusions about hyperspectral imaging models. The best models were those built with all three genotypes to encompass the most genetic and physiological variability.

This experiment also proved that partial least squares models built with one genotype can accurately predict other genotypes of sorghum for both relative water content and nitrogen content. We can see this through the coefficients of determination for all of the relative water contents that are all above 0.75. For the nitrogen content predictions, the coefficients of determination were all over 0.57. While this is not a strong prediction, it does indicate that we are more likely than not to predict the correct nitrogen content.

This experiment also proves that we can build robust models, often equally robust models, using only the spectral features as opposed to the spectral and the morphological features. This could become important as more handheld spectrometers are taken to the field.

Nitrogen and water signals are also confounded so it is important to account for both water and nitrogen in our models by using both nitrogen and water treatments. If we do not account for differing levels of nitrogen in our relative water content predictions, we end up with four distinct groups in the graph. If we do not account for differing levels of water in our nitrogen content models, we end up with decreased predictive power in our models.

Finally, when developing nitrogen prediction models, we discovered a curious phenomenon where the hyperspectral models of some genotypes are more predictive than the hyperspectral models of certain other genotype.

The next chapter in this thesis will cover another hyperspectral imaging study utilizing six genotypes of maize to predict both relative water content and nitrogen content. We then use the sorghum calibration data to attempt to predict the maize reference measurements. Finally, we will combine both the sorghum and maize experimental data.

CHAPTER 3: MAIZE MULTIPLE GENOTYPE STUDY

3.1 Introduction

Maize (*Zea mays* L.), also known as corn, is a close cousin of sorghum (*Sorghum bicolor* (L.) Moench). Maize is a C4 grass that was domesticated around 10,000 years ago in central Mexico from the progenitor teosinte (Corn: plant, 2018). Maize performs best on well-drained and well-aerated soils but it is also quite tolerant to a variety of soils except for dense clay soils or very sandy soils (Maize, FAO, 2018). Maize is fairly sensitive to drought and salinity and exhibits poor adaptation to low fertility soils, such as soils deficient in nitrogen. Maize is considered both less drought tolerant than sorghum and less adapted to low nitrogen conditions. These features of maize make it a key target for nitrogen and water use efficiency improvements. Another incentive to improve maize is that it is the most important cereal grain in the world and is used widely for human food, livestock feed, biofuels, and industrial applications (Maize, FAO, 2018).

Many of the same challenges face maize breeders and sorghum breeders. The challenge is developing a quick, high-throughput, accurate system to identify the genotypes that have the highest relative water contents and nitrogen contents under stress conditions. Phenomics, particularly through hyperspectral imaging, could provide a quick, high-throughput and accurate solution. Phenomics is broadly defined as the intense and detailed study of the physical aspects of the plant and relate the phenotype to the genotype (Araus and Cairns, 2014). However, as previously mentioned, the greatest bottleneck to these accurate predictions in phenomics is genetic variation in crop species.

In previous studies, there has been a distinct lack of genetic diversity represented in the experimental designs. Several recent studies used only one cultivar to study either drought or

nitrogen (Moshou et al., 2014; Pandey et al., 2017; Corti et al., 2017). A handful of other studies used two cultivars (Nigon et al., 2015; Ge et al., 2016; Bhugra et al., 2017), while a few others used three genotypes (Li et al., 2014; Kersting et al., 2012; and Behmann et al., 2014). One of the few studies that included genetic variation in a study of drought or nitrogen stresses was a study out of Italy that assessed the effects of drought on oak foliage (Cotrozzi et al., 2017). This study used oak seeds collected from individual mothers in four different regions of Central America, which encompassed four different countries and a wide range of genetics.

Our goal is to develop maize phenotyping models that represent a wide range of genetics in the hopes that these are more universal models that can be used to predict the nitrogen content and relative water content of a variety of maize genotypes. To this end, we developed an experiment using six genotypes of maize representing elite temperate and tropical germplasm.

3.2 Materials and Methods

3.2.1 Maize Seed Sources

The six genotypes used for this multiple genotype study were selected from a variety of sources having specific reactions to drought and nitrogen stresses. The B73xMo17 hybrid is a classic hybrid developed in 1973 that remained the preeminent hybrid in the United States corn industry for five to seven years (Hoegemeyer, 2014). This is a cross between the Iowa Stiff Stalk Synthetic heterotic group and the Lancaster Sure Crop (non-stiff stalk) heterotic group. P1105AM was selected as a more modern commercial hybrid from the Aquamax© brand of Dupont Pioneer. The Aquamax lines are touted as having superior drought tolerance.

The Tuinstra lab has been involved in developing a series of hybrids using a non-stiff stalk male line called PHP02. This is an ex-plant variety protected (ex-PVP) line originally developed

by Pioneer Hi-bred International (PI 601570, USDA GRIN, n.d.). Four of these hybrids were selected for this study, BCC03xPHP02, PHG80xPHP02, CML550xPHP02, and PHJ33xPHP02. Both PHG80 and PHJ33 are ex-PVP lines developed by Pioneer in the 1980s (PI 601037, USDA GRIN, n.d., PI601774, USDA GRIN, n.d.) while BCC03 was developed in Minnesota in the late 1980s by Northrup, King and Company (PI 544065, USDA GRIN, n.d.). Preliminary data from field trials in Arizona suggests that PHJ33xPHP02 yielded well under drought stress while G80xPHP02 and BCC03xPHP02 exhibited greater susceptibility to drought.

CML550 is a CIMMYT maize inbred line released in 2013 (“CIMMYT releases 22 new maize inbred lines for the tropics and subtropics”, 2013). This line is an intermediate maturity line and is characterized as a CIMMYT heterotic group B type and is often used as a seed parent. CML550 generally produces hybrids with very good adaptation to low nitrogen and low water conditions.

3.2.2 Soil Medium

See Section 2.2.2.

3.2.3 Design of Experiment

The design of experiment for this study was a randomized complete block design with twelve blocks. Each combination of six genotypes and four treatments was represented in each block of the design (Table 5).

Table 4. Genotype and treatment combinations evaluated in this experiment

Genotype	<u>Nitrogen (mM)</u>	<u>Water</u>
B73xMo17	40	Fully watered
	40	Severe drought stress
	5	Fully watered
	5	Severe drought stress
BCC03xPHP02	40	Fully watered
	40	Severe drought stress
	5	Fully watered
	5	Severe drought stress
CML550xPHP02	40	Fully watered
	40	Severe drought stress
	5	Fully watered
	5	Severe drought stress
G80xPHP02	40	Fully watered
	40	Severe drought stress
	5	Fully watered
	5	Severe drought stress
P1105AM	40	Fully watered
	40	Severe drought stress
	5	Fully watered
	5	Severe drought stress
PHJ33xPHP02	40	Fully watered
	40	Severe drought stress
	5	Fully watered
	5	Severe drought stress

3.2.4 Application of Stress

See Section 2.2.4.

3.2.5 Automated Imaging System

See Section 2.2.5.

3.2.6 Relative Water Content Measurements

See Section 2.2.6.

3.2.7 Nitrogen Content Measurements

See Section 2.2.7.

3.2.8 Data Processing

See Section 2.2.8.

3.2.9 PLS_ToolBox in MatLab

See Section 2.2.9

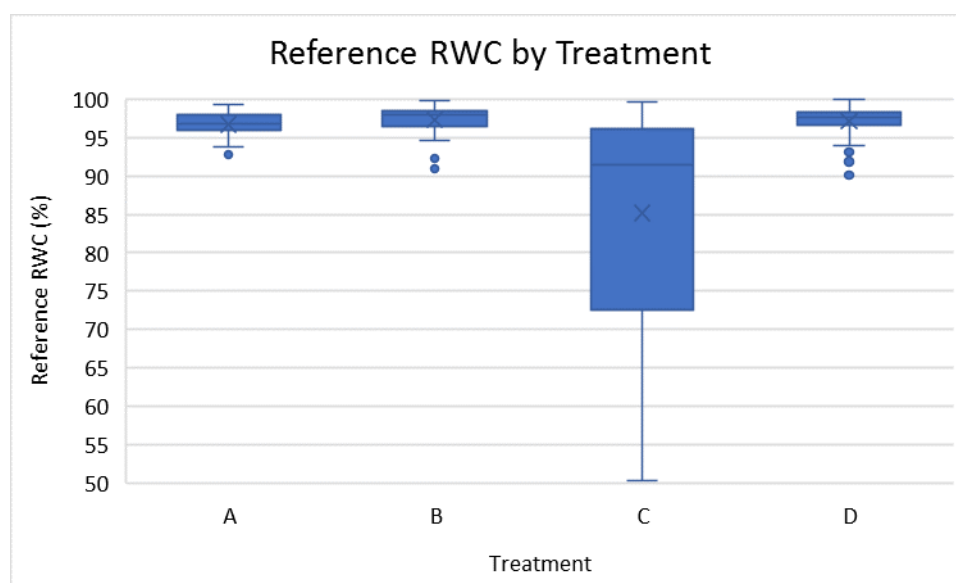
3.3 Results

3.3.1 Relative Water Content Results

The relative water content of the maize plants varied from 50.4% to 100% for the plants in this study (Fig. 31). Treatment C, which was treated with high nitrogen and severe drought stress, displayed the most drought stress while treatment D, which was treated with low nitrogen and severe drought stress, did not display drought stress. The analysis of variance of the RWC is shown in Table 5. The formula used for the ANOVA is:

$$\text{RWC} \sim \text{Treatment} + \text{Genotype} + \text{Treatment} * \text{Genotype}$$

The treatment and genotype main effects were not significant but the treatment by genotype interaction was highly significant (Table 6). An interaction plot was generated (Fig. 32) to visualize the interaction between genotype and treatment. Most of the treatment by genotype interaction resulted from the differential response of the hybrids to treatment C. CML550xPHP02, B73xMo17, and P1105AM had relatively higher RWC values than the other hybrids in the study. CML550xPHP02 had the highest average RWC under treatment C.



A	Well-Watered; 40 mM N
B	Well-Watered; 5 mM N
C	Severe Drought Stress; 40 mM N
D	Severe Drought Stress; 5 mM N

Figure 31. RWC values for maize plants by treatment

Table 5. Analysis of Variance (ANOVA) table of relative water content

ANOVA Table (Type III tests)					
Response: RWC					
	Sum Squares	Df	F Value	Pr(>F)	
(Intercept)	109979	1	2605.1473	<2.2e-16	***
Treatment	262	3	2.0658	0.105321	
Genotype	29	5	0.1353	0.984067	
Treatment x Genotype	1422	15	2.2449	0.005722	**
Residuals	10343	245			
Significance codes: 0 , '***' 0.001, '**' 0.01, '*' 0.05					

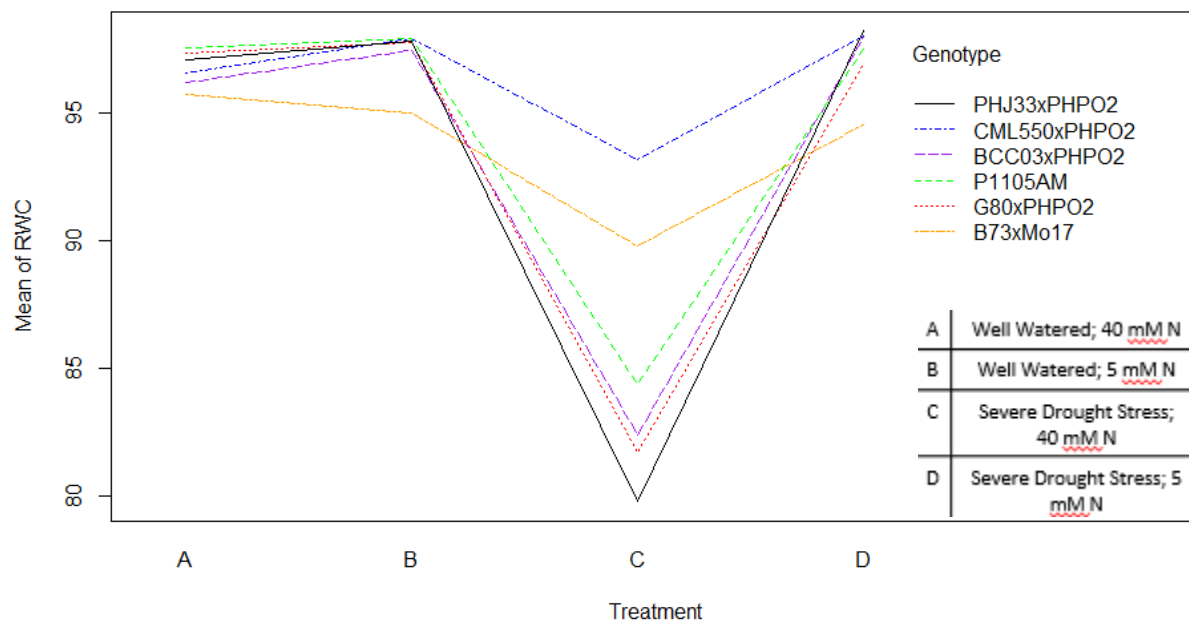


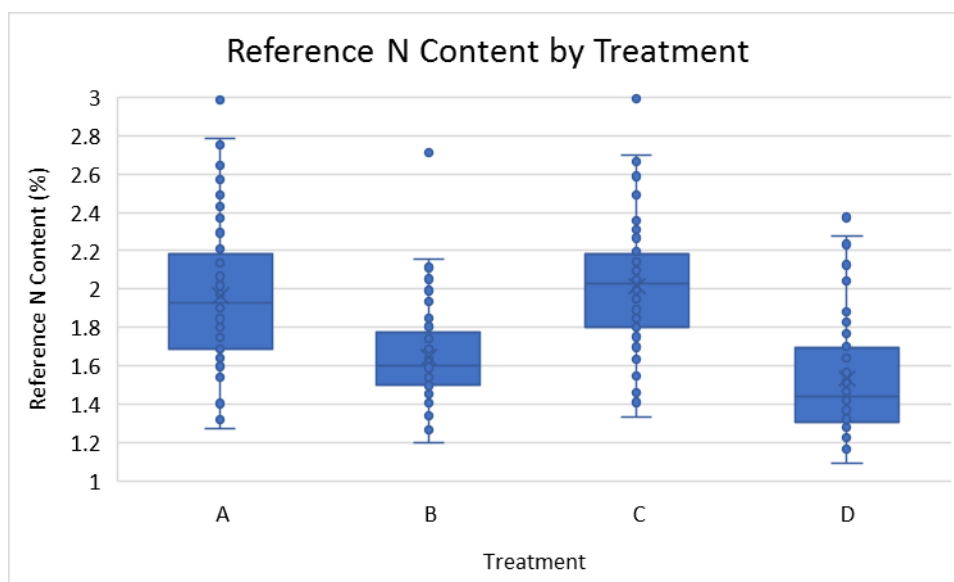
Figure 32. Interaction plot of RWC by genotype for the four treatments

3.3.2 Nitrogen Content Results

The nitrogen content of the maize plants varied from 1.09% to 2.99% of the leaf sample (Fig. 33). The nitrogen content results plotted on this graph indicate that the two low nitrogen treatments are lower than the two high nitrogen treatments. The analysis of variance results of the N content is shown in Table 7. The formula used for the ANOVA is:

$$\text{Ncontent} \sim \text{Treatment} + \text{Genotype} + \text{Treatment} * \text{Genotype}$$

The treatment main effect is highly significant but there is no genotype main effect or interaction affect between treatment and genotype. The plants grown under the low nitrogen treatment did indeed have lower nitrogen contents than those plants grown under the high nitrogen treatments.



A	Well-Watered; 40 mM N
B	Well-Watered; 5 mM N
C	Severe Drought Stress; 40 mM N
D	Severe Drought Stress; 5 mM N

Figure 33. Graph of reference N content by treatment

Table 6. Analysis of Variance (ANOVA) table of reference nitrogen content

ANOVA Table (Type III tests)					
Response: N content					
	Sum Squares	Df	F Value	Pr(>F)	
(Intercept)	49.440	1	531.8543	<2.2e-16	***
Treatment	1.368	3	4.9065	0.002497	**
Genotype	0.686	5	1.4759	0.198271	
Treatment x Genotype	0.871	15	0.6245	0.853699	
Residuals	22.775	245			
Significance codes: 0, '***' 0.001, '**' 0.01, '*' 0.05					

3.3.3 Relative Water Content Models

Partial least squares (PLS) regression was used to model RWC using the hyperspectral data generated in maize. The models built with the spectral and morphological features of the multiple maize genotypes produced the best predictions for RWC. The RWC models were developed for all six genotypes combined and all six genotypes individually for a total of seven RWC models.

The first model was generated using all six genotypes combined and had a coefficient of determination of 0.72 which was higher than any of the individual genotype models (Fig. 34). Models built using the individual hybrids had lower coefficients of determination ranging from 0.43 to 0.69 (Figs. 35-40). The model developed using B73xMo17 had the best coefficient of determination of any of the individual genotype models at 0.69 (Fig. 35), and the model developed using G80xPHP02 had the lowest coefficient of determination at 0.43 (Fig. 38).

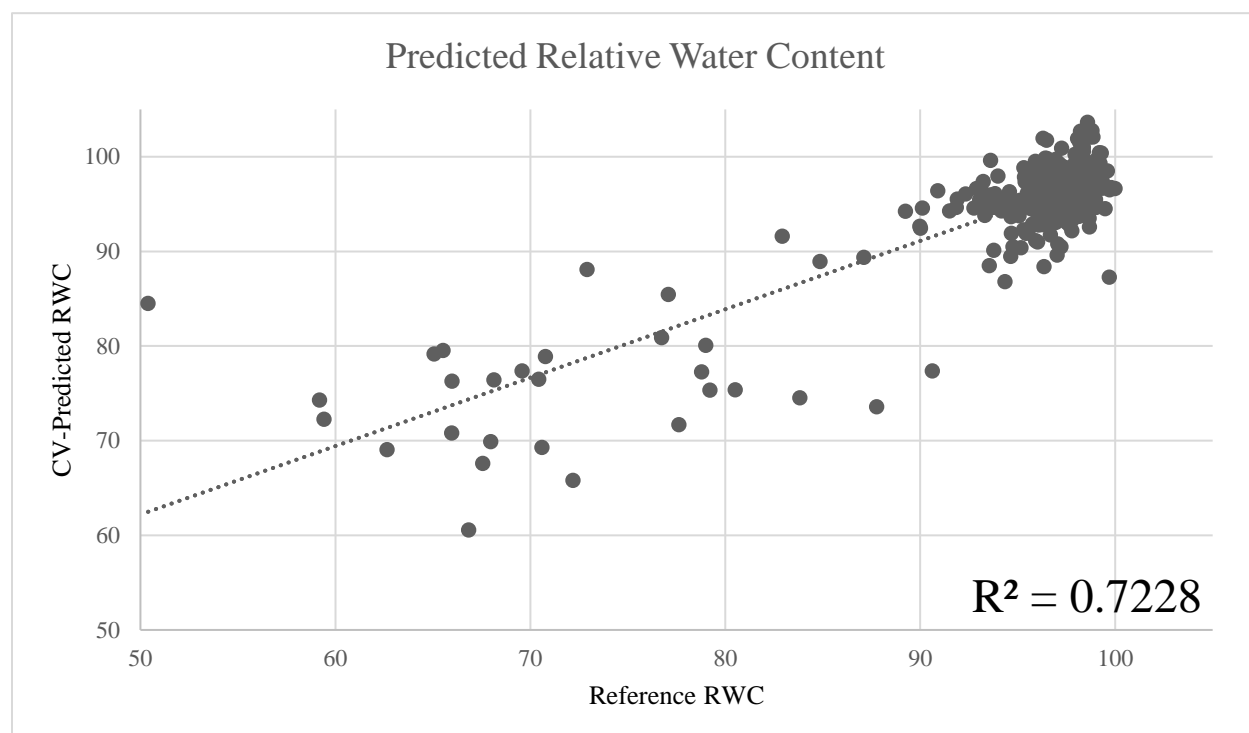


Figure 34. Plot of cross-validated relative water content against reference relative water content for the model built with all six genotypes.

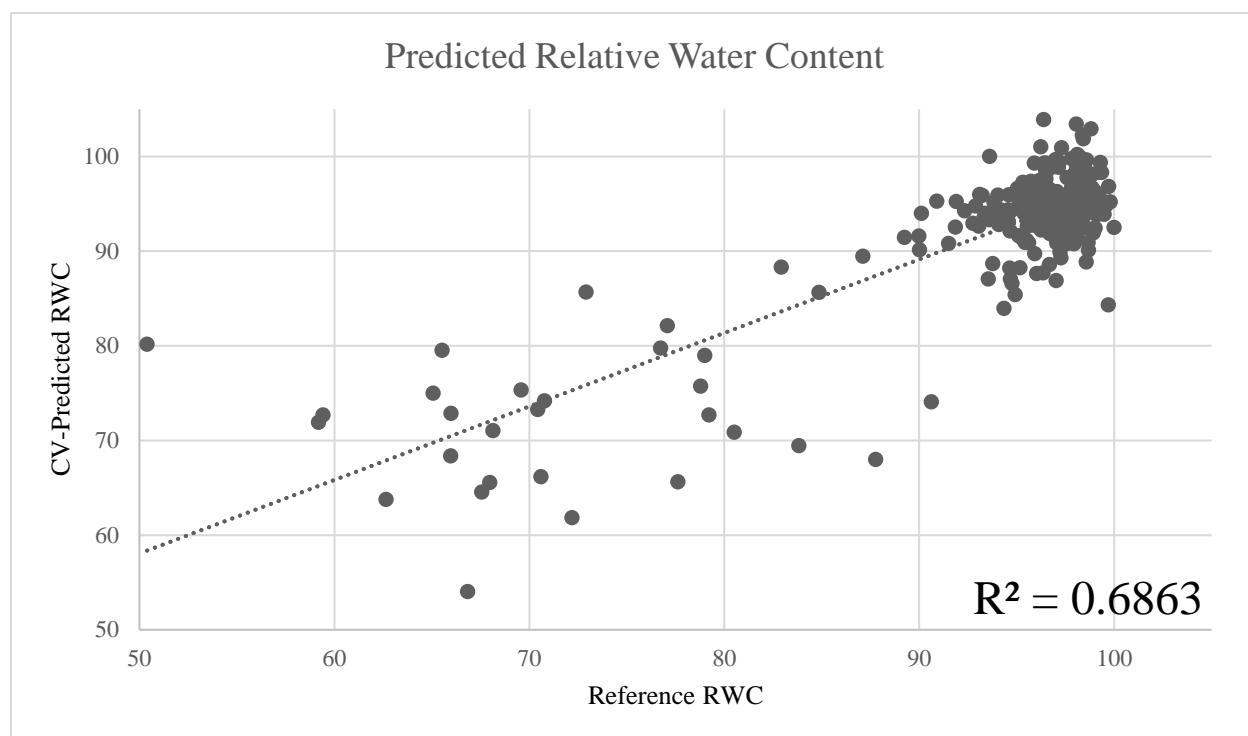


Figure 35. Plot of cross-validated relative water content against reference relative water content for the model built with B73xMo17.

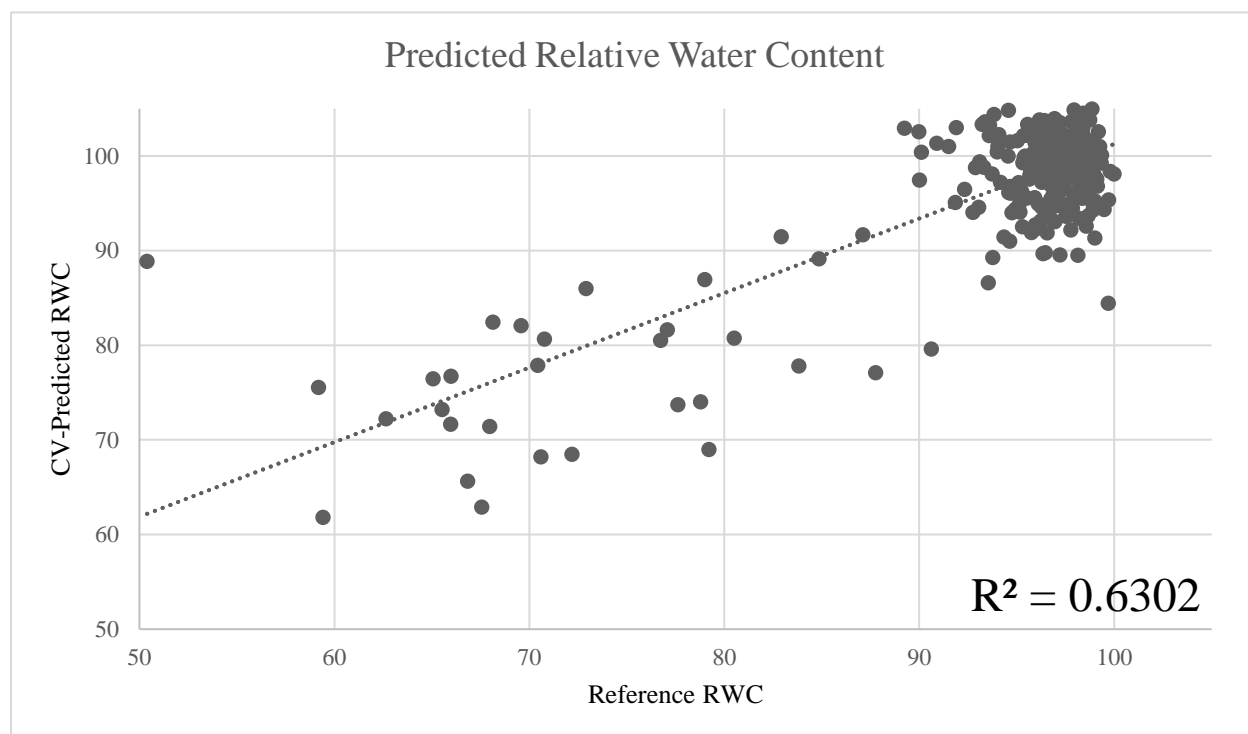


Figure 36. Plot of cross-validated relative water content against reference relative water content for the model built with BCC03xPHP02.

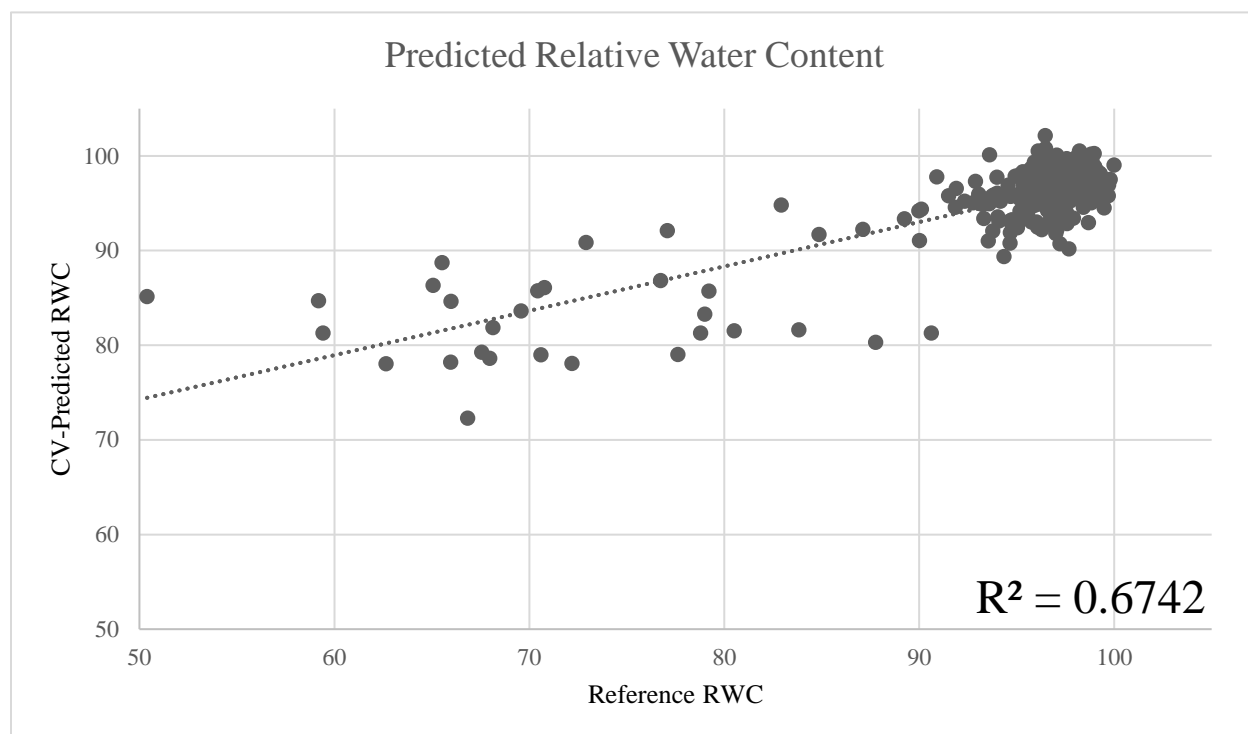


Figure 37. Plot of cross-validated relative water content against reference relative water content for the model built with CML550xPHP02.

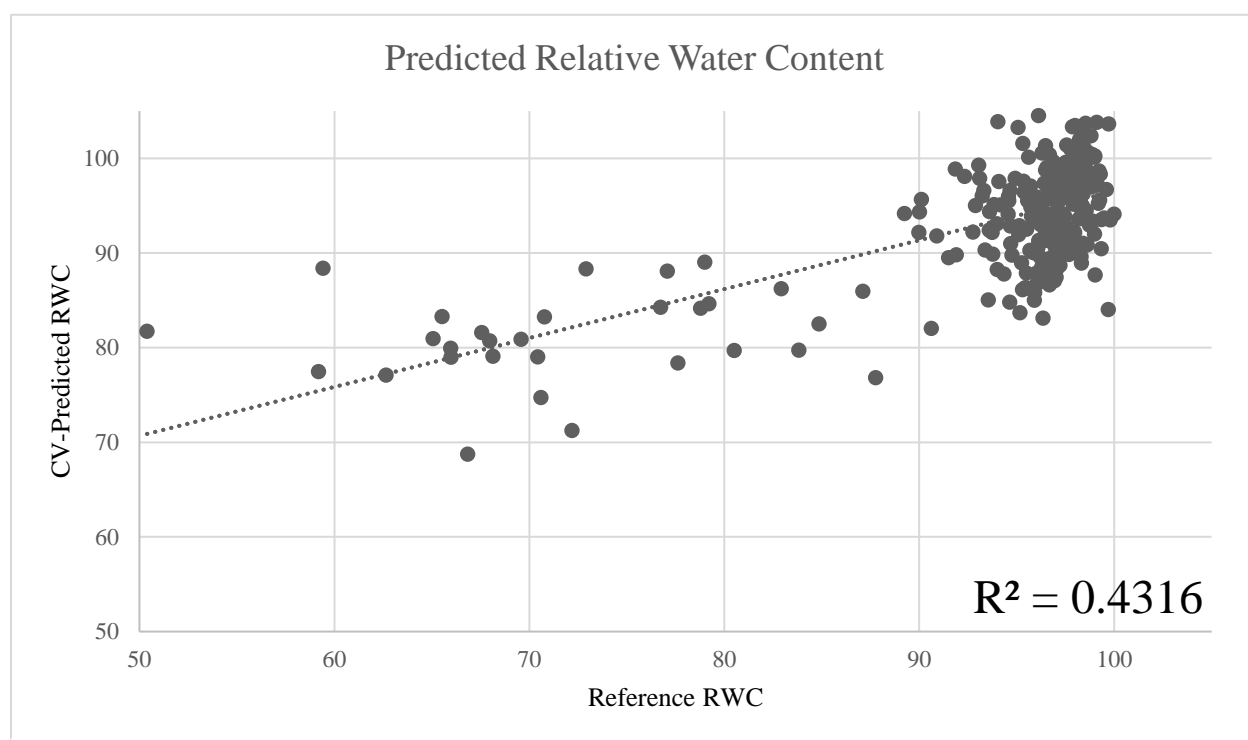


Figure 38. Plot of cross-validated relative water content against reference relative water content for the model built with G80xPHP02

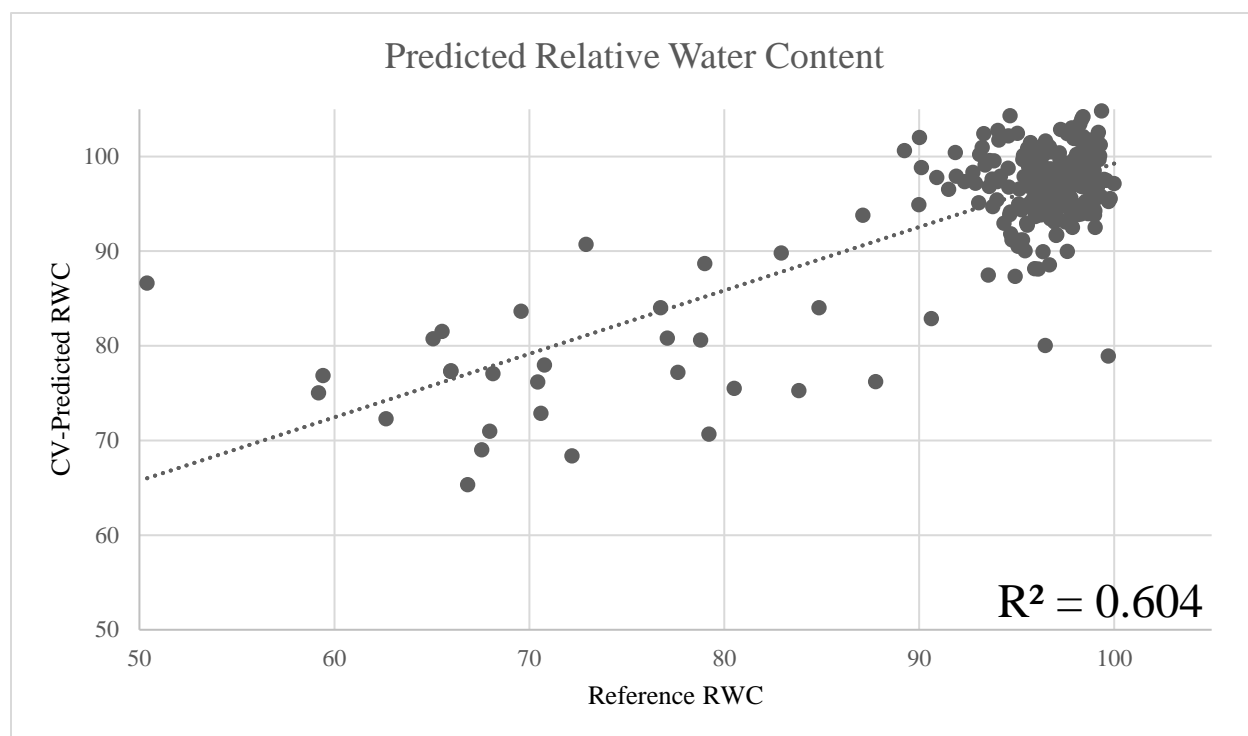


Figure 39. Plot of cross-validated relative water content against reference relative water content for the model built with PHJ33xPHP02

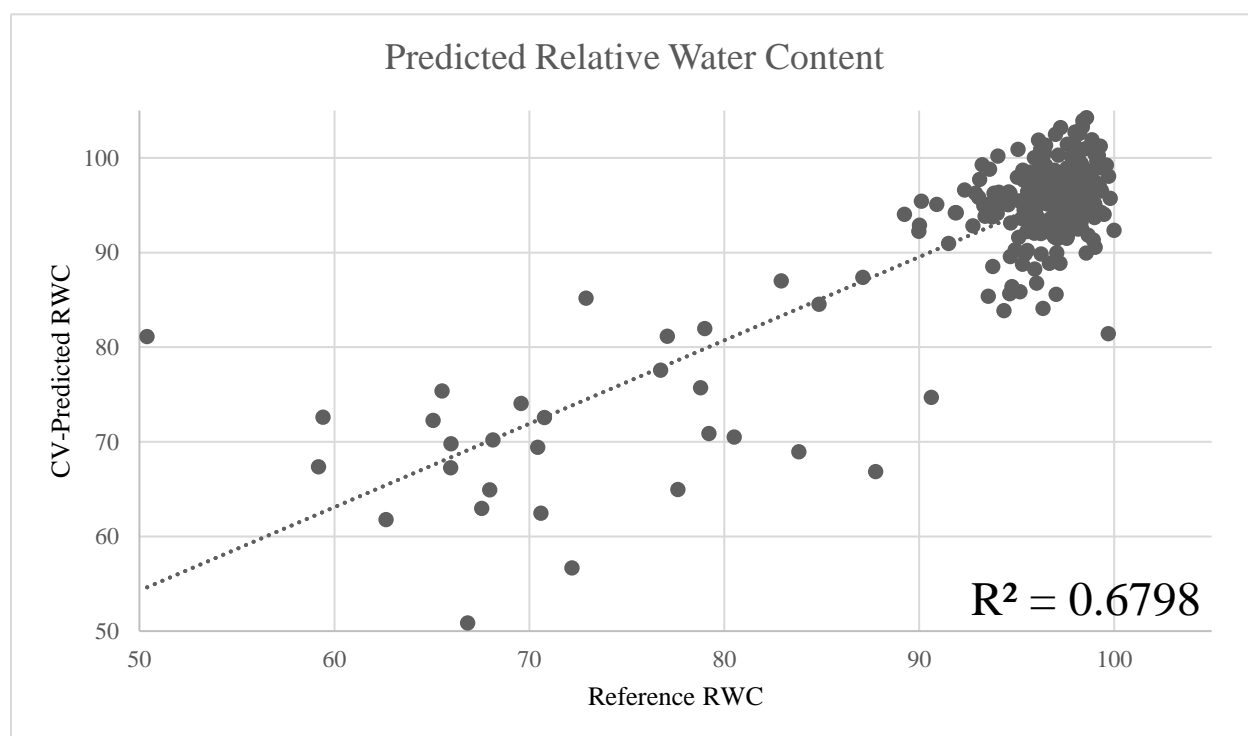


Figure 40. Plot of cross-validated relative water content against reference relative water content for the model built with P1105AM

3.3.4 Summary of all Relative Water Content Models

The seven maize models and the sorghum model were compared for modeling of RWC across all the genotypes. The coefficients of determination for each of the plots are summarized below (Fig. 41). All of the models developed from a single genotype were more accurate predictors of the respective genotype the model was developed from. However, the combined maize model that was developed using all of the hybrids had the highest prediction of all genotypes together with a coefficient of determination of 0.72. The models developed using B73xMo17, P1105AM, and CML550xPHPO2 hybrids were also good models with high coefficients of determination. The model developed using G80xPHPO2 performed quite poorly. The sorghum model that did not use maize training data performed poorly as well.

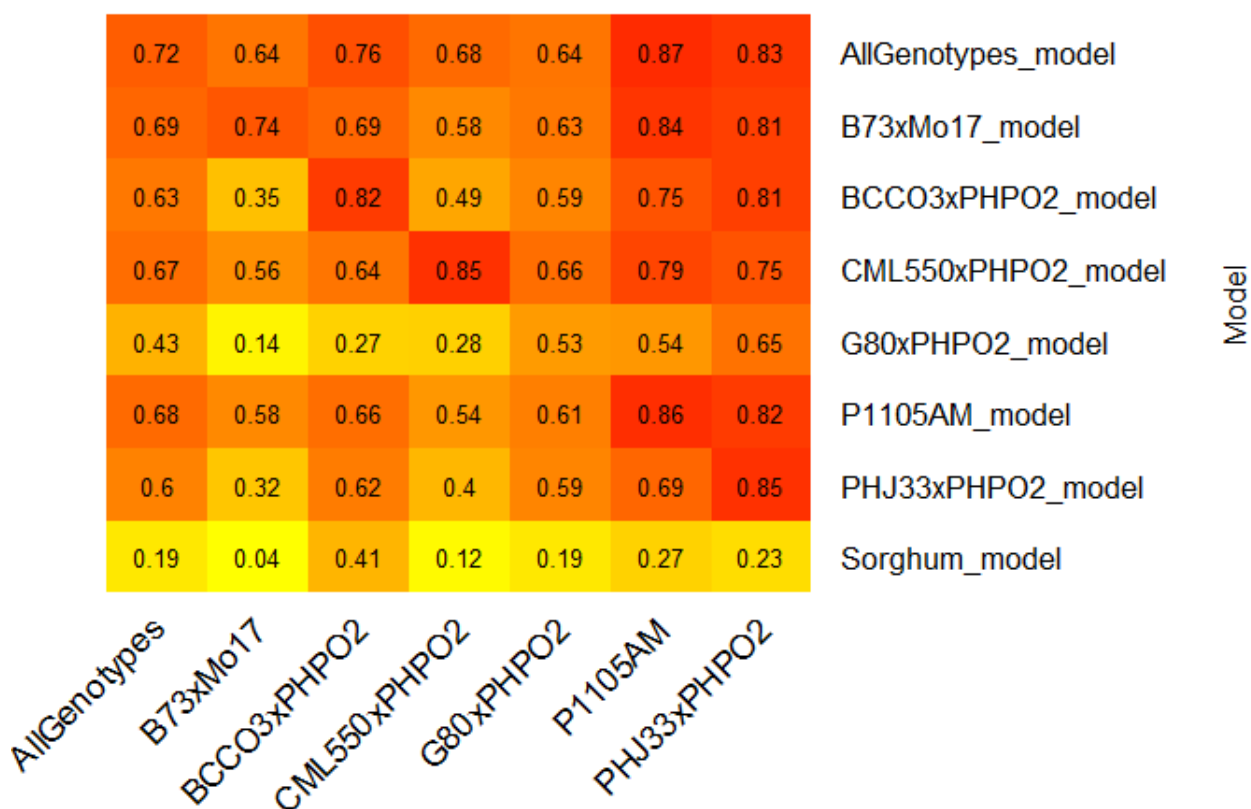


Figure 41. Heatmap of all coefficients of determination for relative water content models; _s_ represents spectral only models and _sm_ represents spectral and morphological models

3.3.5 Nitrogen Content Models

Seven new spectral and morphological feature models were generated to predict the nitrogen content of maize plants. These models were built using either all of the genotypes or with individual hybrid performance data. The model built using all of the hybrids exhibited the highest coefficient of determination of 0.64 (Fig. 42). Several of the models developed based on the individual hybrid performance were also highly predictive with BCC03xPHP02 exhibiting a coefficient of determination of 0.59 (Fig. 44). For BCC03xPHP02 the coefficient of determination was 0.59 (Fig. 43), CML550xPHP02 exhibits a coefficient of determination of 0.50 (Fig. 45), G80xPHP02 exhibits a coefficient of determination of 0.48 (Fig. 46), the P1105AM model displayed a coefficient of determination of 0.61 (Fig. 47), and finally for the model built using PHJ33xPHP02 the coefficient of determination is 0.59 (Fig. 48).

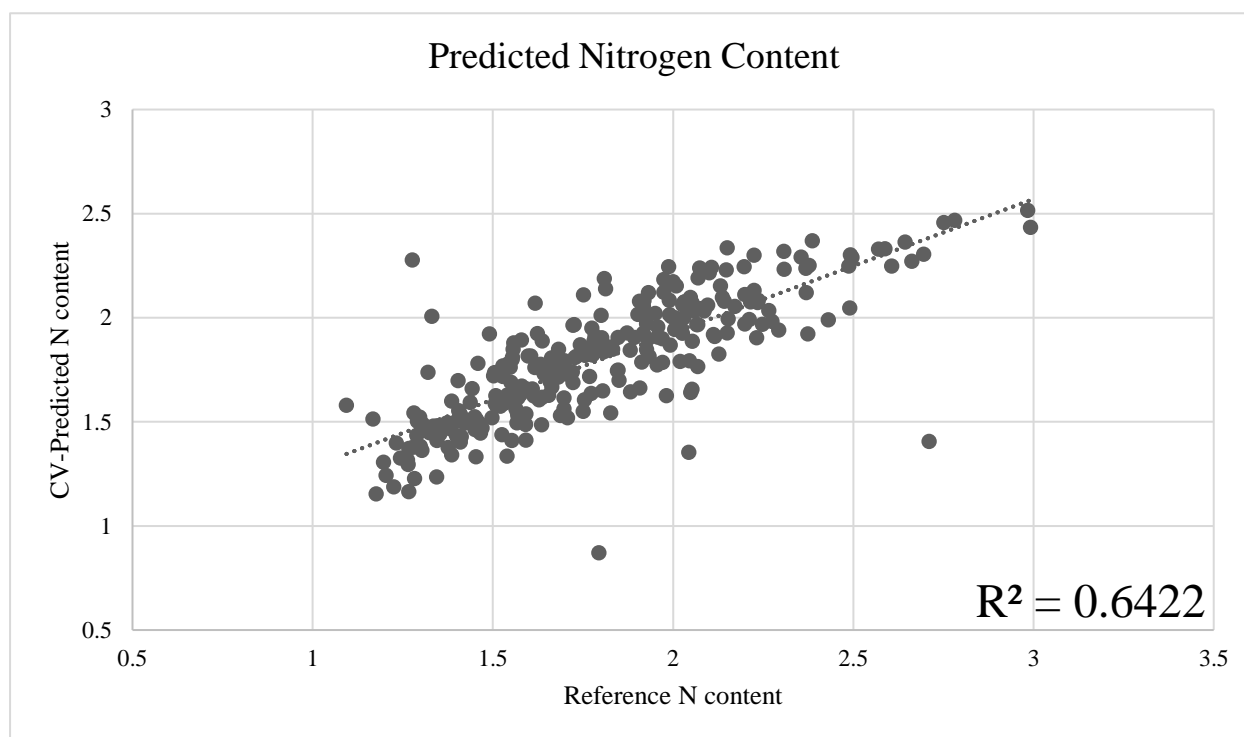


Figure 42. Plot of cross-validated nitrogen content against reference nitrogen content for the model built with all six genotypes

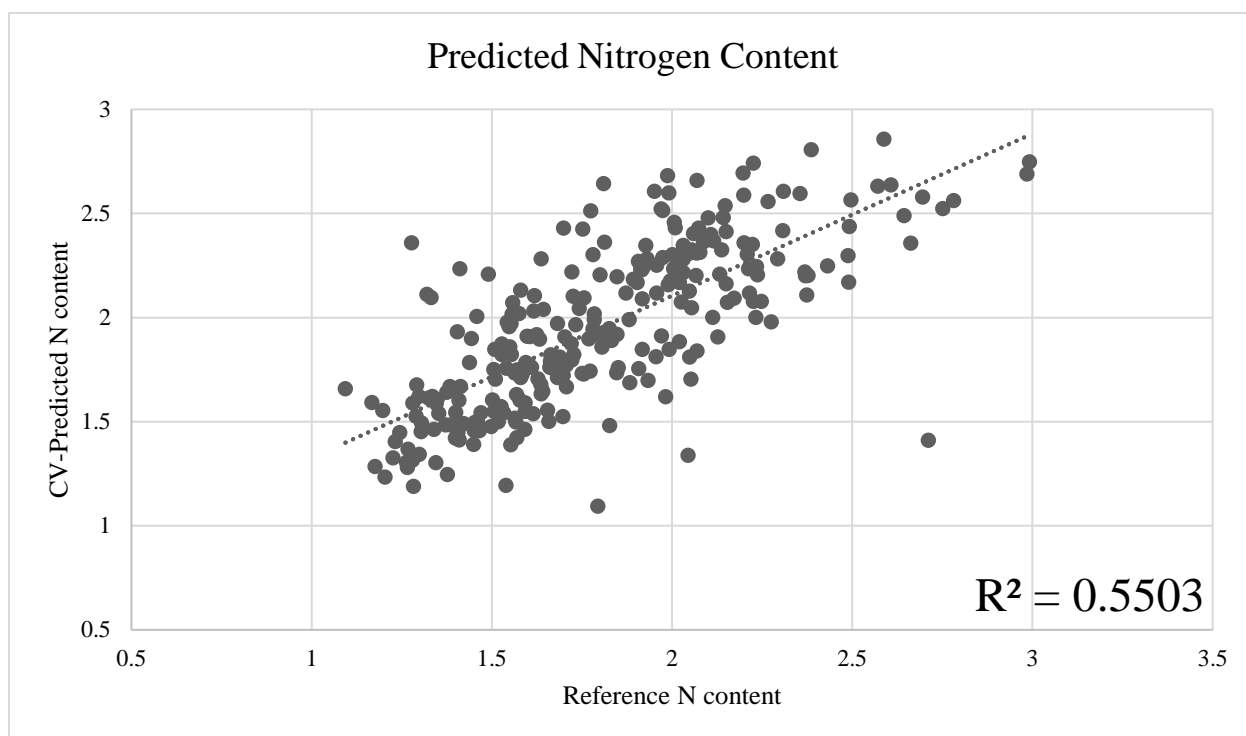


Figure 43. Plot of cross-validated nitrogen content against reference nitrogen content for the model built with B73xMo17

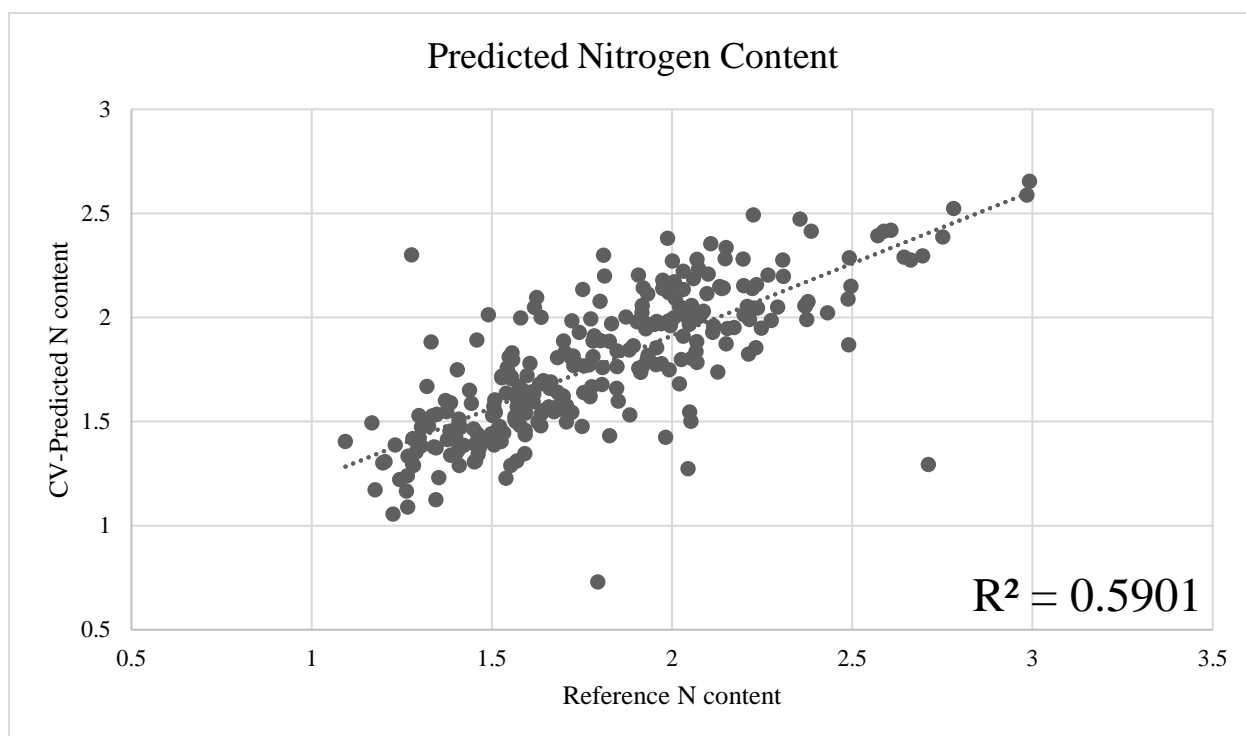


Figure 44. Plot of cross-validated nitrogen content against reference nitrogen content for the model built with BCC03xPHP02

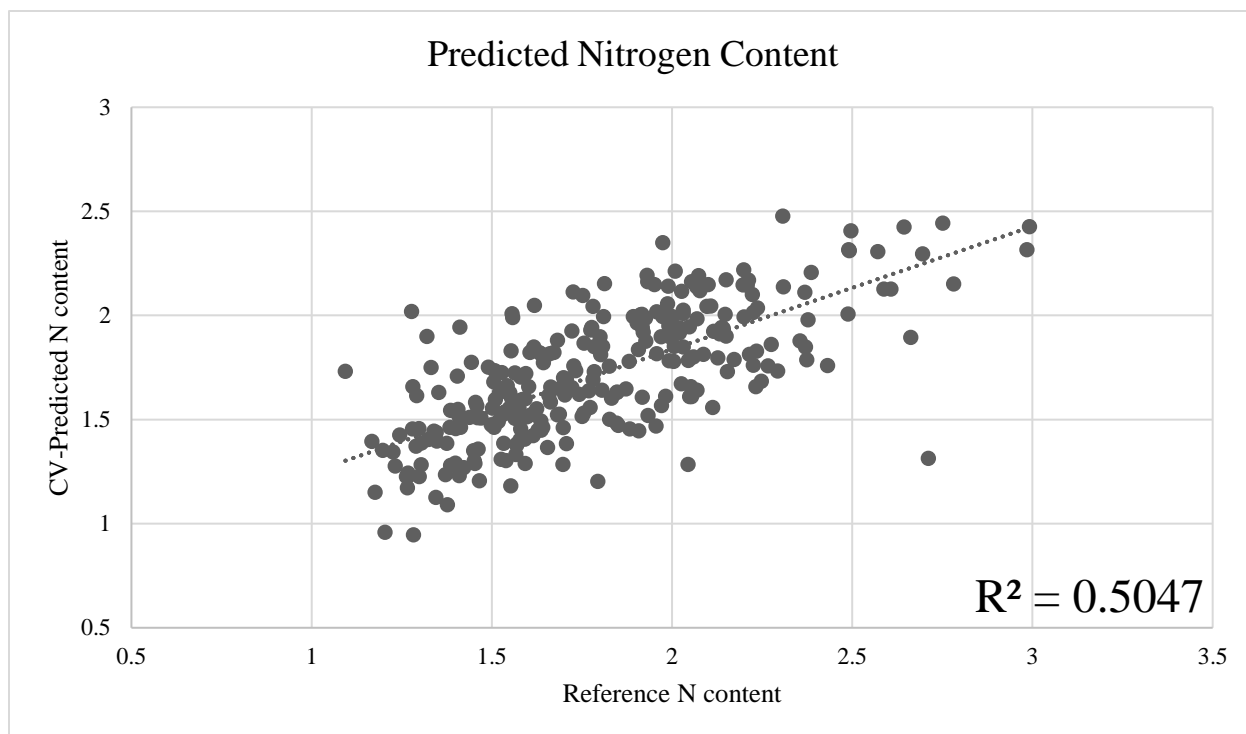


Figure 45. Plot of cross-validated nitrogen content against reference nitrogen content for the model built with CML550xPHP02

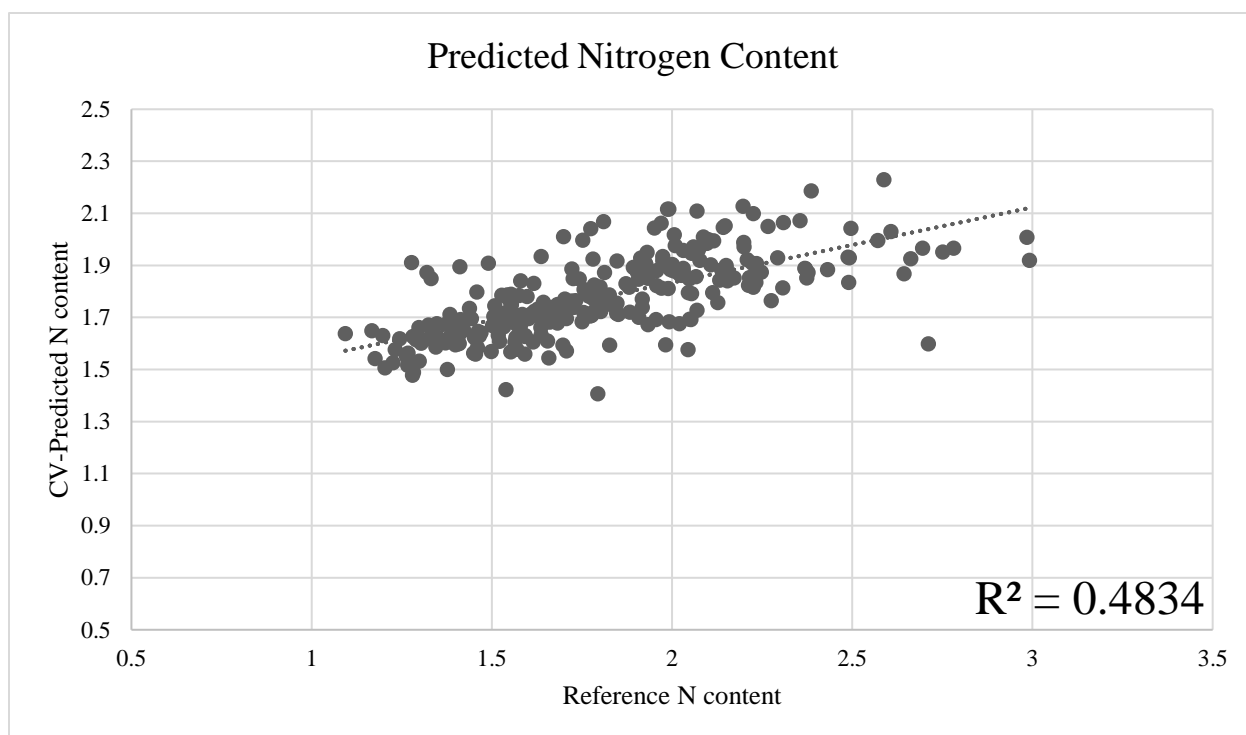


Figure 46. Plot of cross-validated nitrogen content against reference nitrogen content for the model built with G80xPHP02

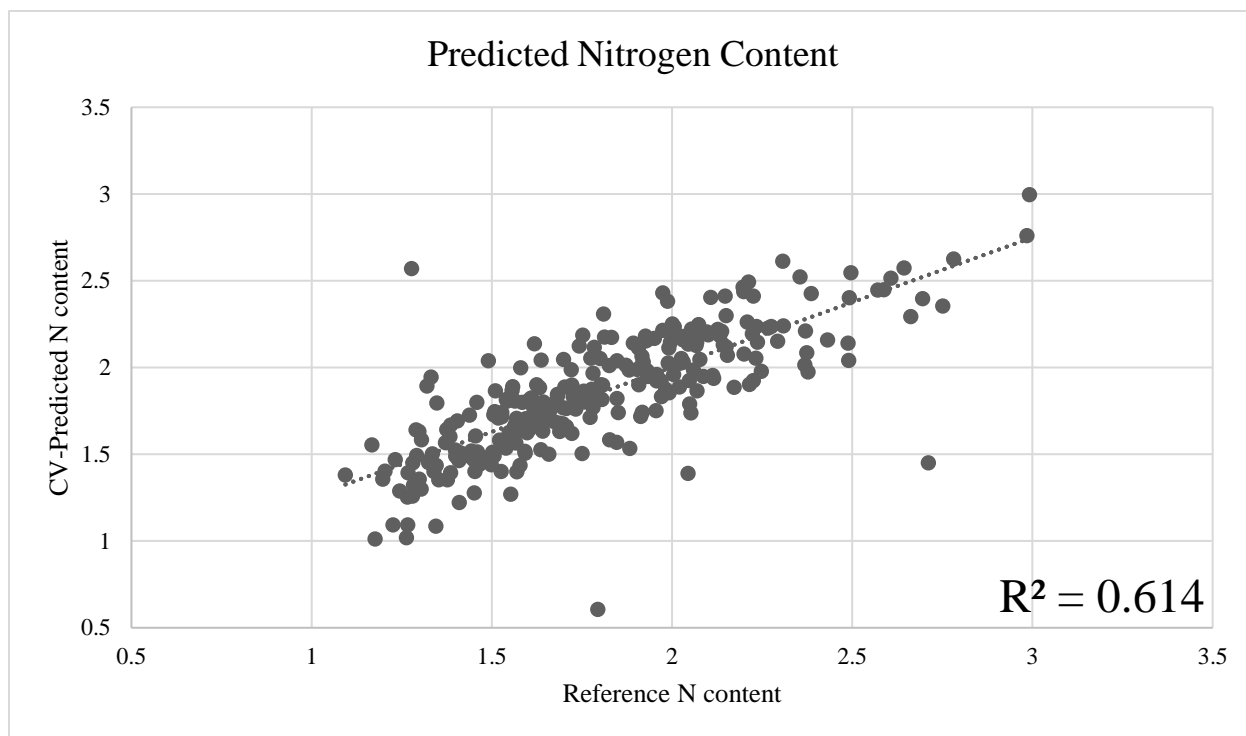


Figure 47. Plot of cross-validated nitrogen content against reference nitrogen content for the model built with P1105AM

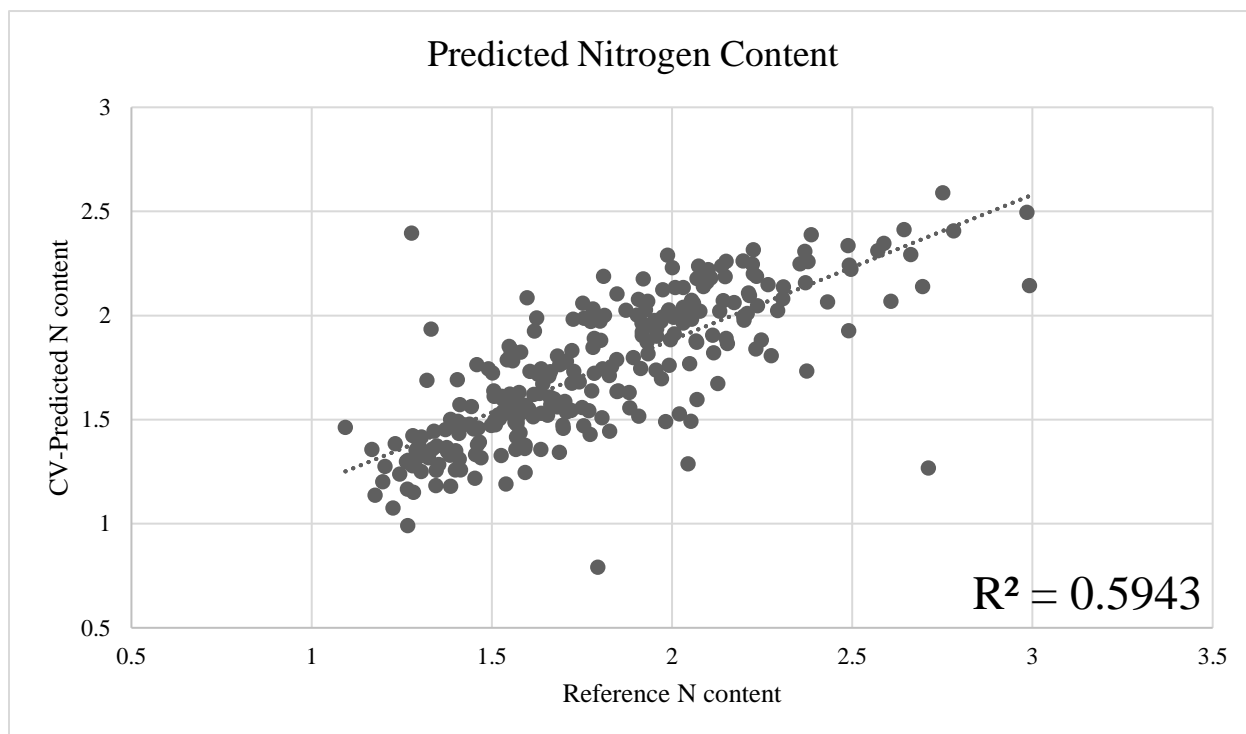


Figure 48. Plot of cross-validated nitrogen content against reference nitrogen content for the model built with PHJ33xPHP02

3.3.6 Summary of all Nitrogen Content Models

The seven maize models and the sorghum model were compared for modeling of N content across all the genotypes. The coefficients of determination for each of the plots are summarized in Figure 49. The combined model using the data from all genotypes was the best predictor of N content, but all the individual models predicted the respective genotype well. The exception to this was the G80xPHP02 hybrid. None of the models predicted this hybrid well. This is different than the RWC predictions in which none of the G80xPHP02 models predicted the other hybrids well. The sorghum model that contained no maize training data was fairly accurate at predicting the N content of the maize genotypes collectively and was particularly good at predicting the N contents of P1105AM and PHJ33xPHP02.

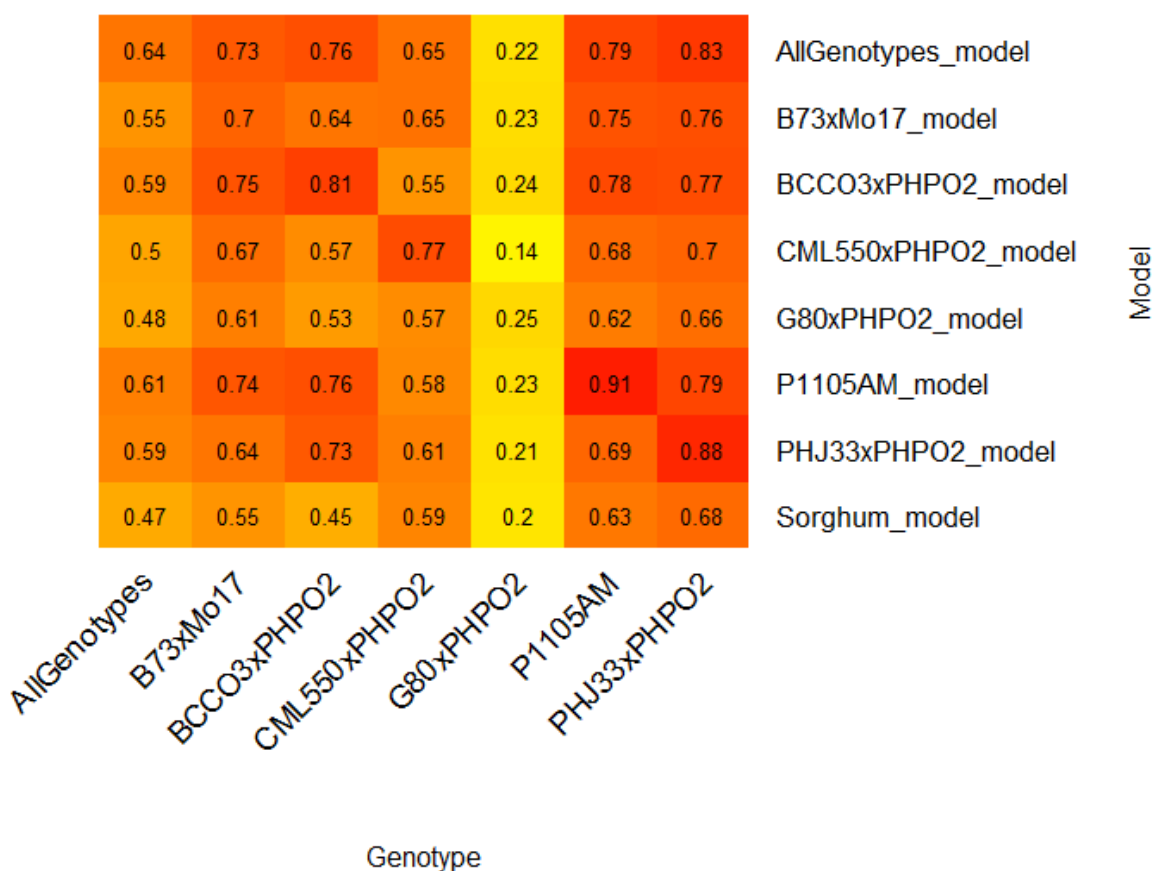


Figure 49. Heatmap of all coefficients of determination of all nitrogen content models; _s_ represents spectral only models and _sm_ represents spectral and morphological models

3.3.7 Models built using PHP02 Half-Siblings

In addition to the models developed using all six genotypes, models were also generated using the data from the four PHP02 half-sibling hybrids. The resulting predicted relative water content is graphed against the reference relative water in Fig. 50. The coefficient of determination for this model was slightly but not significantly higher than the model based on the six hybrids.

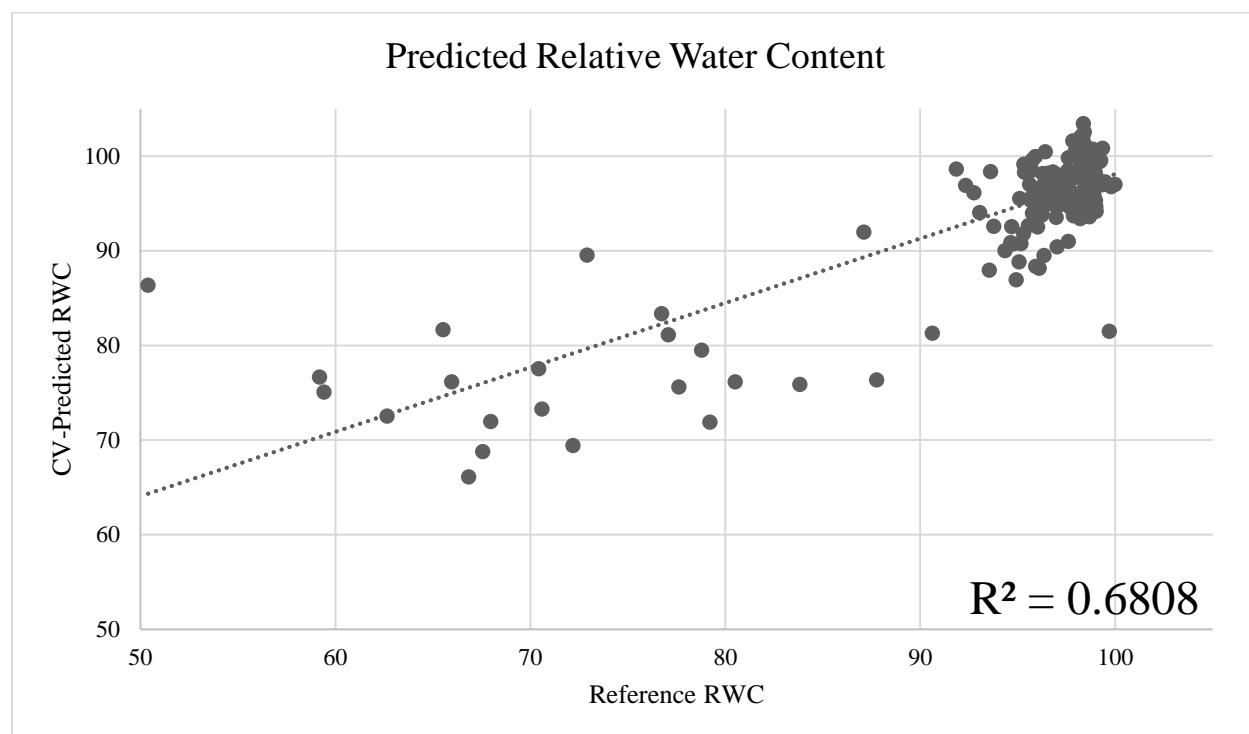


Figure 50. Plot of reference RWC against cross-validated predicted RWC for a model built using the spectral and morphological features of the four PHP02 half-siblings

3.3.8 Models built using Sorghum Data

The sorghum calibration experiment from the previous chapter was the first experiment performed on the new automated imaging system at Purdue. Given morphological and anatomical similarities between maize and sorghum, we attempted to use the sorghum model to predict the relative water content and nitrogen content of maize plants in this study.

3.3.8.1 Relative Water Content Model

The spectral and morphological sorghum model did not predict RWC in maize so the spectral sorghum model for RWC was used to yield a better prediction of RWC in maize (Fig. 51). The coefficient of determination for this model was 0.187.

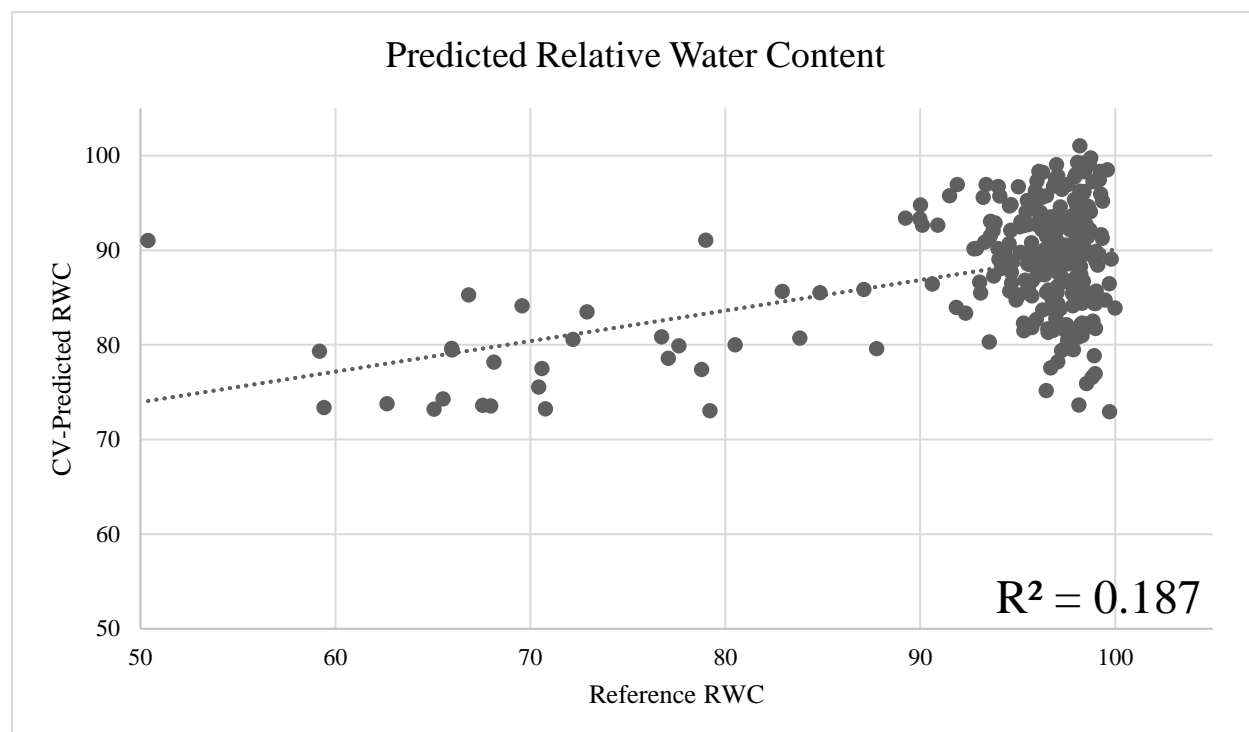


Figure 51. Plot of RWC against cross-validated predicted RWC of the maize multiple genotype study using the sorghum calibration RWC model

3.3.8.2 Nitrogen Content Model

We also attempted to use the sorghum model to predict the N content of maize. Nitrogen content predictions of maize plants were predicted using the sorghum model with spectral and morphological features. The sorghum spectral and morphological models did not predict nitrogen content in maize very well; however, the spectral only sorghum models were more highly predictive of maize nitrogen content with a coefficient of determination of 0.47 (Fig. 52).

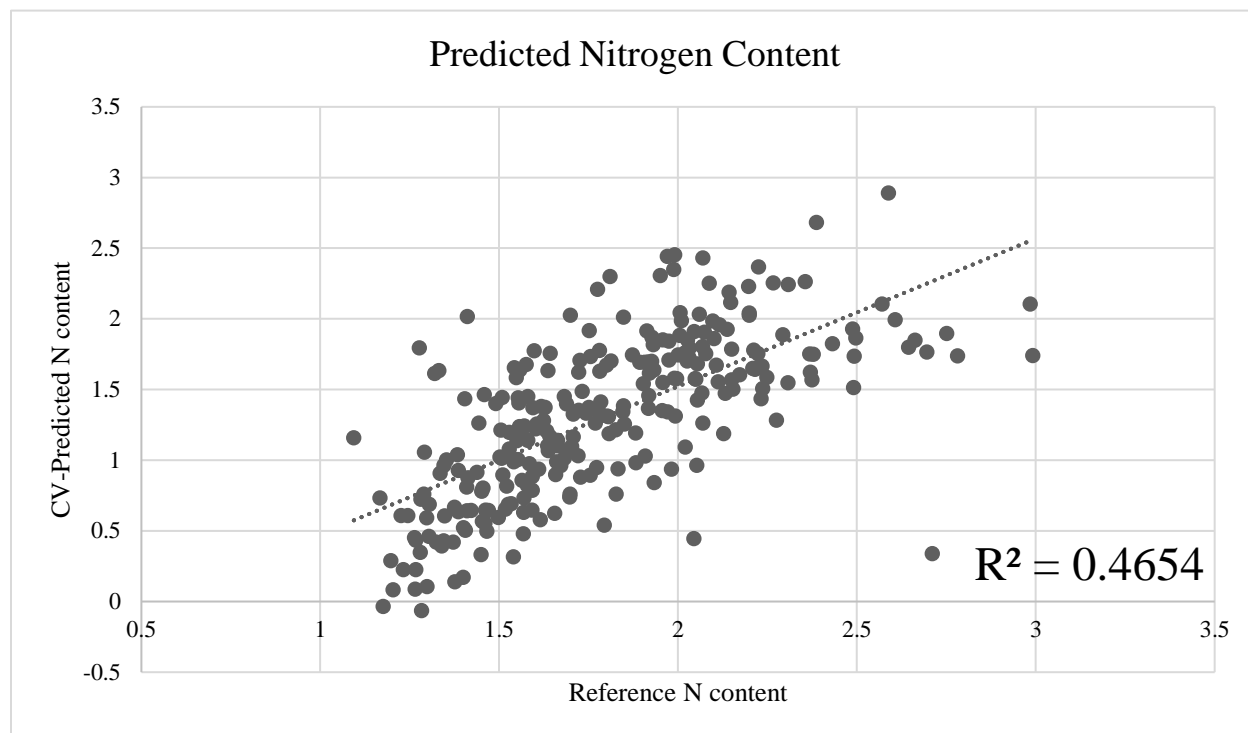


Figure 52. Plot of N content against cross-validated predicted N content of the maize multiple genotype study using the sorghum calibration spectral nitrogen content model

3.3.9 Combining Sorghum Calibration Data and Maize Multiple Genotype Data

Since the sorghum models were not highly predictive of the maize data, we decided to combine both the sorghum and the maize data to develop new relative water content and nitrogen content models.

3.3.9.1 Relative Water Content Model

Two relative water content models were developed from the combined sorghum and maize data using both the spectral and morphological features of the entire dataset and the spectral only features of the entire data set to predict both maize and sorghum combined in one dataset. The spectral and morphological model and the spectral only model were compared to the reference RWC values from the entire dataset (Figs. 53 and 54) with coefficients of determination of 0.85 and 0.8, respectively. These coefficients of determination are a large improvement over the original maize models and are comparable to the sorghum models.

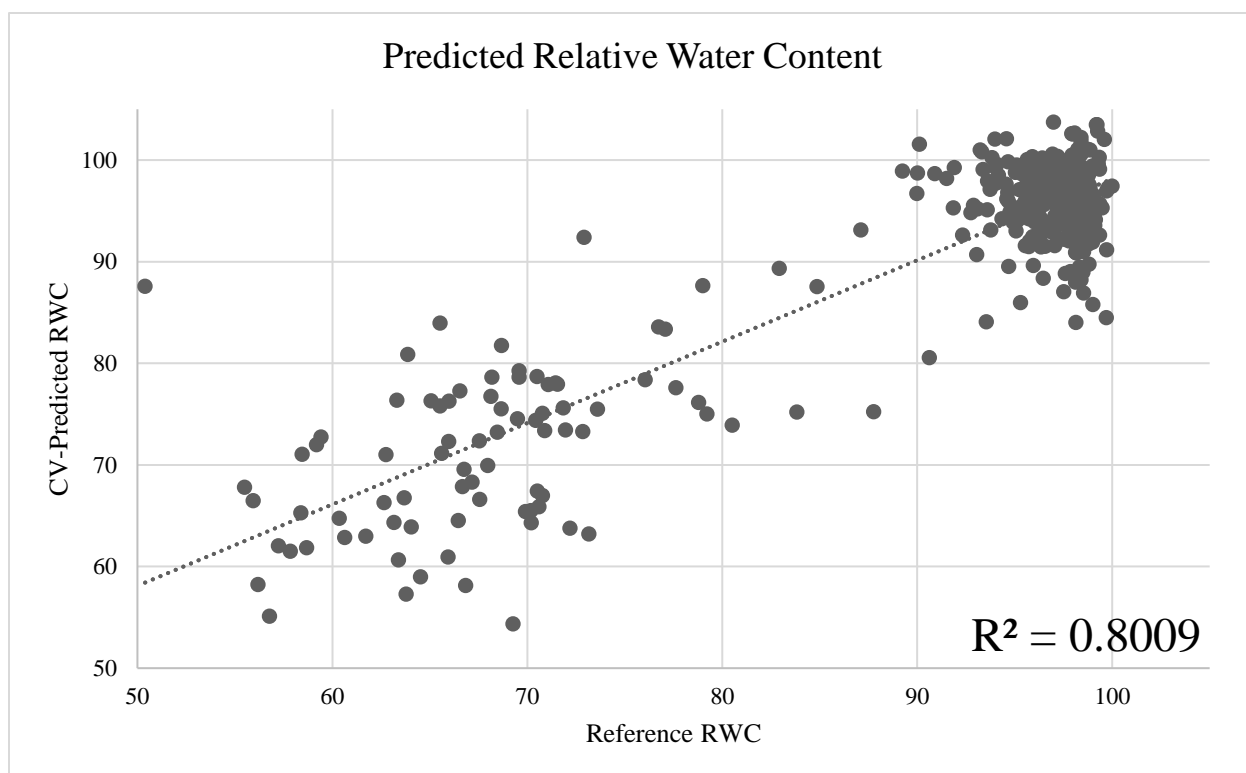


Figure 53. Plot of cross-validated relative water content against reference relative water content generated using the spectral and morphological features of the sorghum and maize data

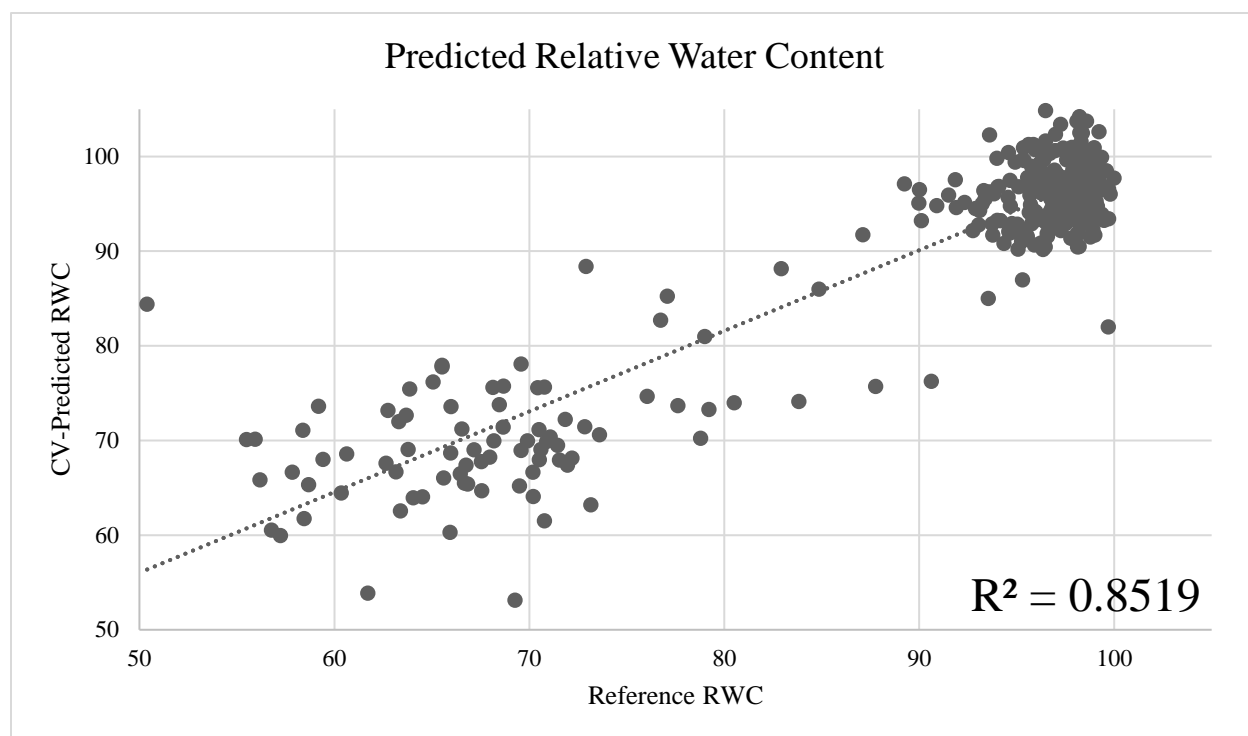


Figure 54. Plot of cross-validated predicted relative water content against reference relative water content generated using the spectral features of the sorghum and maize data

3.3.9.2 Nitrogen Content Model

Nitrogen content models were also generated using combined sorghum and maize data. The first model was built using the spectral and morphological features of the entire dataset while the second model was generated using only the spectral features of the dataset. Again, both the spectral and morphological model and the spectral only model were compared with the reference nitrogen content data from the entire sorghum and maize dataset (Figs. 55 and 56) with coefficients of determination of 0.66 and 0.65, respectively. These coefficients of determination are an improvement from the maize study and are slightly worse than the sorghum models.

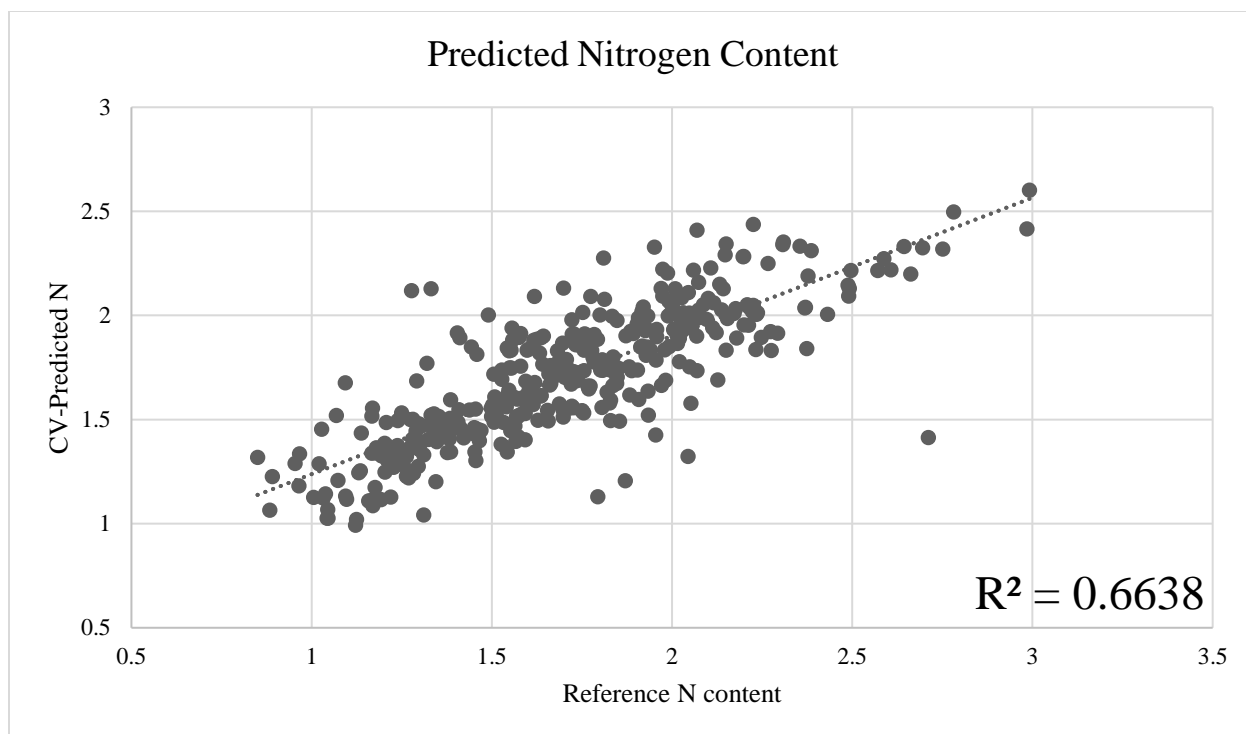


Figure 55. Plot of cross-validated nitrogen content against reference nitrogen content generated using the spectral and morphological features of sorghum and maize

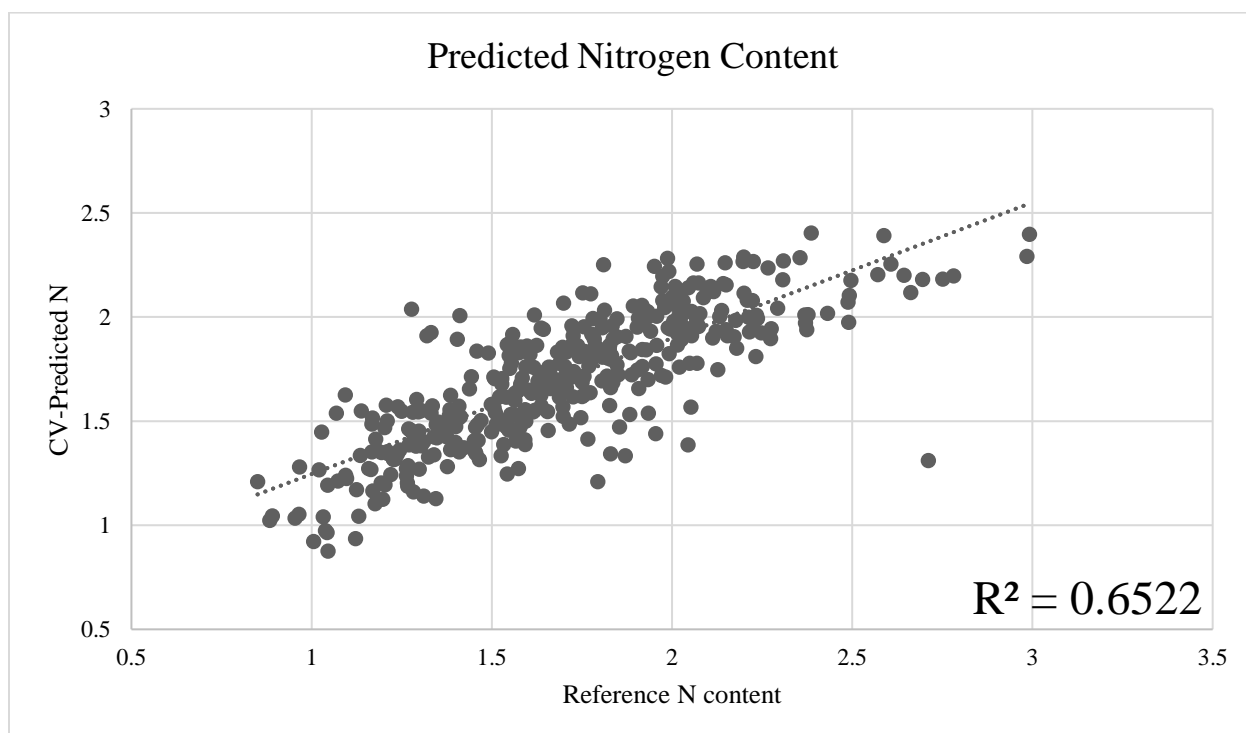


Figure 56. Plot of cross-validated nitrogen content against reference nitrogen content generated using the spectral features of sorghum and maize

3.3.10 Principal Component Analysis

A principal component analysis was performed on all the maize spectral and morphological features to compare the genotypes (Fig. 57). The two principal components (PC1 and PC2) explain 93% of the total variation. Confidence ellipses summarize the mean point of each genotype. All of the mean points are centered on relatively the same area and there are no differentiating features between any of the six genotypes.

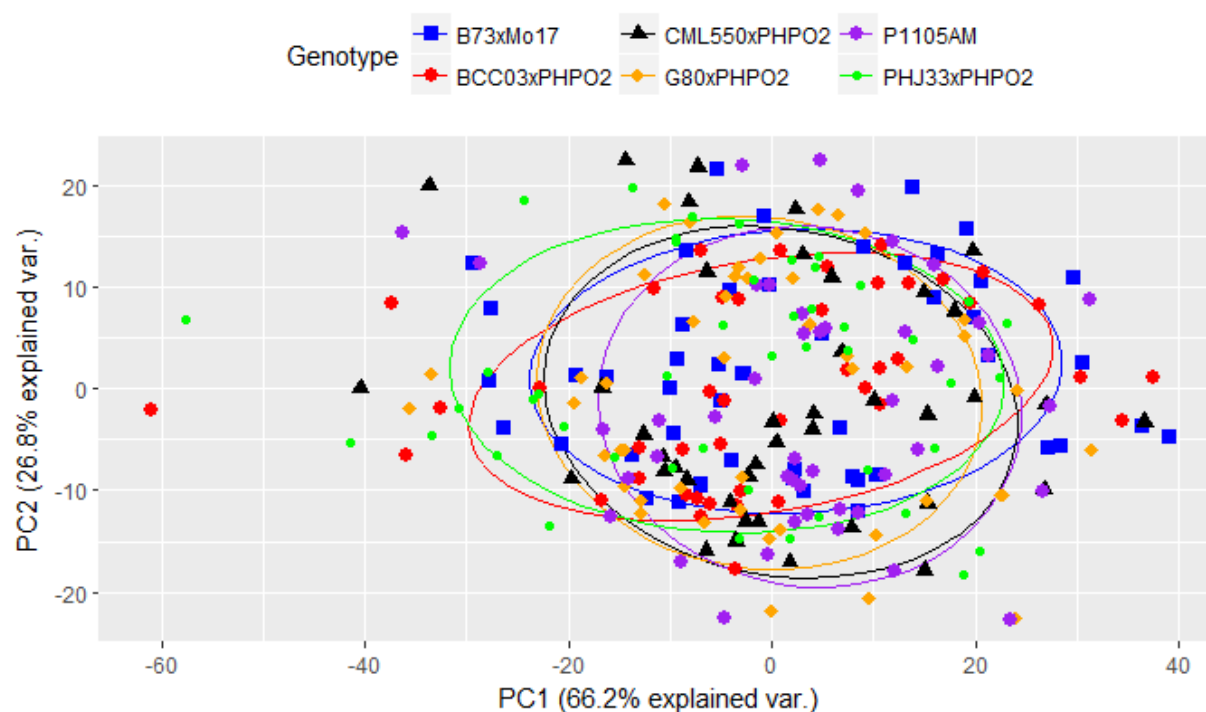


Figure 57. Principal Component Analysis of all spectral and morphological features

3.4 Discussion

3.4.1 Reference Measurements

The RWC measurements were distributed from approximately 50% to 100%. Many of the plants in the drought treatment groups exhibited high RWC. In particular, the smaller plants with lower leaf area in the low nitrogen treatments did not get drought stressed in treatment D. The treatment and treatment by genotype interaction effects were significant for RWC. The greatest variability in RWC occurred in treatment C and several of the genotypes performed better than the others. The genotype least affected by the drought stress was CML550xPHP02 which was reported by CIMMYT to produce hybrids that are well adapted to drought and low-N environments (“CIMMYT releases 22 new maize inbred lines for the tropics and subtropics”, 2013). The other genotype that maintained a higher RWC in treatment C was B73xMo17.

The N contents of plants exhibited variation from around 1% to 3%. The ANOVA showed that only the treatment effect was significant. The interaction of treatment and genotype was not significant; however, the interaction plot shows that all of the genotypes reacted in a similar fashion to the low N treatments except for G80xPHP02, which does not decrease as much under the low nitrogen treatments even though it is not considered significant, it may explain some of the difficulty of predicting this hybrid, G80xPHP02.

3.4.2 Models

For this maize experiment, the RWC predictions were not as high as the sorghum calibration study; however, it is difficult to tell if this is due to experimental design or the six genotypes. This was such a large experiment that we could not run the entire experiment on the conveyor belt. The plants were grown in a greenhouse without the constant movement to reduce

microenvironmental variation. Other PLS regression studies that have evaluated multiple genotypes of a single species have evaluated up to two genotypes. Ge et al. (2016) used PLS regression to predict the water status of two genotypes of maize. This study found that when the predicted values were compared to the reference values, the coefficient of determination was 0.87. The best RWC model developed from the six maize genotypes had a coefficient of determination of 0.72. Several other models developed with a single genotypes, namely B73xMo17 and CML550xPHP02, had coefficients of determination almost as high at 0.69 and 0.67 respectively. The poorest performing model was the one developed from G80xPHP02 which was a poor predictor of every genotype including G80xPHP02.

The Li et al. (2013) used a dataset containing the data from two cultivars of wheat. This dataset had a coefficient of determination of 0.79 when the predicted values were compared to the reference values. Nigon et al. (2014) modeled the leaf N concentration in two genotypes of potato over a growing season with multiple imaging dates. The coefficient of determination across all dates when the predicted values were compared to the reference values was 0.78. The best model developed from the data of all six genotypes of maize had a coefficient of determination of 0.64 when the predictions are compared to the reference measurements of all six genotypes.

While this is the best model for predicting N content of all the genotypes it is only slightly better than many of the other models such as the model built using P1105AM. It is in these predictions (Fig. 51) that it becomes clearer that the genotype might affect the prediction, particularly for nitrogen. For example, when the model built using the BCC03xPHP02 genotype is used to predict the nitrogen content of P1105AM, the coefficient of determination is 0.78, but when that same model is used to predict the nitrogen content of CML550xPHP02 and compared to the reference measurements, the coefficient of determination is 0.55.

Unlike the RWC models, the nitrogen content model built using G80xPHP02 appears no worse than any of the other models; however, every single model is an extremely poor predictor of the reference measurements from G80xPHP02. Even the model built using the G80xPHP02 data is not a good predictor of N content. The nitrogen content measurements for this genotype could be bad data and the true nitrogen content were not accurately measured. However, the standards in the nitrogen content assays were measured and recorded correctly. Another explanation could be that G80xPHP02 is genetically different from the rest of these genotypes. This is why a principal component analysis was performed to see if G80xPHP02 was centered on another area of the PCA. However, all the genotypes appear to be similar in the PCA (Fig. 57). In the PCA, we can also see that G80xPHP02 is rather noisy with many of the points falling outside of the confidence ellipses. I believe either the nitrogen content measurements are bad or there is too much noise in the data.

In an attempt to improve the water content models, we then hypothesized that the predictions may be more accurate for the PHP02 half-sibling lines. The model represented in Fig. 52 is a relative water content model with a coefficient of determination of 0.68 when the predictions of the PHP02 half-siblings were compared to the reference measurements of the PHP02 half-siblings. This is slightly better than the model built with all genotypes but is not a large improvement over the model generated with all six genotypes.

3.4.3 Predicting Across Species

The final models built from this experimental data included the sorghum calibration data. The first predictions from both of the experiments combined used the sorghum models to predict the maize reference measurements. The sorghum RWC models yielded a coefficient of determination of only 0.187 when the predicted RWC was compared to the reference RWC for all

the maize data. This is not a very predictive model and should not be used to predict RWC. The nitrogen content models were better than the RWC models with a coefficient of determination of 0.465 when comparing all maize data. These models were developed using only sorghum data and used to predict maize.

Pandey et al. (2017) also performed PLS regression to predict water and nitrogen status of maize and soybean. The coefficient of determination for the water status was 0.97 when comparing the predicted values to the reference values while the N content prediction was 0.88 when comparing the predicted values to the reference values. However, this study didn't treat the same plants with both nitrogen and water treatments, and the plants were all sampled at the same time, under the same treatments, and the same environment.

We also combined both the sorghum and maize data together to generate new models using both the spectral features and the spectral and morphological features. These models were used to predict both sorghum and maize relative water contents and nitrogen contents. The predicted RWC using spectral and morphological features compared to the reference relative water contents produced a model with a coefficient of determination of 0.85 while the model using the spectral only features yielded a coefficient of determination of 0.8. This large increase in the coefficient of determination could be due to the fact that combining the two datasets resulted in a more even spectrum of relative water content from 50% to 100%.

The model for predicting N content using the spectral and morphological features of sorghum and maize had a coefficient of determination of 0.66. The nitrogen content model built using the spectral only features of the combined dataset has a coefficient of determination of 0.65. The relative water content models and the nitrogen content models built using the combined data

across species with six genotypes of maize and three genotypes of sorghum were highly predictive of the respective reference measurements.

3.5 Conclusion

The goal of the maize multiple genotype study was to develop models that can span multiple genotypes of a species. Previous studies have not included more than three genotypes and the pervasive thought in hyperspectral imaging is that models that are predictive of multiple genotypes cannot be built. This study has shown that predictive models of relative water content and nitrogen content can be built for six genotypes of maize.

When looking at the nitrogen models, we discovered that none of the models predicted the G80xPHP02 genotype very well and we did not find a good reason why that may be. We also see that some genotypes are better predictors of other genotypes like we saw in the sorghum calibration experiment. This may be related to genetic relatedness so we evaluated models developed using half-siblings and found we could increase the coefficients of determination when the predicted values were compared to the reference values. We found that the models were not better than the models built with all six genotypes.

Finally, we also evaluated the predictions across two different species: maize and sorghum. We first used the sorghum models to predict the maize phenotypes. The coefficients of determination for the RWC and N content phenotypes were 0.187 and 0.465, respectively, which are not very predictive for either trait. However, when new models were developed using the combined maize and sorghum data, the coefficients of determination for both RWC and N content jump to 0.85 and 0.66, respectively. These models produce excellent predictions and provide a broad inference for predictions across the two key crop species, in two different experiments, under two different environments. We would recommend the maize and sorghum combined models for

future analyses because these models span two species, a range of water and nitrogen contents, and two experiments to avoid overfitting of the model.

With all we have learned about developing the experimental designs and utilizing the hyperspectral imaging system in the greenhouse, we believe that we can go forward with this system and develop experiments with less variability and noise in the hyperspectral data and in the plants involved in the experiment. This, in turn, will result in models with higher coefficients of determination. I believe we can begin using this system to evaluate more genotypes and the respective responses to low water and nitrogen inputs.

REFERENCES

- 2018 Corn Hybrid-Herbicide Management Guide** Adequate Tolerance Requires Careful Management Crop Response Warning Insufficient Data Herbicide Families. (2018). Retrieved March 20, 2018, from <https://www.pioneer.com/CMRoot/pioneer/us/products/stewardship/2018-corn-herbicide-response-ratings.pdf>
- Accession: PI 550473 - GRIN-Global Web v 1.10.1.5. (n.d.). Retrieved March 20, 2018, from <https://npgsweb.ars-grin.gov/gringlobal/accessiondetail.aspx?accid=PI+550473>
- Accession: PI 544065 - GRIN-Global Web v 1.10.1.5. (n.d.). Retrieved March 20, 2018, from <https://npgsweb.ars-grin.gov/gringlobal/accessiondetail.aspx?id=1439001>
- Accession: PI 558532 - GRIN-Global Web v 1.10.1.5. (n.d.). Retrieved March 20, 2018, from <https://npgsweb.ars-grin.gov/gringlobal/accessiondetail.aspx?id=1453504>
- Accession: PI 601037 - GRIN-Global Web v 1.10.1.5. (n.d.). Retrieved March 20, 2018, from <https://npgsweb.ars-grin.gov/gringlobal/accessiondetail.aspx?id=1157676>
- Accession: PI 601570 - GRIN-Global Web v 1.10.1.5. (n.d.). Retrieved March 20, 2018, from <https://npgsweb.ars-grin.gov/gringlobal/accessiondetail.aspx?id=1185648>
- Agapiou, A., Hadjimitsis, D., & Alexakis, D. (2012). Evaluation of Broadband and Narrowband Vegetation Indices for the Identification of Archaeological Crop Marks. *Remote Sensing*, 4(12), 38
- Araus, J. L., Slafer, G. A., Reynolds, M. P., & Royo, C. (2002). Plant breeding and drought in C3 cereals: what should we breed for? *Annals of Botany*, 89 Spec No(7), 925–40. <https://doi.org/10.1093/AOB/MCF049>
- Araus, J. L., & Cairns, J. E. (2014). Field high-throughput phenotyping: the new crop breeding frontier. *Trends in Plant Science*, 19(1), 52–61. <https://doi.org/10.1016/j.tplants.2013.09.008>
- Azedo-Silva, J., Osorio, J., Fonseca, F., & Correia, M. J. (2004). Effects of soil drying and subsequent re-watering on the activity of nitrate reductase in roots and leaves of *Helianthus annuus*. *Functional Plant Biology*, 31(6), 611–621. <https://doi.org/10.1071/FP04018>
- Bausch, W. C., Duke, H. R., & Iremonger, C. J. (1996). Assessment of Plant Nitrogen in Irrigated Corn. In *Precision Agriculture* (pp. 23–32). American Society of Agronomy, Crop Science Society of America, Soil Science Society of America. <https://doi.org/10.2134/1996.precisionagproc3.c3>

- Bedoya, C. A., Dreisigacker, S., Hearne, S., Franco, J., Mir, C., Prasanna, B. M., Warburton, M. L. (2017). Genetic diversity and population structure of native maize populations in Latin America and the Caribbean. *PLOS ONE*, 12(4), e0173488. <https://doi.org/10.1371/journal.pone.0173488>
- Behmann, J., Steinrücken, J., & Plümer, L. (2014). Detection of early plant stress responses in hyperspectral images. *ISPRS Journal of Photogrammetry and Remote Sensing*, 93, 98–111. <https://doi.org/10.1016/J.ISPRSJPRS.2014.03.016>
- Bhugra, S., Agarwal, N., Yadav, S., Banerjee, S., Chaudhury, S., & Lall, B. (2017). Extraction of Phenotypic Traits for Drought Stress Study Using Hyperspectral Images. In *Pattern Recognition and Machine Intelligence* (pp. 608–614). Springer, Cham. https://doi.org/10.1007/978-3-319-69900-4_77
- Borrell, A. K., Bidinger, F. R., & Sunitha, K. (1999). Stay-Green Trait Associated with Yield in Recombinant Inbred Sorghum Lines Varying in Rate of Leaf Senescence. *International Sorghum and Millets Newsletter*, 40, 31–34. Retrieved from <http://oar.icrisat.org/1778/>
- Borlaug, N. E., & Dowsell, C. R. (n.d.). Feeding a world of ten billion people: A 21 st century challenge.
- Borrell, A.K. and Hammer, G.L. 2000. Nitrogen dynamics in stay-green and senescent sorghum hybrids grown under varying levels of water supply. *Crop Science*, 40(4), 1295-1307.
- Borrell, A. K., Hammer, G. L., & Henzell, R. G. (2000). Does Maintaining Green Leaf Area in Sorghum Improve Yield under Drought? II. Dry Matter Production and Yield. *Crop Science*, 40(4), 1037–1048. <https://doi.org/10.2135/cropsci2000.4041037x>
- Borrell, A. K., Mullet, J. E., George-Jaeggli, B., van Oosterom, E. J., Hammer, G. L., Klein, P. E., & Jordan, D. R. (2014). Drought adaptation of stay-green sorghum is associated with canopy development, leaf anatomy, root growth, and water uptake. *Journal of Experimental Botany*, 65(21), 6251–63. <https://doi.org/10.1093/jxb/eru232>
- Campbell, J., & Wynne, R. (2011). *Introduction to Remote Sensing* (5th ed.). New York, NY: The Guilford Press.
- Cattivelli, L., Rizza, F., Badeck, F.-W., Mazzucotelli, E., Mastrangelo, A. M., Francia, E., Stanca, A. M. (2008). Drought tolerance improvement in crop plants: An integrated view from breeding to genomics. *Field Crops Research*, 105(1–2), 1–14. <https://doi.org/10.1016/j.fcr.2007.07.004>
- Chapin, F. S. (1991). Effects of Multiple Environmental Stresses on Nutrient Availability and Use. In *Response of Plants to Multiple Stresses* (pp. 67–88). Elsevier. <https://doi.org/10.1016/B978-0-08-092483-0.50008-6>

- Charney, J. G. (1975). Dynamics of deserts and drought in the Sahel. *Quarterly Journal of the Royal Meteorological Society*, 101(428), 193–202. <https://doi.org/10.1002/qj.49710142802>
- Chun, L., Mi, G., Li, J., Chen, F., & Zhang, F. (2005). Genetic Analysis of Maize Root Characteristics in Response to Low Nitrogen Stress. *Plant and Soil*, 276(1–2), 369–382. <https://doi.org/10.1007/s11104-005-5876-2>
- CIMMYT releases 22 new maize inbred lines for the tropics and subtropics | CIMMYT. International Maize and Wheat Improvement Center. (2013). Retrieved March 20, 2018, from <https://www.cimmyt.org/cimmyt-releases-22-new-maize-inbred-lines-for-the-tropics-and-subtropics/>
- Clifton, K. E., & Clifton, L. M. (1991). A field method for the determination of total nitrogen in plant tissue. *Communications in Soil Science and Plant Analysis*, 22(9–10), 851–860.
- Cornic, G., & Massacci, A. (1996). Leaf Photosynthesis Under Drought Stress. In *Photosynthesis and the Environment* (pp. 347–366). Dordrecht: Kluwer Academic Publishers. https://doi.org/10.1007/0-306-48135-9_14
- Corti, M., Marino Gallina, P., Cavalli, D., & Cabassi, G. (2017). Hyperspectral imaging of spinach canopy under combined water and nitrogen stress to estimate biomass, water, and nitrogen content. *Biosystems Engineering*, 158, 38–50. <https://doi.org/10.1016/J.BIOSYSTEMSENG.2017.03.006>
- Cotrozzi, L., Couture, J. J., Cavender-Bares, J., Kingdon, C. C., Fallon, B., Pilz, G., ... Townsend, P. A. (2017). Using foliar spectral properties to assess the effects of drought on plant water potential. *Tree Physiology*, 37(11), 1582–1591. <https://doi.org/10.1093/treephys/tpx106>
- Crafts-Brandner, S. J., Holzer, R., & Feller, U. (1998). Influence of nitrogen deficiency on senescence and the amounts of RNA and proteins in wheat leaves. *Physiologia Plantarum*, 102(2), 192–200. <https://doi.org/10.1034/j.1399-3054.1998.1020206.x>
- Cramer, M. D., Hawkins, H.-J., & Verboom, G. A. (2009). The importance of nutritional regulation of plant water flux. *Oecologia*, 161(1), 15–24. <https://doi.org/10.1007/s00442-009-1364-3>
- Dai, A. (2011). Drought under global warming: a review. *Wiley Interdisciplinary Reviews: Climate Change*, 2(1), 45–65. <https://doi.org/10.1002/wcc.81>
- Deng, Z., Cao, S., Tang, Y., Lu, W., & Zhang, R. (2001). Comparison on some aspects of photosynthetic declination of wild rice and cultivated rice. *Acta Agronomica Sinica*, 27, 453–459. <https://doi.org/10.1111/j.1365-3040.2009.02054.x>
- Dial, H., & Tucson Plant Materials Center, U. (n.d.). Plant Guide Sorghum: *Sorghum bicolor* (L.) Moench Plant Symbol = SOBI2.

- Estrada-Campuzano, G., Miralles, D. J., & Slafer, G. A. (2008). Genotypic variability and response to water stress of pre- and post-anthesis phases in triticale. *European Journal of Agronomy*, 28(3), 171–177. <https://doi.org/10.1016/J.EJA.2007.07.005>
- Farooq, M., Wahid, A., Kobayashi, N., Fujita, D., & Basra, S. M. A. (2009). Plant drought stress: effects, mechanisms and management. *Agronomy for Sustainable Development*, 29(1), 185–212. <https://doi.org/10.1051/agro:2008021>
- Farooq, M., Wahid, A., Kobayashi, N., Fujita, D., & Basra, S. M. A. (2009). Plant drought stress: effects, mechanisms and management. *Agronomy for Sustainable Development*, 29(1), 185–212. <https://doi.org/10.1051/agro:2008021>
- Fathi, A., & Tari, D. B. (2016). Effect of Drought Stress and its Mechanism in Plants. *International Journal of Life Sciences*, 10(1), 1–6. <https://doi.org/10.3126/ijls.v10i1.14509>
- Fierer, N., & Schimel, J. P. (2002). Effects of drying–rewetting frequency on soil carbon and nitrogen transformations. *Soil Biology and Biochemistry*, 34(6), 777–787. [https://doi.org/10.1016/S0038-0717\(02\)00007-X](https://doi.org/10.1016/S0038-0717(02)00007-X)
- Filella, I., Amaro, T., Araus, J. L., & Penuelas, J. (1996). Relationship between photosynthetic radiation-use efficiency of barley caeopies and the photochemical reflectance index (PRI). *Physiologia Plantarum*, 96, 211–216. Retrieved from <https://onlinelibrary.wiley.com/doi/pdf/10.1111/j.1399-3054.1996.tb00204.x>
- Fluorescence vs. Transmittance. (n.d.). Retrieved January 1, 2016, from http://botit.botany.wisc.edu/botany_130/photosynthesis/Fluorescence.html
- Franke, J., Menz, G., Oerke, E.-C., & Rascher, U. (2005). Comparison of multi- and hyperspectral imaging data of leaf rust infected wheat plants. In M. Owe & G. D'Urso (Eds.), *Remote Sensing for Agriculture, Ecosystems, and Hydrology VII* (p. 59761D). International Society for Optics and Photonics. <https://doi.org/10.1117/12.626531>
- Galinat, W.C. (1971) The Origin of Maize. *Annual Review of Genetics*. 5 447-478. <https://www.annualreviews.org/doi/pdf/10.1146/annurev.ge.05.120171.002311>
- Gamon, J., Serrano, L., & Surfus, J. (1997) The photochemical reflectance index: an optical indicator of photosynthetic radiation use efficiency across species, functional types, and nutrient levels. *Oecologia*, 112(4) 492-501. https://www.researchgate.net/publication/226117209_The_Photochemical_Reflectance_Index_An_Optical_Indicator_of_Photosynthetic_Radiation_Use_Efficiency_across_Species_Functional_Types_and_Nutrient_Levels
- Ge, Y., Bai, G., Stoerger, V., & Schnable, J. C. (2016). Temporal dynamics of maize plant growth, water use, and leaf water content using automated high throughput RGB and hyperspectral imaging. *Computers and Electronics in Agriculture*, 127, 625–632. <https://doi.org/10.1016/J.COMPAG.2016.07.028>

- Gelli, M., Duo, Y., Konda, A., Zhang, C., Holding, D., & Dweikat, I. (2014). Identification of differentially expressed genes between sorghum genotypes with contrasting nitrogen stress tolerance by genome-wide transcriptional profiling. *BMC Genomics*, *15*(1), 179. <https://doi.org/10.1186/1471-2164-15-179>
- Gente, R., Born, N., Voß, N., Sannemann, W., Léon, J., Koch, M., & Castro-Camus, E. (2013). Determination of Leaf Water Content from Terahertz Time-Domain Spectroscopic Data. *Journal of Infrared, Millimeter, and Terahertz Waves*, *34*(3), 316–323. <https://doi.org/10.1007/s10762-013-9972-8>
- Gitelson, A., & Solovchenko, A. (2017). Generic Algorithms for Estimating Foliar Pigment Content. *Geophysical Research Letters*, *44*(18), 9293–9298. <https://doi.org/10.1002/2017GL074799>
- Govender, M., Chetty, K., & Bulcock, H. (2007). A review of hyperspectral remote sensing and its application in vegetation and water resource studies. *Water SA*, *33*(2).
- Halkier, B. A., & Moller, B. L. (1989). Biosynthesis of the Cyanogenic Glucoside Dhurrin in Seedlings of *Sorghum bicolor* (L.) Moench and Partial Purification of the Enzyme System Involved. *Plant Physiology*, *90*(4), 1552–1559. <https://doi.org/10.1104/pp.90.4.1552>
- Hansen, P. M., & Schjoerring, J. K. (2003). Reflectance measurement of canopy biomass and nitrogen status in wheat crops using normalized difference vegetation indices and partial least squares regression. *Remote Sensing of Environment*, *86*(4), 542–553. [https://doi.org/10.1016/S0034-4257\(03\)00131-7](https://doi.org/10.1016/S0034-4257(03)00131-7)
- Harlan, J. R., & de Wet, J. M. J. (1972). A Simplified Classification of Cultivated Sorghum1. *Crop Science*, *12*(2), 172–176. <https://doi.org/10.2135/cropsci1972.0011183X001200020005x>
- Harrison, M. T., Tardieu, F., Dong, Z., Messina, C. D., & Hammer, G. L. (2014). Characterizing drought stress and trait influence on maize yield under current and future conditions. *Global Change Biology*, *20*(3), 867–878. <https://doi.org/10.1111/gcb.12381>
- Hauck, R. D., & Tucker, T. C. (1984). Diagnosis of Nitrogen Deficiency in Plants. In *Nitrogen in Crop Production* (pp. 249–262). <https://doi.org/10.2134/1990.nitrogenincropproduction.c16>
- He, M., & Dijkstra, F. A. (2014). Drought effect on plant nitrogen and phosphorus: a meta-analysis. *New Phytologist*, *204*(4), 924–931. <https://doi.org/10.1111/nph.12952>
- Heckathorn, S. A., DeLucia, E. H., & Zielinski, R. E. (1997). The contribution of drought-related decreases in foliar nitrogen concentration to decreases in photosynthetic capacity during and after drought in prairie grasses. *Physiologia Plantarum*, *101*(1), 173–182. <https://doi.org/10.1111/j.1399-3054.1997.tb01834.x>

- Hoegemeyer, T. (2014). History of the US Hybrid Corn Seed Industry. Retrieved from http://imbgil.cropsci.illinois.edu/school/2014/11_THOMAS_HOEGEMEYER.pdf
- Houle, D., Govindaraju, D. R., & Omholt, S. (2010). Phenomics: the next challenge. *Nature Reviews. Genetics*, 11(12), 855–66. <https://doi.org/10.1038/nrg2897>
- Huang, J., Minnis, P., Yan, H., Yi, Y., Chen, B., Zhang, L., & Ayers, J. K. (2010). Dust aerosol effect on semi-arid climate over Northwest China detected from A-Train satellite measurements. *Atmospheric Chemistry and Physics*, 10(14), 6863–6872. <https://doi.org/10.5194/acp-10-6863-2010>
- Huang, J., Ji, M., Xie, Y., Wang, S., He, Y., & Ran, J. (2016). Global semi-arid climate change over last 60 years. *Climate Dynamics*, 46(3), 1131–1150. <https://doi.org/10.1007/s00382-015-2636-8>
- Huang, Z.-A., Jiang, D.-A., Yang, Y., Sun, J.-W., & Jin, S.-H. (2004). Effects of Nitrogen Deficiency on Gas Exchange, Chlorophyll Fluorescence, and Antioxidant Enzymes in Leaves of Rice Plants. *Photosynthetica*, 42(3), 357–364. <https://doi.org/10.1023/B:PHOT.0000046153.08935.4c>
- Inada, K., Matsuura, A., & Yamane, M. (1992). Interspecific Differences in the Mechanism of Drought Tolerance among Four Cereal Crops. *Japanese Journal of Crop Science*, 61, 87–95. Retrieved from https://www.jstage.jst.go.jp/article/jcs1927/61/1/61_1_87/_pdf/-char/en
- Jain, N., Ray, S. S., Singh, J. P., & Panigrahy, S. (2007). Use of hyperspectral data to assess the effects of different nitrogen applications on a potato crop. *Precision Agriculture*, 8(4), 225–239. <https://doi.org/10.1007/s11119-007-9042-0>
- Jamieson, P. D., Martin, R. J., & Francis, G. S. (1995). Drought influences on grain yield of barley, wheat, and maize. *New Zealand Journal of Crop and Horticultural Science*, 23(1), 55–66.
- Jurgens, C. (1997). The modified normalized difference vegetation index (mNDVI) a new index to determine frost damages in agriculture based on Landsat TM data. *International Journal of Remote Sensing*, 18(17), 3583–3594. <https://doi.org/10.1080/014311697216810>
- Karper, R. E. (1949). Registration of Sorghum Varieties, V1. *Texas Agricultural Experiment Station Publication*. Retrieved from <https://billrooney.tamu.edu/research/files/germplasm/Tx643-Tx645SorghumInbredsWebsite.pdf>
- Kebede, H., Subudhi, P. K., Rosenow, D. T., & Nguyen, H. T. (2001). Quantitative trait loci influencing drought tolerance in grain sorghum (*Sorghum bicolor* L. Moench). *Theoretical and Applied Genetics*, 103(2–3), 266–276. <https://doi.org/10.1007/s001220100541>

- Kersting, K., Xu, Z., Wahabzada, M., Bauckhage, C., Thureau, C., Roemer, C., Pluemer, L. (n.d.). Pre-Symptomatic Prediction of Plant Drought Stress Using Dirichlet-Aggregation Regression on Hyperspectral Images. *Proceedings of the Twenty-Sixth AAAI Conference of Artificial Intelligence*. Retrieved from <https://pdfs.semanticscholar.org/2daf/f1c4c2971b994e9770bfdec9328b77d20dd3.pdf>
- Khamis, S., Lamaze, T., Lemoine, Y., & Foyer, C. (1990). Adaptation of the Photosynthetic Apparatus in Maize Leaves as a Result of Nitrogen Limitation : Relationships between Electron Transport and Carbon Assimilation. *Plant Physiology*, 94(3), 1436–43. <https://doi.org/10.1104/PP.94.3.1436>
- Lamb, J. A., Fernandez, F. G., & Kaiser, D. E. (2014). Nutrient Management: Understanding Nitrogen in Soils: Extension Specialists in Nutrient Management. *University of Minnesota Extension Publication*, (AG-FO-3770-B). Retrieved from <https://www.extension.umn.edu/agriculture/nutrient-management/nitrogen/understanding-nitrogen-in-soils/docs/AG-FO-3770-B.pdf>
- Lee, D., Nguyen, V., & Littlefield, S. (2008). Comparison of methods for determination of nitrogen levels in soil, plant and body tissues, and water. *Communications in Soil Science and Plant Analysis*, 27(3–4), 783–793.
- Li, F., Mistele, B., Hu, Y., Chen, X., & Schmidhalter, U. (2014). Reflectance estimation of canopy nitrogen content in winter wheat using optimised hyperspectral spectral indices and partial least squares regression. *European Journal of Agronomy*, 52, 198–209. <https://doi.org/10.1016/J.EJA.2013.09.006>
- Loh, F., Grabosky, J., & Bassuk, N. (2002). Using the SPAD 502 Meter to Assess Chlorophyll and Nitrogen Content of Benjamin Fig and Cottonwood Leaves. *HortTechnology*, 12(4).
- Marschner, H. (1995). 8 – Functions of Mineral Nutrients: Macronutrients. In *Mineral Nutrition of Higher Plants* (pp. 229–312). <https://doi.org/10.1016/B978-012473542-2/50010-9>
- Meena, A. K., Gurjar, D., Patil, S. S., & Kumhar, B. L. (2017). Concept of Heterotic Group and its Exploitation in Hybrid Breeding. *International Journal of Current Microbiology and Applied Sciences*, 6(6), 61–73. <https://doi.org/10.20546/ijcmas.2017.606.007>
- Miller, A. J., & Cramer, M. D. (2005). Root Nitrogen Acquisition and Assimilation. *Plant and Soil*, 274(1–2), 1–36. <https://doi.org/10.1007/s11104-004-0965-1>
- Mithofer, A., & Boland, W. (2012). Plant Defense Against Herbivores: Chemical Aspects. *Annu. Rev. Plant Biol.*, 63, 431–50. <https://doi.org/10.1146/annurev-arplant-042110-103854>
- Monneveux, P., Zaidi, P. H., & Sanchez, C. (2005). Population Density and Low Nitrogen Affects Yield-Associated Traits in Tropical Maize. *Crop Science*, 45(2), 535. <https://doi.org/10.2135/cropsci2005.0535>

- Monteiro, S. T., Minekawa, Y., Kosugi, Y., Akazawa, T., & Oda, K. (2007). Prediction of sweetness and amino acid content in soybean crops from hyperspectral imagery. *ISPRS Journal of Photogrammetry and Remote Sensing*, 62(1), 2–12. <https://doi.org/10.1016/j.isprsjprs.2006.12.002>
- Moshou, D., Pantazi, X.-E., Kateris, D., & Gravalos, I. (2014). Water stress detection based on optical multisensor fusion with a least squares support vector machine classifier. *Biosystems Engineering*, 117, 15–22. <https://doi.org/10.1016/J.BIOSYSTEMSENG.2013.07.008>
- Mu, X., Chen, Q., Chen, F., Yuan, L., & Mi, G. (2016). Within-Leaf Nitrogen Allocation in Adaptation to Low Nitrogen Supply in Maize during Grain-Filling Stage. *Frontiers in Plant Science*, 7, 699. <https://doi.org/10.3389/fpls.2016.00699>
- Muñoz-Huerta, R., Guevara-Gonzalez, R., Contreras-Medina, L., Torres-Pacheco, I., Prado-Olivarez, J., & Ocampo-Velazquez, R. (2013). A Review of Methods for Sensing the Nitrogen Status in Plants: Advantages, Disadvantages and Recent Advances. *Sensors*, 13(8), 10823–10843. <https://doi.org/10.3390/s130810823>
- Nam, N. H., Chauhan, Y. S., & Johansen, □□□ C. (2018). Effect of timing of drought stress on growth and grain yield of extra-short-duration pigeonpea lines. *Journal of Agricultural Science*, 136, 179–189. Retrieved from <https://www.cambridge.org/core/services/aop-cambridge-core/content/view/8810DC53EE3CCB98C144290D4F80B95D/S0021859601008607a.pdf/div-class-title-effect-of-timing-of-drought-stress-on-growth-and-grain-yield-of-extra-short-duration-pigeonpea-lines-div.pdf>
- Nigon, T. J., Mulla, D. J., Rosen, C. J., Cohen, Y., Alchanatis, V., Knight, J., & Rud, R. (2015). Hyperspectral aerial imagery for detecting nitrogen stress in two potato cultivars. *Computers and Electronics in Agriculture*, 112, 36–46. <https://doi.org/10.1016/J.COMPAG.2014.12.018>
- Nonami, H. (1998). Plant water relations and control of cell elongation at low water potentials. *Journal of Plant Research*, 111(3), 373–382. <https://doi.org/10.1007/BF02507801>
- O 'Toole, J. C., & Cruz, R. T. (1980). Response of Leaf Water Potential, Stomatal Resistance, and Leaf Rolling to Water Stress. *Plant Physiology*, 65, 428–432. Retrieved from <http://www.plantphysiol.org/content/plantphysiol/65/3/428.full.pdf>
- Otegui, M. E., Andrade, F. H., & Suero, E. E. (1995). Growth, water use, and kernel abortion of maize subjected to drought at silking. *Field Crops Research*, 40(2), 87–94. [https://doi.org/10.1016/0378-4290\(94\)00093-R](https://doi.org/10.1016/0378-4290(94)00093-R)
- Palmer, W. C. (1965). *Meteorological Drought. Research Paper No. 45, 1965, 58 p.* Washington, D.C. Retrieved from <https://www.ncdc.noaa.gov/temp-and-precip/drought/docs/palmer.pdf>

- Pandey, P., Ge, Y., Stoerger, V., & Schnable, J. C. (2017). High Throughput In vivo Analysis of Plant Leaf Chemical Properties Using Hyperspectral Imaging. *Frontiers in Plant Science*, 8, 1–12. <https://doi.org/10.3389/fpls.2017.01348>
- Parks, S. E., Irving, D. E., & Milham, P. J. (2012). A critical evaluation of on-farm rapid tests for measuring nitrate in leafy vegetables. *Scientia Horticulturae*, 134, 1–6. <https://doi.org/10.1016/j.scienta.2011.10.015>
- Paterson, A. H., Bowers, J. E., Bruggmann, R., Dubchak, I., Grimwood, J., Gundlach, H., Rokhsar, D. S. (2009). The Sorghum bicolor genome and the diversification of grasses. *Nature*, 457(7229), 551–556. <https://doi.org/10.1038/nature07723>
- Peel, M. C., Finlayson, B. L., & McMahon, T. A. (2007). Updated world map of the Koppen-Geiger climate classification. *Hydrology and Earth System Sciences Discussions, European Geosciences Union*, 4(2), 439–473.
- Peguero-Pina, J. J., Morales, F., Flexas, J., Gil-Pelegrín, E., & Moya, I. (2008). Photochemistry, remotely sensed physiological reflectance index and de-epoxidation state of the xanthophyll cycle in *Quercus coccifera* under intense drought. *Oecologia*, 156(1), 1–11. <https://doi.org/10.1007/s00442-007-0957-y>
- Penuelas, J., Baret, F., & Filella, I. (1995). Semi-empirical indices to assess carotenoids/chlorophyll a ratio from leaf spectral reflectance. *Photosynthetica*, 31(2), 221–230. Retrieved from https://www.creaf.uab.es/global-ecology/Pdfs_UEG/Photosyn1995.pdf
- Peñuelas, J., Gamon, J. A., Fredeen, A. L., Merino, J., & Field, C. B. (1994). Reflectance indices associated with physiological changes in nitrogen- and water-limited sunflower leaves. *Remote Sensing of Environment*, 48(2), 135–146. [https://doi.org/10.1016/0034-4257\(94\)90136-8](https://doi.org/10.1016/0034-4257(94)90136-8)
- Petiole sap nitrate guidelines. (2011). Retrieved from http://msue.anr.msu.edu/news/petiole_sap_nitrate_guidelines
- PLS_Toolbox. (2018). Manson, WA: Eigenvector Research, Inc.
- Pontes, F. V. M., Carneiro, M. C., Vaitsman, D. S., da Rocha, G. P., da Silva, L. I. D., Neto, A. A., & Monteiro, M. I. C. (2009). A simplified version of the total kjeldahl nitrogen method using an ammonia extraction ultrasound-assisted purge-and-trap system and ion chromatography for analyses of geological samples. *Analytica Chimica Acta*, 632(2), 284–288. <https://doi.org/10.1016/j.aca.2008.11.011>
- Quinby, J. R. (1974). *Sorghum Improvement and the Genetics of Growth*. College Station, Texas: Texas A&M University Press.

- Rao, K. P. C. (2008). Changes in dry land agriculture in the semi-arid tropics of India, 1975-2004. *The European Journal of Development Research*, 20(4), 562–578. <https://doi.org/10.1080/09578810802469366>
- Reddy, A. R., Chaitanya, K. V., & Vivekanandan, M. (2004). Drought-induced responses of photosynthesis and antioxidant metabolism in higher plants. *Journal of Plant Physiology*, 161(11), 1189–1202. <https://doi.org/10.1016/J.JPLPH.2004.01.013>
- Reflectance & Transmittance. (2016). Retrieved January 1, 2016, from <http://oceanoptics.com/measurementtechnique/reflectance-transmittance/>
- Ren, S., Chen, X., & An, S. (2017). Assessing plant senescence reflectance index-retrieved vegetation phenology and its spatiotemporal response to climate change in the Inner Mongolian Grassland. *International Journal of Biometeorology*, 61(4), 601–612. <https://doi.org/10.1007/s00484-016-1236-6>
- Ribaut, J.-M., Betran, J., Monneveux, P., & Setter, T. (2009). Drought Tolerance in Maize. In *Handbook of Maize: It's Biology* (pp. 311–344). New York, NY: Springer New York. https://doi.org/10.1007/978-0-387-79418-1_16
- Rosenow, D. T., Peterson, G. C., Rooney, W. L., & Collins, S. D. (n.d.). Release of A/BTx643, A/BTx644 and A/BTx645 sorghum inbred parental lines. *Texas AgriLife Research and Extension Center Publication*. Retrieved from <https://billrooney.tamu.edu/research/files/germplasm/Tx643-Tx645SorghumInbredsWebsite.pdf>
- Rosso, P. H., Ustin, S. L., & Hastings, A. (2005). Mapping marshland vegetation of San Francisco Bay, California, using hyperspectral data. *International Journal of Remote Sensing*, 26(23), 5169–5191.
- Rotenberg, E., & Yakir, D. (2010). Contribution of semi-arid forests to the climate system. *Science*, 327(5964), 451–4. <https://doi.org/10.1126/science.1179998>
- Rouphael, Y., Cardarelli, M., Schwarz, D., Franken, P., & Colla, G. (2012). Effects of Drought on Nutrient Uptake and Assimilation in Vegetable Crops. In *Plant Responses to Drought Stress* (pp. 171–195). Berlin, Heidelberg: Springer Berlin Heidelberg. https://doi.org/10.1007/978-3-642-32653-0_7
- Saengwilai, P., Nord, E. A., Chimungu, J. G., Brown, K. M., & Lynch, J. P. (2014). Root cortical aerenchyma enhances nitrogen acquisition from low-nitrogen soils in maize. *Plant Physiology*, 166(2), 726–35. <https://doi.org/10.1104/pp.114.241711>
- Samborski, S. M., Tremblay, N., & Fallon, E. (2009). Strategies to Make Use of Plant Sensors-Based Diagnostic Information for Nitrogen Recommendations. *Agronomy Journal*, 101(4), 800–816. <https://doi.org/10.2134/agronj2008.0162Rx>

- Sanaullah, M., Rumpel, C., Charrier, X., & Chabbi, A. (2012). How does drought stress influence the decomposition of plant litter with contrasting quality in a grassland ecosystem? *Plant and Soil*, 352(1), 277–288. <https://doi.org/10.1007/s11104-011-0995-4>
- Sanchez, P. A. (2002). Ecology. Soil fertility and hunger in Africa. *Science (New York, N.Y.)*, 295(5562), 2019–20. <https://doi.org/10.1126/science.1065256>
- Sardans, J., & Penuelas, J. (2012). The Role of Plants in the Effects of Global Change on Nutrient Availability and Stoichiometry in the Plant-Soil System. *Plant Physiology*, 160(4), 1741–1761. <https://doi.org/10.1104/pp.112.208785>
- Schimel, J., Balser, T. C., & Wallenstein, M. (2007). Microbial Stress-Response Physiology and its Implications for Ecosystem Function. *Ecology*, 88(6), 1386–1394. <https://doi.org/10.1890/06-0219>
- Schittenhelm, S., & Schroetter, S. (2014). Comparison of Drought Tolerance of Maize, Sweet Sorghum and Sorghum-Sudangrass Hybrids. *Journal of Agronomy and Crop Science*, 200(1), 46–53. <https://doi.org/10.1111/jac.12039>
- Schubert, S. D., Stewart, R. E., Wang, H., Barlow, M., Berbery, E. H., Cai, W., Zhou, T. (2016). Global Meteorological Drought: A Synthesis of Current Understanding with a Focus on SST Drivers of Precipitation Deficits. *Journal of Climate*, 29. <https://doi.org/10.1175/JCLI-D-15-0452.1>
- Shao, H.-B., Chu, L.-Y., Jaleel, C. A., Manivannan, P., Panneerselvam, R., & Shao, M.-A. (2009). Understanding water deficit stress-induced changes in the basic metabolism of higher plants - biotechnologically and sustainably improving agriculture and the ecoenvironment in arid regions of the globe. *Critical Reviews in Biotechnology*, 29(2), 131–51. <https://doi.org/10.1080/07388550902869792>
- Stagakis, S., Markos, N., Sykioti, O., & Kyparissis, A. (2010). Monitoring canopy biophysical and biochemical parameters in ecosystem scale using satellite hyperspectral imagery: An application on a *Phlomis fruticosa* Mediterranean ecosystem using multiangular CHRIS/PROBA observations. *Remote Sensing of Environment*, 114(5), 977–994. <https://doi.org/10.1016/j.rse.2009.12.006>
- Stephens, J. C., Miller, F. R., & Rosenow, D. T. (1967). Conversion of Alien Sorghums to Early Combine Genotypes1. *Crop Science*, 7(4), 396. <https://doi.org/10.2135/cropsci1967.0011183X000700040036x>
- Sutton, L. (2012). Vegetation Indices Enhancing green vegetation using mathematical equations and transformations. Retrieved from http://web.pdx.edu/~nauna/resources/8-2012_lecture1-vegetationindices.pdf

- Swain, S., Rundquist, D., Arkebauer, T. J., Narumalani, S., & Wardlow, B. (2012). Non-invasive estimation of relative water content in soybean leaves using infrared thermography. *Israel Journal of Plant Sciences*, 60(1/2), 25–36.
- Tanksley, S. D., & McCouch, S. R. (1997). Seed banks and molecular maps: unlocking genetic potential from the wild. *Science*, 277(5329), 1063–6. <https://doi.org/10.1126/science.277.5329.1063>
- Teal, R. K., Tubana, B., Girma, K., Freeman, K. W., Arnall, D. B., Walsh, O., & Raun, W. R. (2006). In-Season Prediction of Corn Grain Yield Potential Using Normalized Difference Vegetation Index. *Agronomy Journal*, 98(6), 1488–1494. <https://doi.org/10.2134/agronj2006.0103>
- The Importance of Sorghum. (2010). Retrieved from <http://biosorghum.org/>
- Thenkabail, A., Lyon, P., & Huete, J. (2011). *Hyperspectral Remote Sensing of Vegetation*. CRC Press. <https://doi.org/10.1201/b11222>
- Townshend, J. R. G., & Justice, C. O. (1986). Analysis of the dynamics of African vegetation using the normalized difference vegetation index. *International Journal of Remote Sensing*, 7(11), 1435–1445.
- Tremblay, N., Wang, Z., & Cerovic, Z. (2012). Sensing crop nitrogen status with fluorescence indicators. A review. *Agronomy for Sustainable Development*, 32(2), 451–464. <https://doi.org/10.1007/s13593-011-0041-1>
- Tuinstra, M. R., Grote, E. M., Goldsbrough, P. B., & Ejeta, G. (1996). Identification of Quantitative Trait Loci Associated with Pre-Flowering Drought Tolerance in Sorghum. *Crop Science*, 36(5), 1337. <https://doi.org/10.2135/cropsci1996.0011183X003600050043x>
- Turner, M. G., Gardner, R. H., & O'Neill, R. V., Robert V. (2001). *Landscape ecology in theory and practice : pattern and process*. Springer. Retrieved from https://books.google.com/books/about/Landscape_Ecology_in_Theory_and_Practice.html?id=RENW9Nq6IDYC
- Turner, N. C. (1981). Techniques and Experimental Approaches for the Measurements of Plant Water Status. *Plant and Soil*, 58, 339–366.
- Ulaby, F. T., & Bush, T. F. (1976). Monitoring Wheat Growth with RADAR. *Photogrammetric Engineering and Remote Sensing*, 42(4), 557–568.
- Underwood, E., Ustin, S., & DiPietro, D. (2003). Mapping nonnative plants using hyperspectral imagery. *Remote Sensing of Environment*, 86(2), 150–161. [https://doi.org/10.1016/S0034-4257\(03\)00096-8](https://doi.org/10.1016/S0034-4257(03)00096-8)

- Unkovich, M., Herridge, D., Peoples, M., Cadisch, G., Boddey, R., Giller, K., Chalk, P. (2008). *Measuring plant-associated nitrogen fixation in agricultural systems*. Canberra, Australia: Australian Centre for International Agricultural Research.
- van Heerwaarden, J., Hufford, M. B., & Ross-Ibarra, J. (2012). Historical genomics of North American maize. *Proceedings of the National Academy of Sciences*, 109(31), 12420–12425.
- van Oosterom, E. J., Borrell, A. K., Deifel, K. S., & Hammer, G. L. (2011). Does Increased Leaf Appearance Rate Enhance Adaptation to Postanthesis Drought Stress in Sorghum? *Crop Science*, 51(6), 2728–2740. <https://doi.org/10.2135/cropsci2011.01.0031>
- Wahid, A., Gelani, S., Ashraf, M., & Foolad, M. R. (2007). Heat tolerance in plants: An overview. *Environmental and Experimental Botany*, 61, 199–223. <https://doi.org/10.1016/j.envexpbot.2007.05.011>
- Wahid, A., & Rasul, E. (2004). Photosynthesis in leaf, stem, flower, and fruit. In *Handbook of Photosynthesis* (2nd ed., pp. 479–497). CRC Press Florida. Retrieved from <https://pdfs.semanticscholar.org/3d35/9f4443bb8267219a7cdc2af9133d21e76dee.pdf>
- Walulu, R. S., Rosenow, D. T., Wester, D. B., & Nguyen, H. T. (1994). Inheritance of the Stay-green Trait in Sorghum. *Crop Science*, 34(4), 970. <https://doi.org/10.2135/cropsci1994.0011183X003400040026x>
- Watson, M. E., & Galliher, T. L. (2001). Comparison of Dumas and Kjeldahl methods with automatic analyzers on agricultural samples under routine rapid analysis conditions. *Communications in Soil Science and Plant Analysis*, 32(13–14), 2007–2019.
- Xiong, D., Chen, J., Yu, T., Gao, W., Ling, X., Li, Y., Huang, J. (2015). SPAD-based leaf nitrogen estimation is impacted by environmental factors and crop leaf characteristics. *Scientific Reports*, 5, 13389. <https://doi.org/10.1038/srep13389>
- Xu, W., Subudhi, P. K., Crasta, O. R., Rosenow, D. T., Mullet, J. E., & Nguyen, H. T. (2000). Molecular mapping of QTLs conferring stay-green in grain sorghum (*Sorghum bicolor* L. Moench). *Genome*, 43, 461–469.
- Xue, Y., Sellers, P. J., Zeng, F. J., & Schlosser, C. A. (1997). The Impact of Desertification in the Mongolian and the Inner Mongolian Grassland on the Regional Climate. *Journal of Climate*, 10, 374–6. [https://doi.org/10.1175/1520-0442\(1996\)009<2173:TIODIT>2.0.CO;2](https://doi.org/10.1175/1520-0442(1996)009<2173:TIODIT>2.0.CO;2)
- Yadav, R. R., Singh, J., Dubey, B., & Chaturvedi, R. (n.d.). Varying strength of relationship between temperature and growth of high-level fir at marginal ecosystems in western Himalaya, India. *Current Science*, 86(8), 1152–1156. <https://doi.org/10.2307/24109326>
- Zegada-Lizarazu, W., Zatta, A., & Monti, A. (2012). Water uptake efficiency and above- and belowground biomass development of sweet sorghum and maize under different water regimes. *Plant and Soil*, 351(1–2), 47–60. <https://doi.org/10.1007/s11104-011-0928-2>

- Zeng, N., Neelin, J. D., Lau, K.-M., & Tucker, C. J. (1999). Enhancement of Interdecadal Climate Variability in the Sahel by Vegetation Interaction. *Science*, 286(5444), 1537–1540. <https://doi.org/10.1126/science.286.5444.1537>
- Zhao, D., Reddy, K. R., Kakani, V. G., & Reddy, V. R. (2005). Nitrogen deficiency effects on plant growth, leaf photosynthesis, and hyperspectral reflectance properties of sorghum. *European Journal of Agronomy*, 22(4), 391–403. <https://doi.org/10.1016/j.eja.2004.06.005>
- Zhao, T., & Dai, A. (2015). The Magnitude and Causes of Global Drought Changes in the Twenty-First Century under a Low–Moderate Emissions Scenario. *Journal of Climate*, 28, 4490–4512. <https://doi.org/10.1175/JCLI-D-14-00363.1>